X-PEEM for micromagnetism and device physics

Florian Kronast

Magnetic imaging

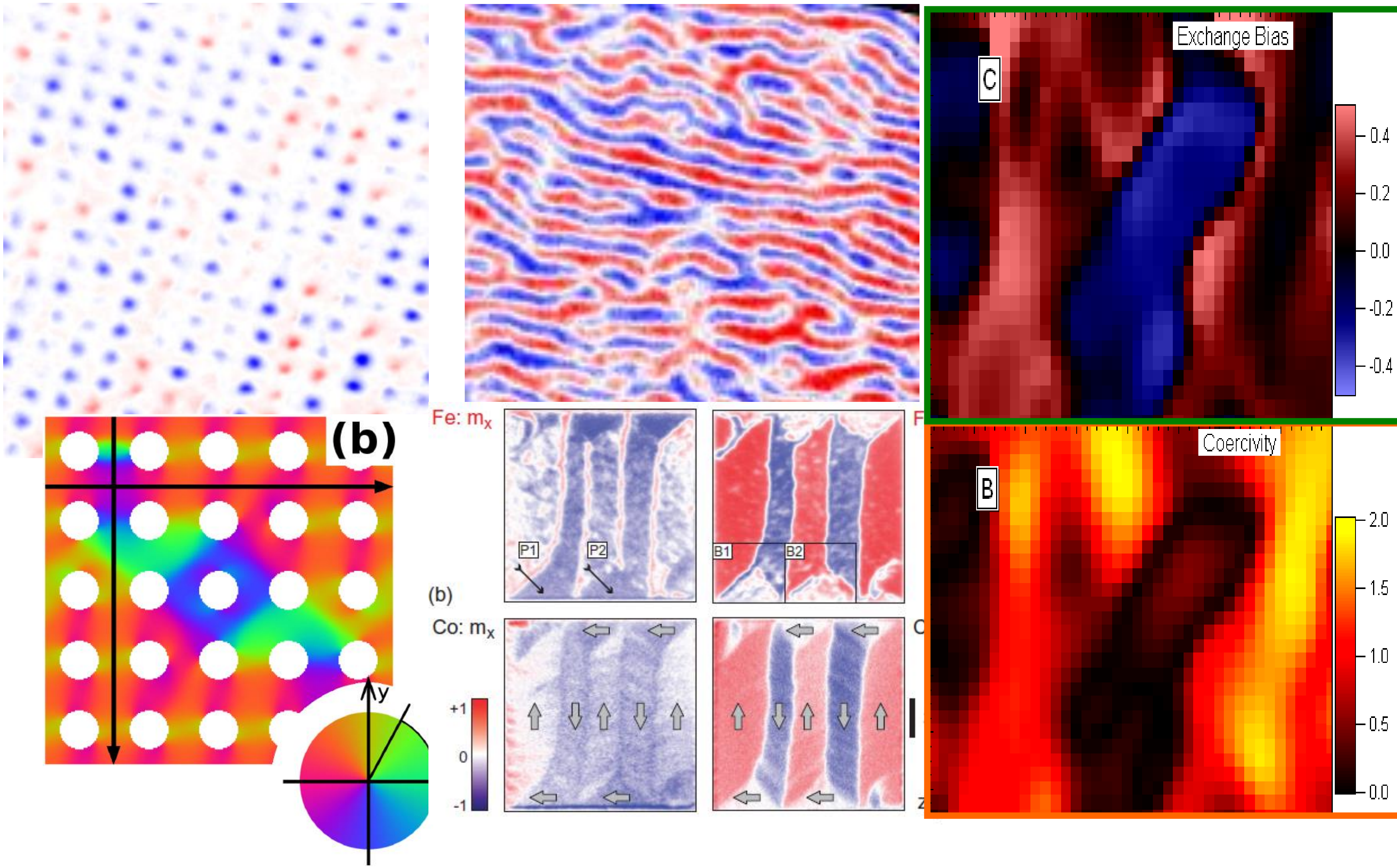

$S_{\text{pin resolved}}$ $P_{\text{hoto}}E_{\text{lectron}}$ E_{mission} $M_{\text{icroscope}}$

Spectromicroscopy & Magnetic imaging on the nanometer scale

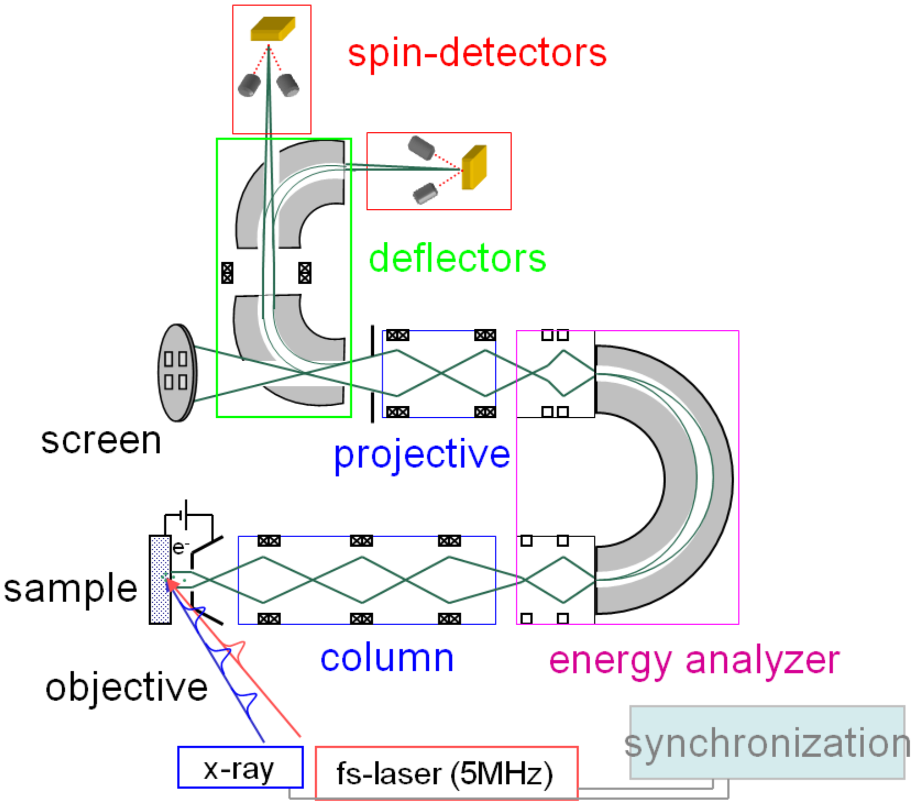

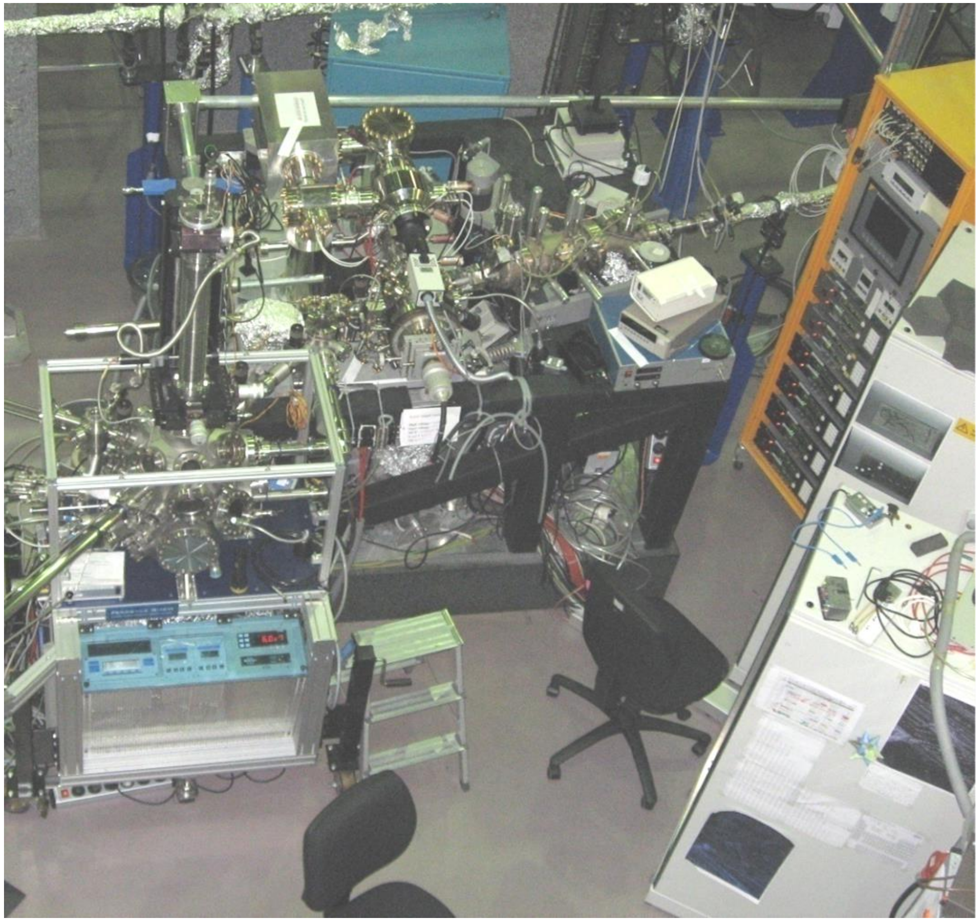

Customized sample holders

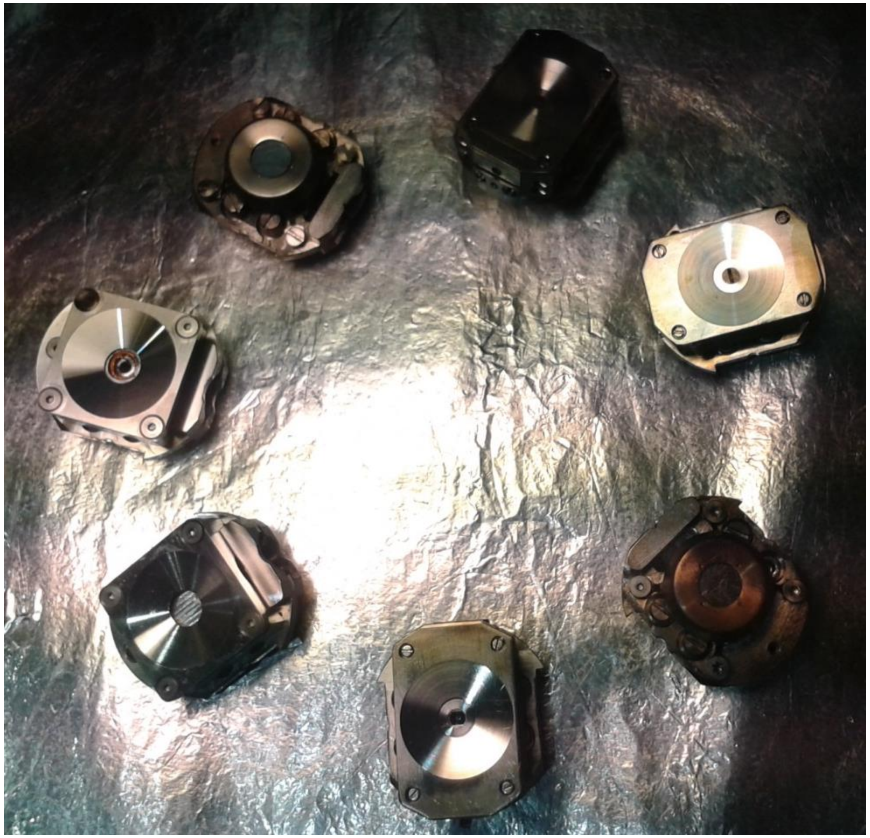

Special sample holders for:

Temperature control

Magnetic field

Electric field

Transport measurements

Laser optics (micro focus)

Cooling upgrade in 2013

Upgrade of the manipulator by a lHe cryostat
Extendend temperature range down to 45K

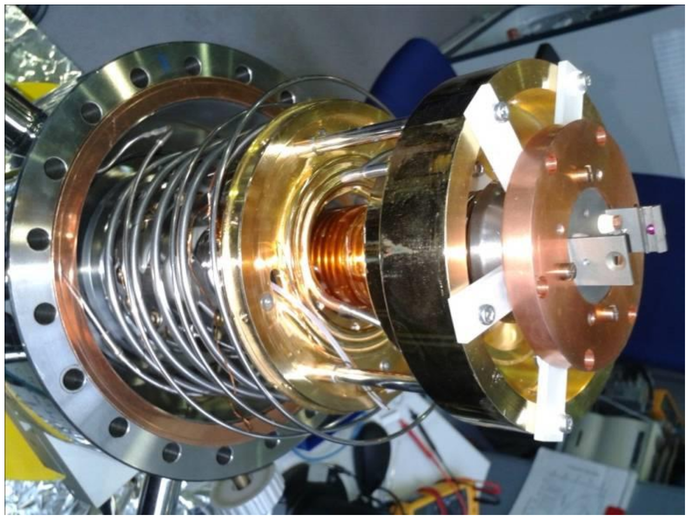

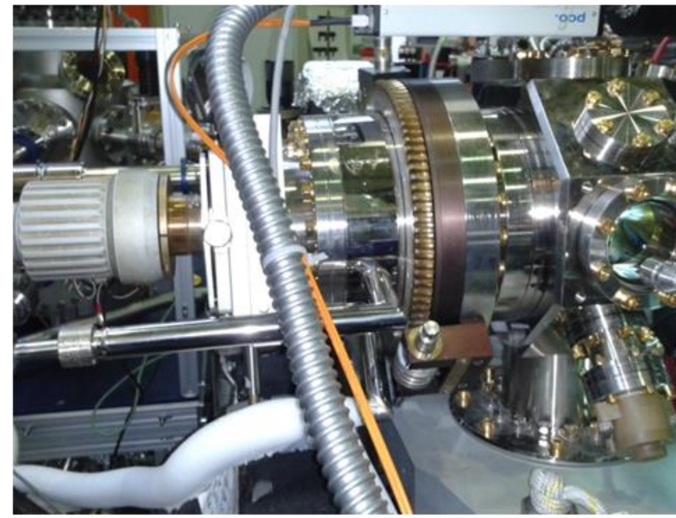

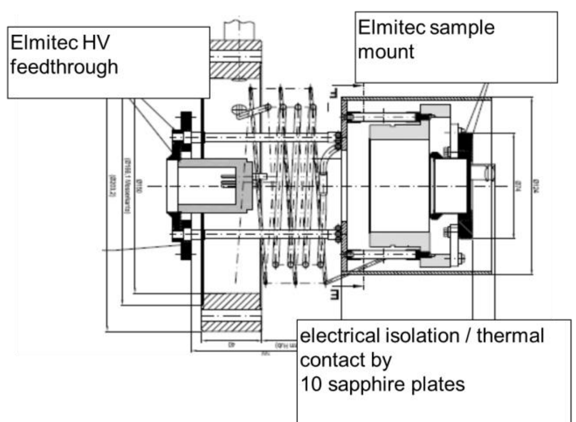

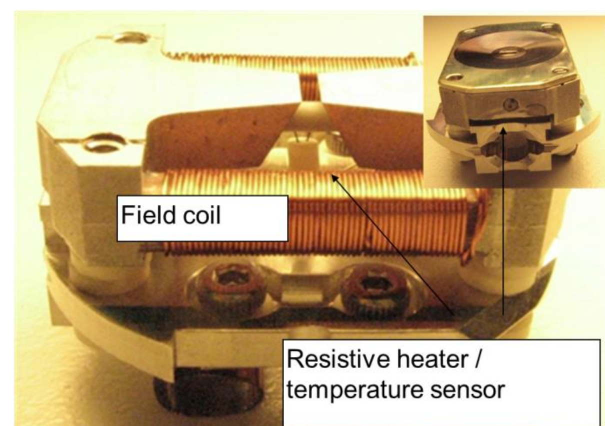

outline

-> Nanoparticles and 3d objects

Thin films and wedge profiles

PEEM with laser excitation

XPS PEEM & SW excitation

outline

-> Nanoparticles and 3d objects

Characterization of individual nanoparticles

PEEM in transmission mode / shadow contrast of 3d objects

Thin films and wedge profiles

XPS PEEM & SW excitation

PEEM with laser excitation

Magnetic Nanoparticles

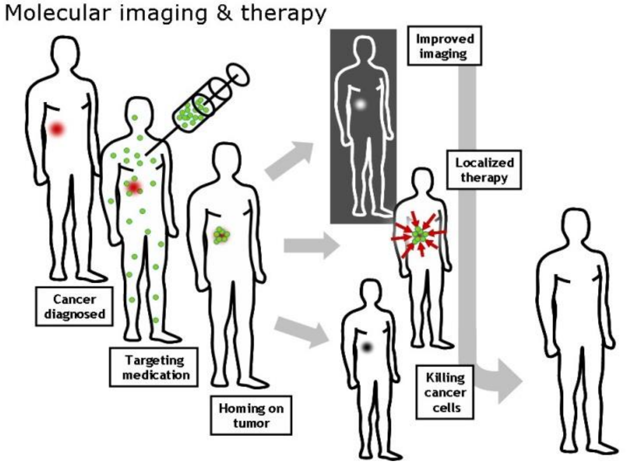

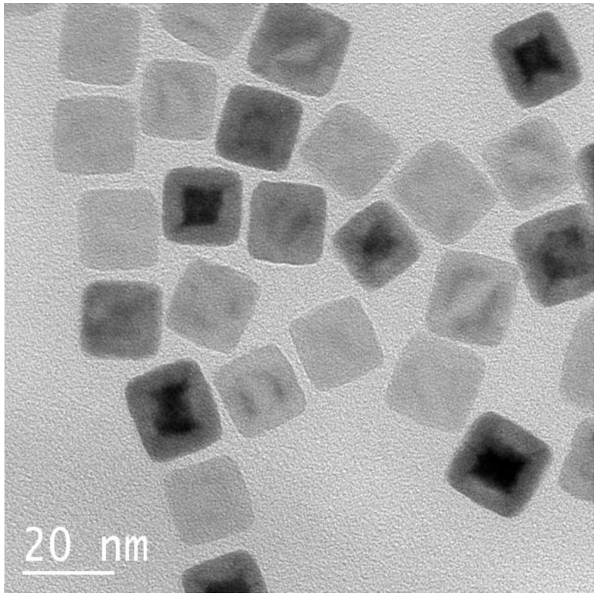

- Biomedical diagnostic and therapeutic applications
  →They can save lives.
- Magnetic data storage media and sensors
- Multifunctional Materials

Structure-function relationship

Ensemble measurements vs.

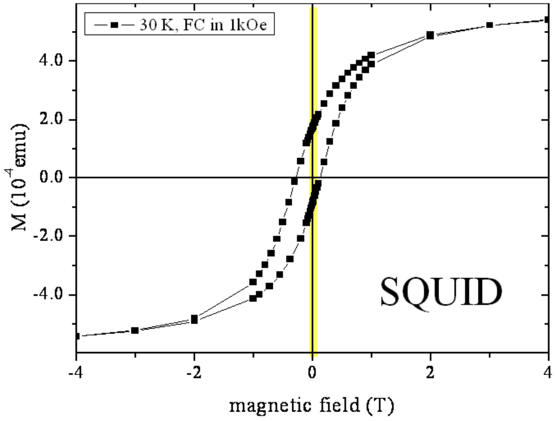

Superparamagnetism

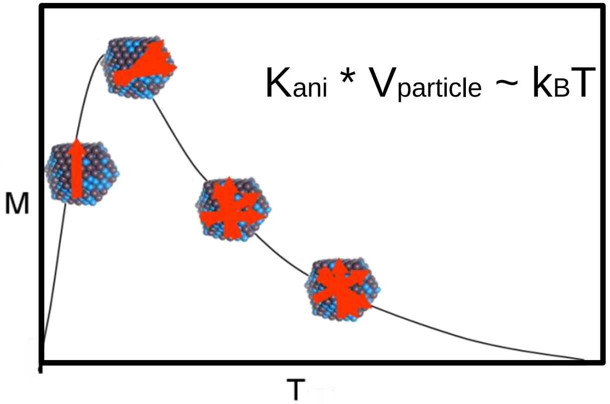

Individual magnetic properties depending on

-composition

-size

-shape

-orientation

-configuration

- particle interactions

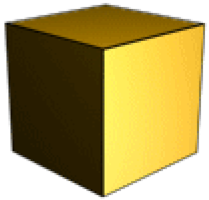

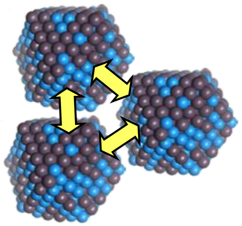

Space resolved magnetospectroscopy

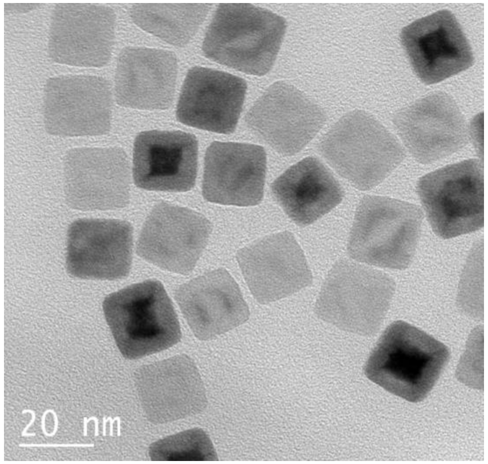

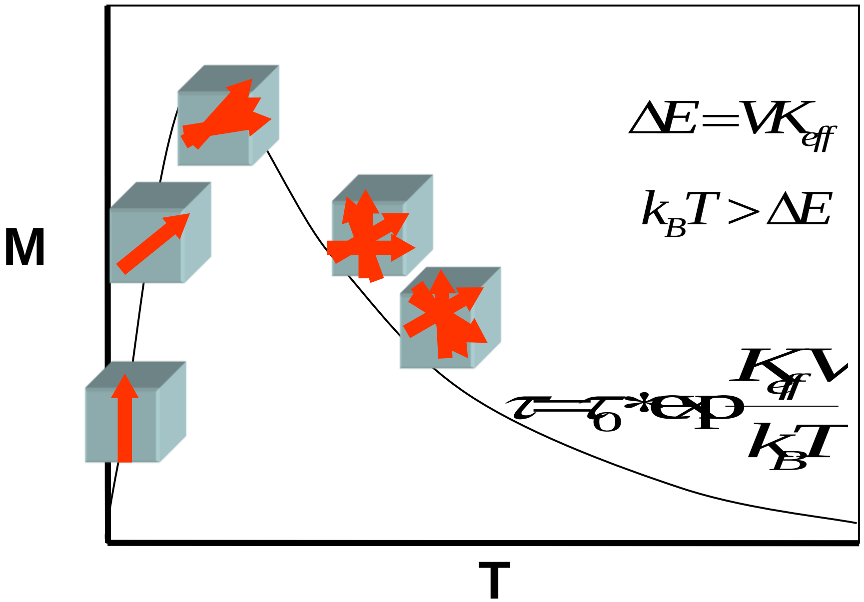

dipolar interactions

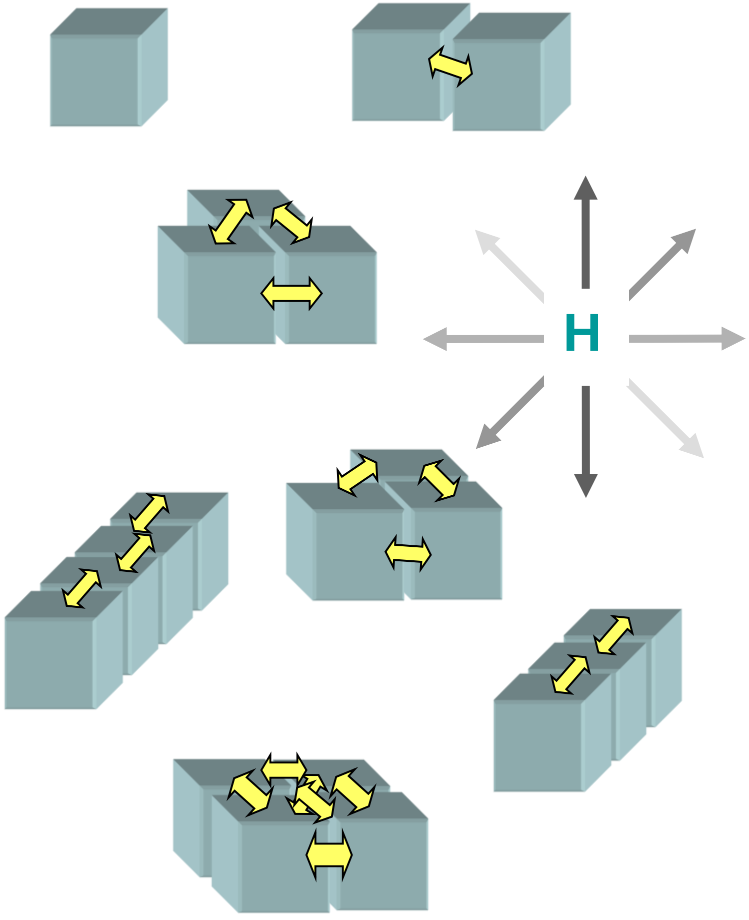

Synthesis and size distribution

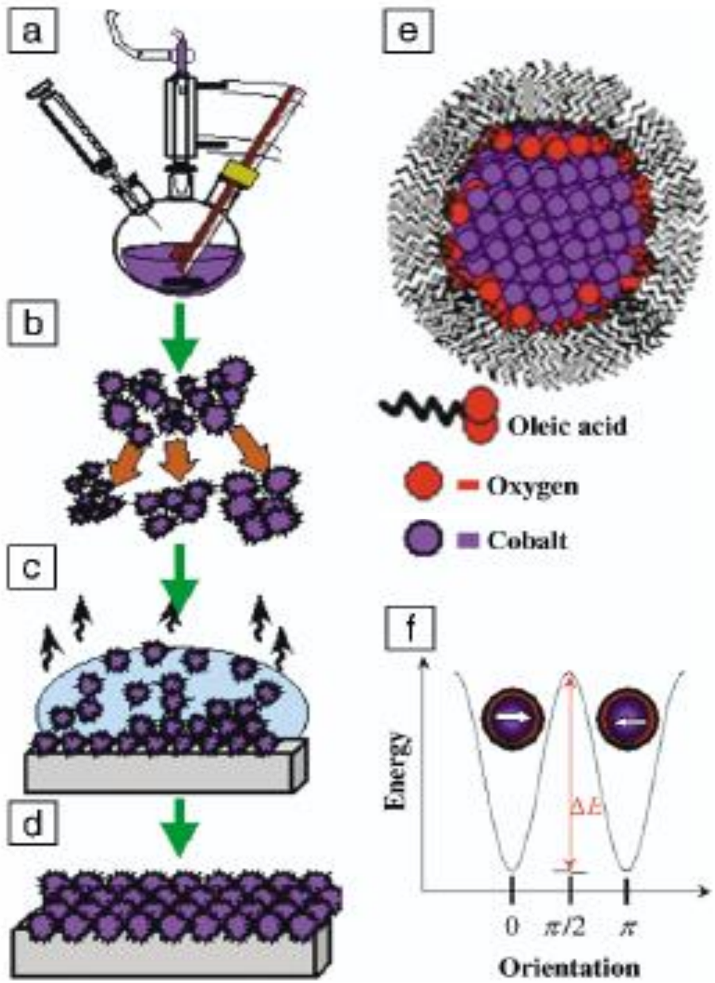

C.B. Murray, MRS Bulletin (2001)

size distribution:

$$N(d) = \frac{1}{\sqrt{2\pi}\,\sigma d} \exp\left[-\frac{1}{2\sigma^2} \ln^2\left(\frac{d}{d_N}\right) \right]$$

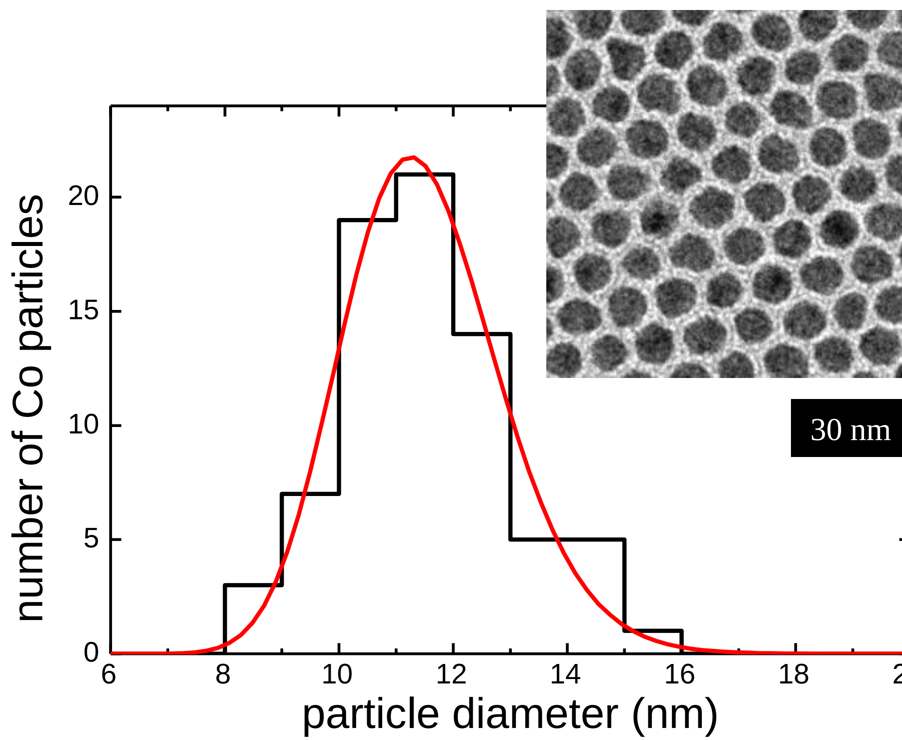

U. Wiedwald, Ph. D. Thesis,
University Duisburg-Essen (2004)

by spin-coating onto a Si wafer
or “Self- Assembly”

Magnetic colloid Fe

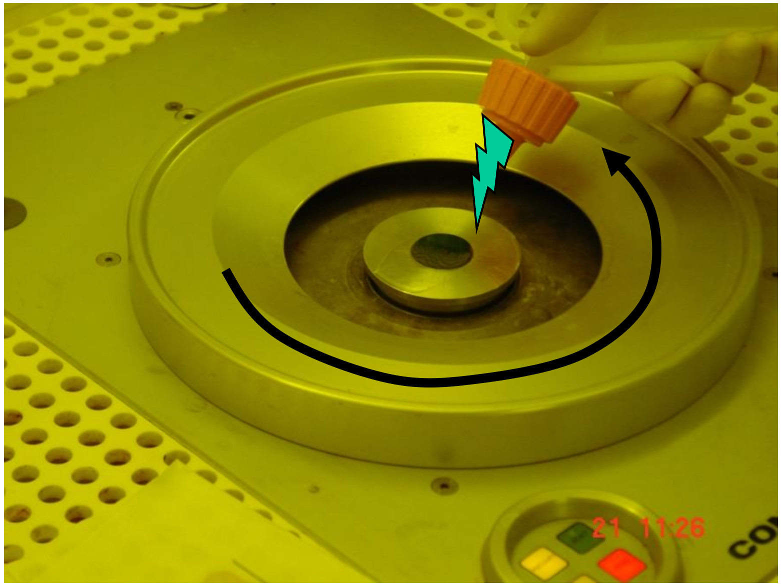

Spin-coating

Two dimensional array of reduced 18nm Fe-cubes

SEM

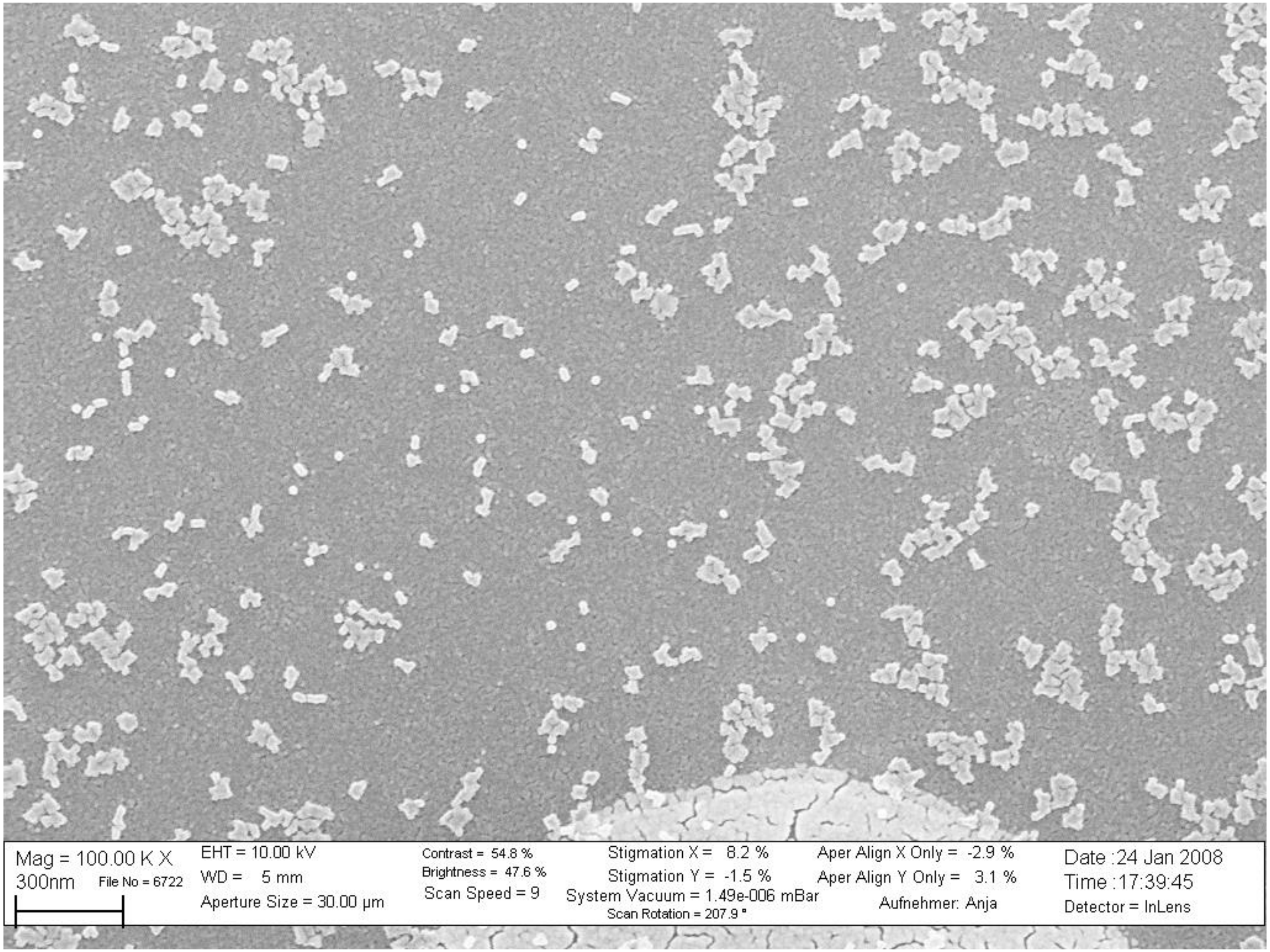

Addressing individual nanoparticles with PEEM and SEM

Experimental Setup

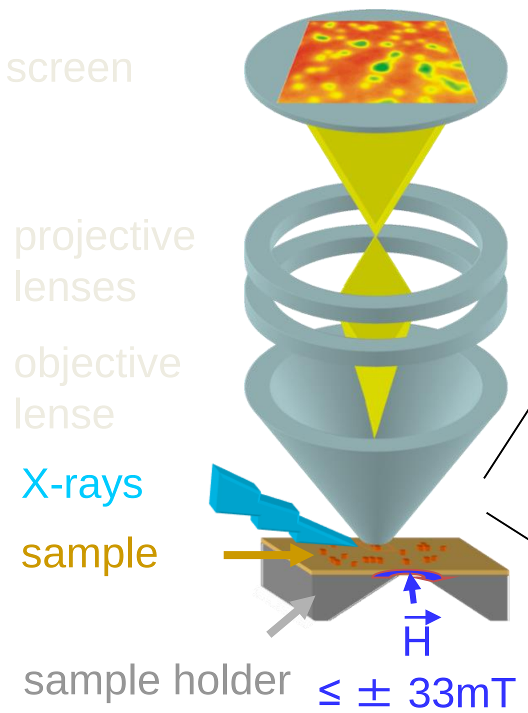

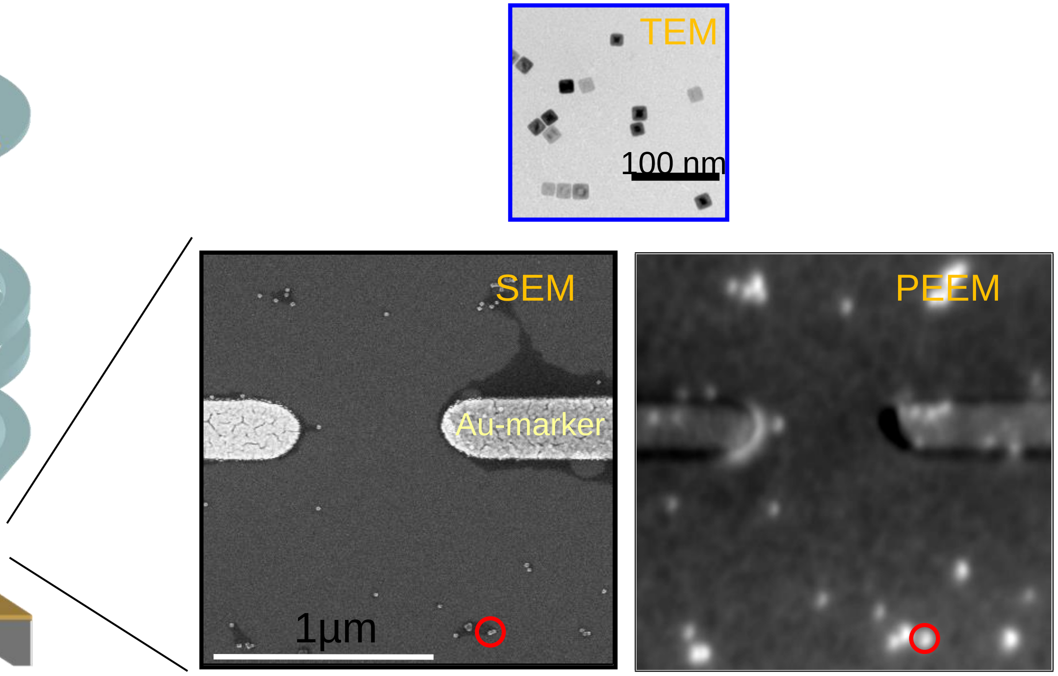

Demands on sample:

- particle separation ~ 100nm
- position markers, to identify particle configurations by SEM
- narrow marker array, as small width as possible

Magnetic micro-spectroscopy of a single dimer

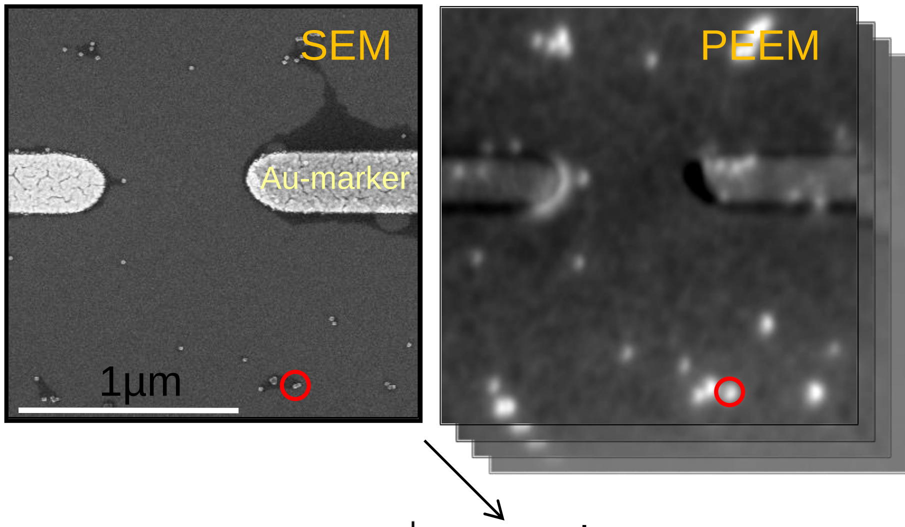

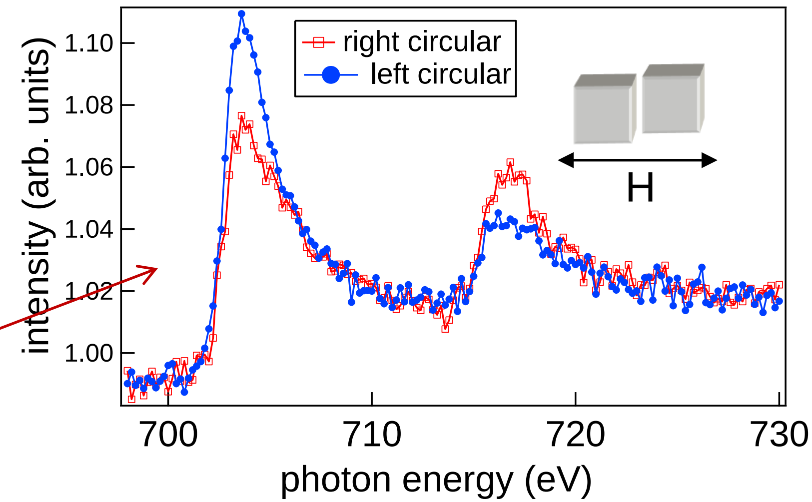

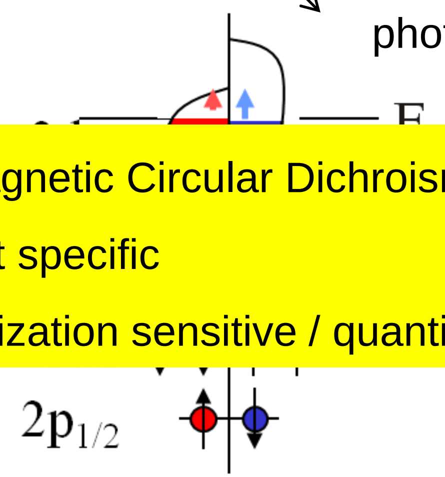

X-ray Magnetic Circular Dichroism (XMCD)

- element specific
- magnetization sensitive / quantitative

maximum contrast for **k** || **M**

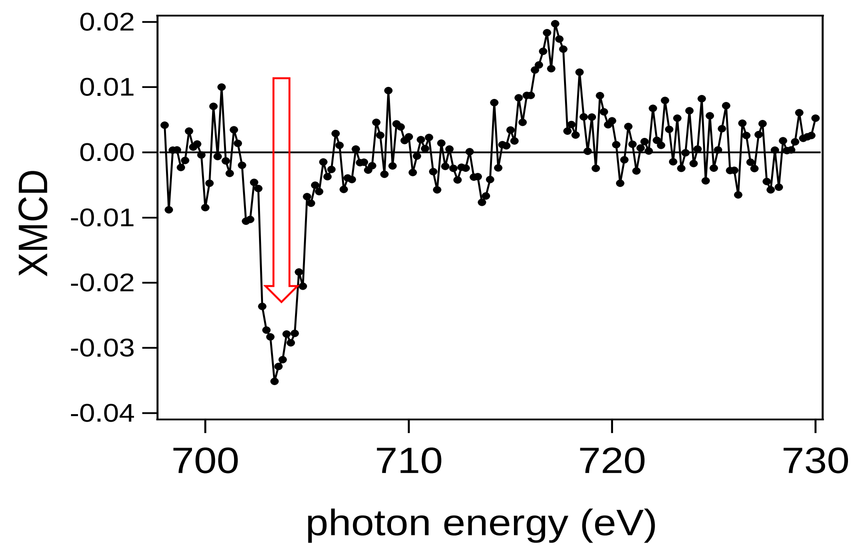

F.Kronast et al.,Nano Lett. 2011, 11, 1710–1715

Magnetic hysteresis of a single dimer

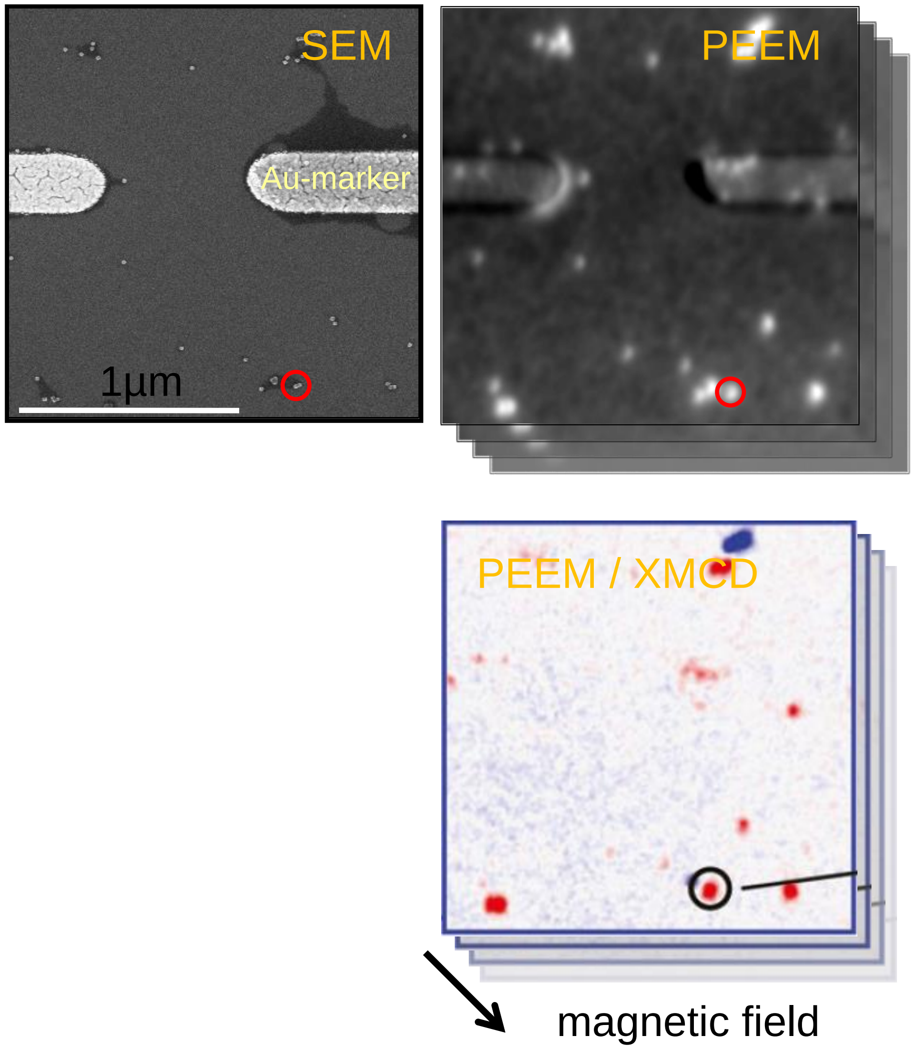

- aquisition time 8-20h
- PEEM fov 3-5µm
- simultaneous recording of several 100 hystersis

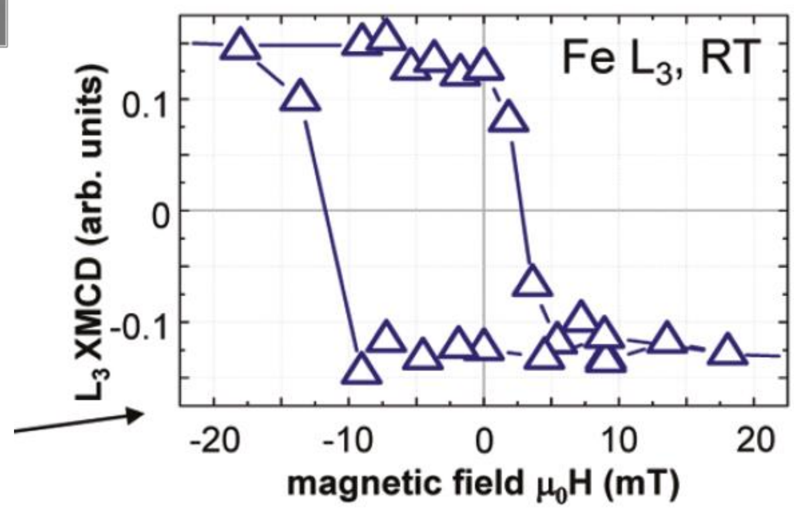

F.Kronast et al.,Nano Lett. 2011, 11, 1710–1715

Recording hysteresis of individual Fe nanocubes

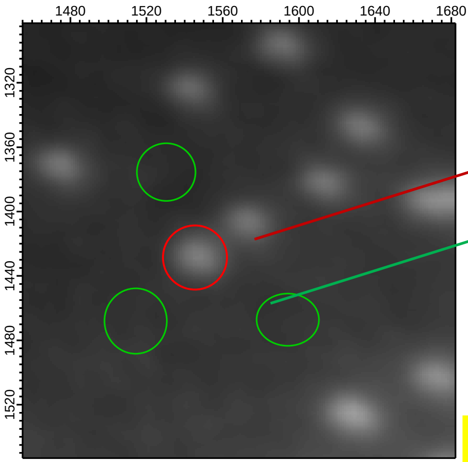

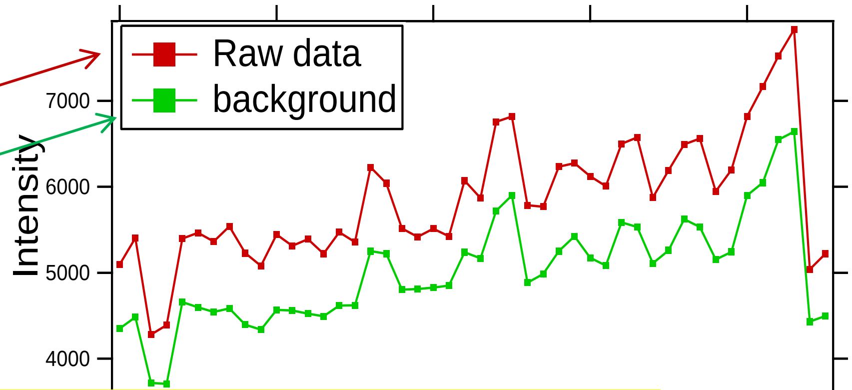

After normalization the Fe L_3 XMCD signal is proportional to the average magnetic moment per Fe atom in each configuration

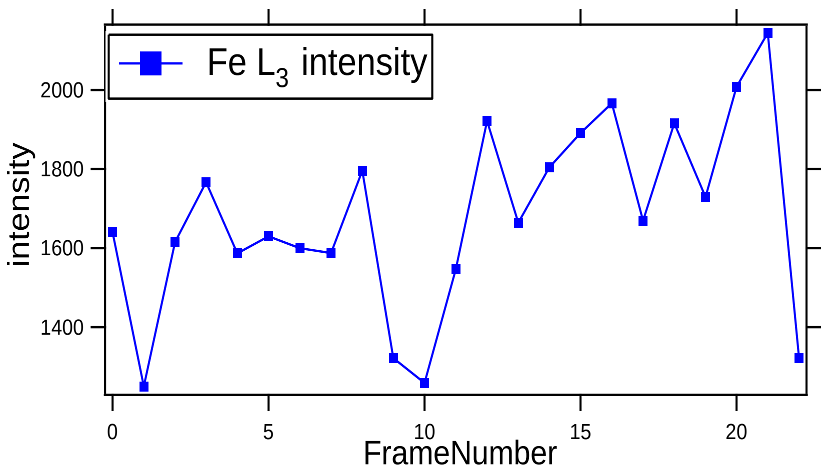

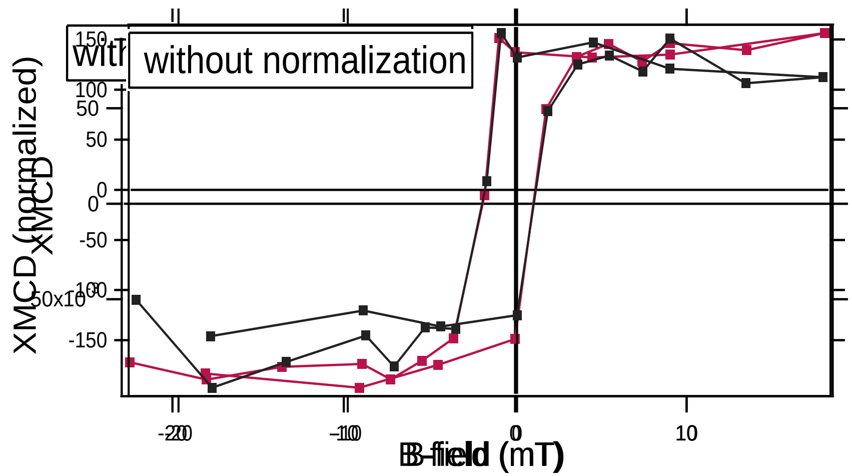

F.Kronast et al.,Nano Lett. 2011, 11, 1710–1715

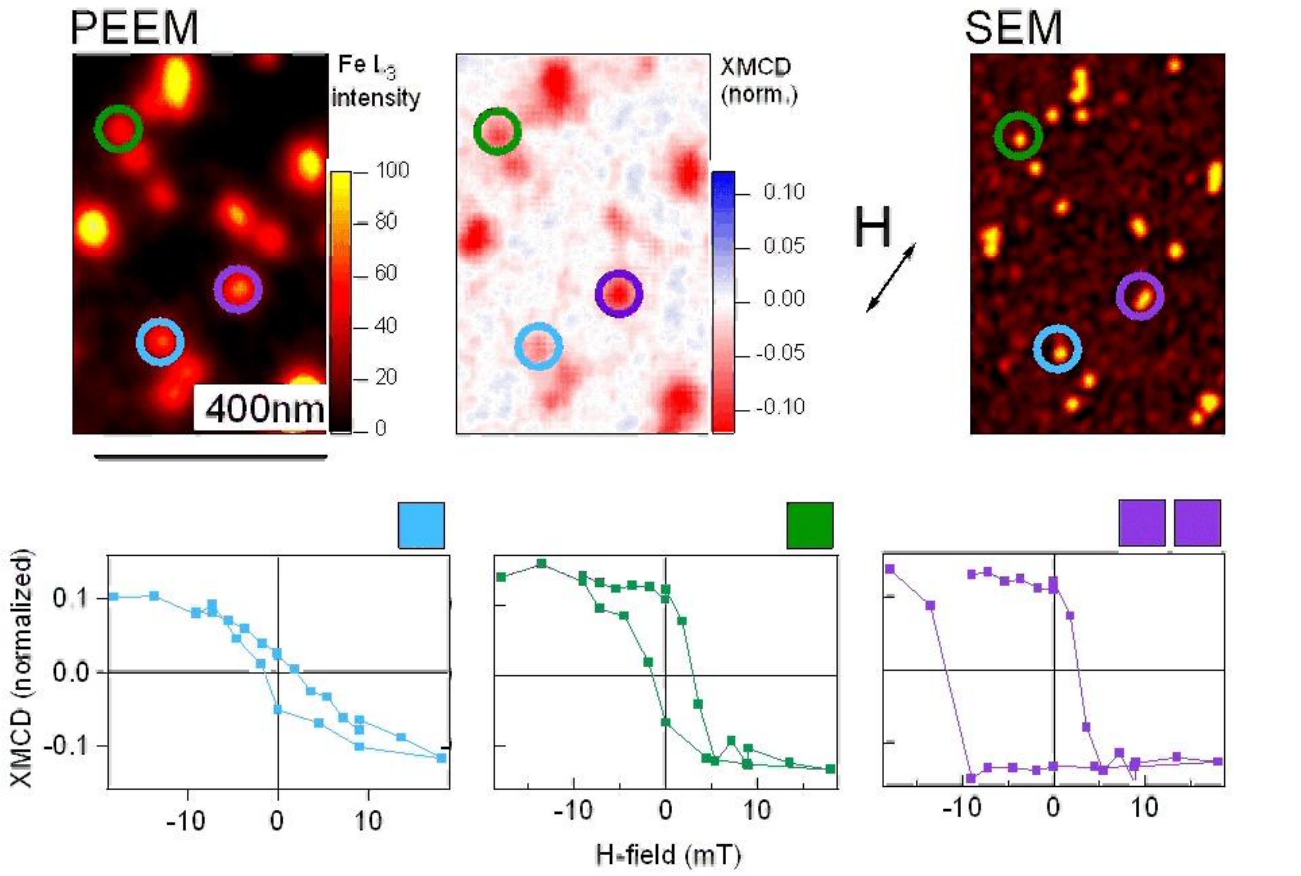

Movie: In this movie, the read out of the XMCD signal for three different particle configurations and the resulting hysteresis loops are illustrated.

F.Kronast et al.,Nano Lett. 2011, 11, 1710–1715

PEEM allows parallel acquisition of many hysteresis

SEM overview

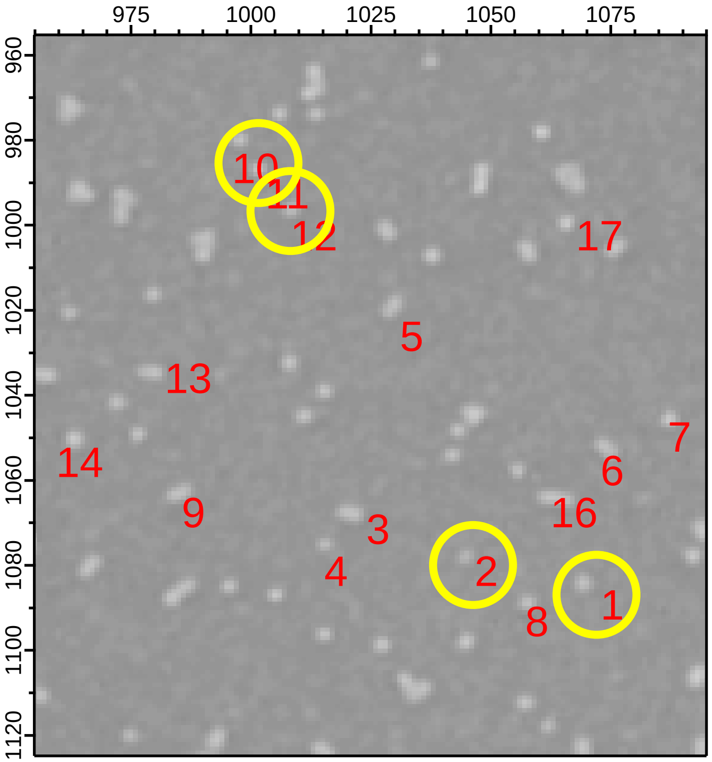

Monomer

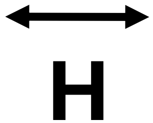

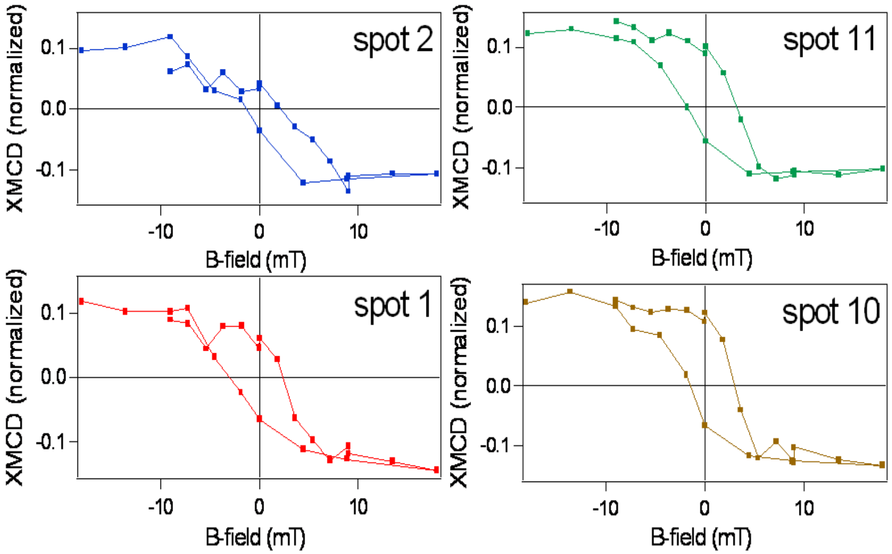

Systematic investigation of different nanocube configurations

SEM overview

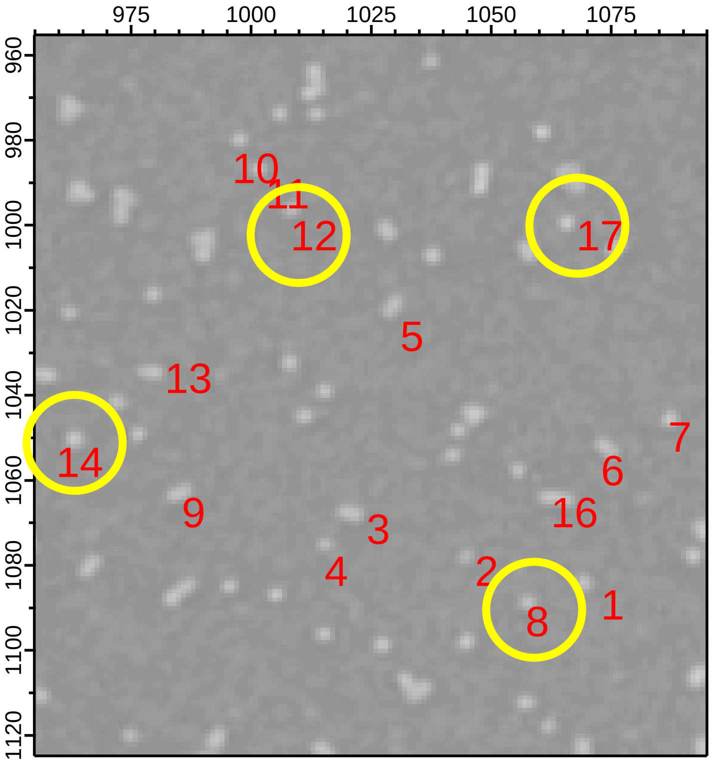

Monomer

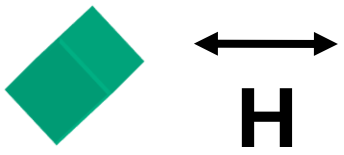

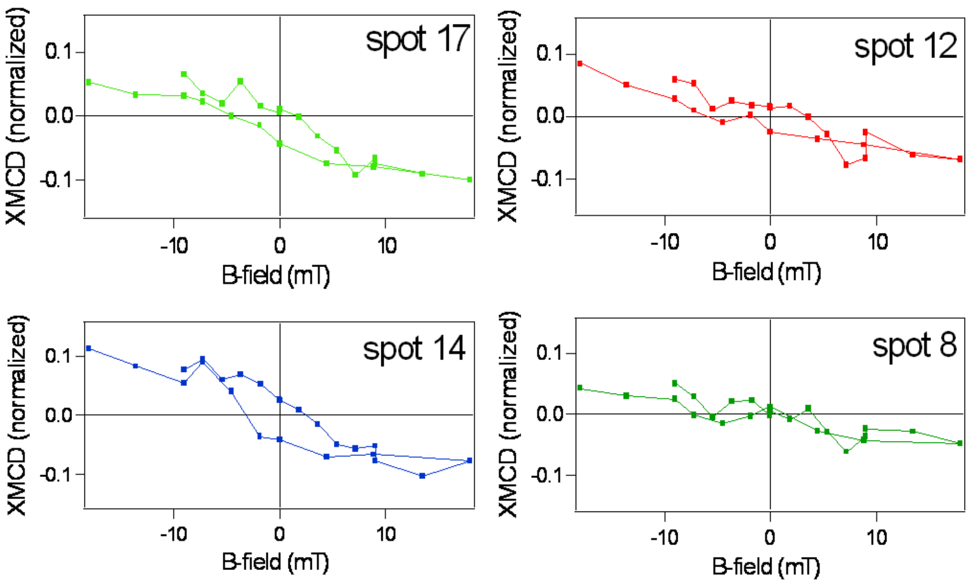

Systematic investigation of different nanocube configurations

SEM overview

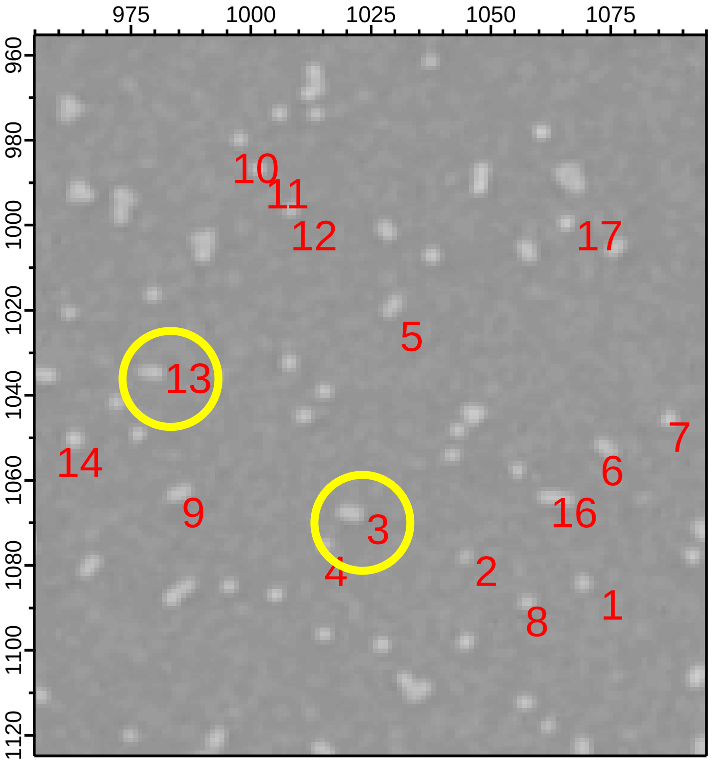

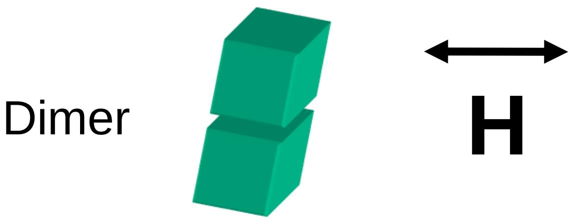

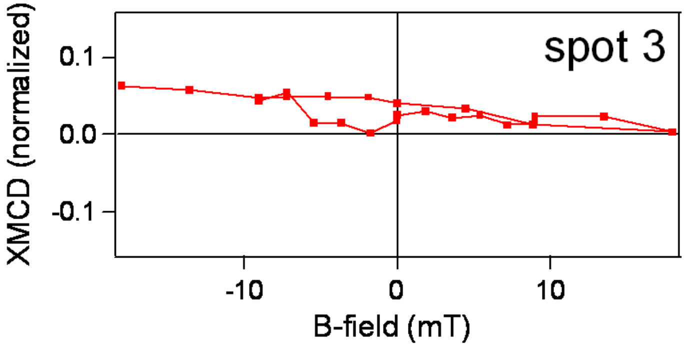

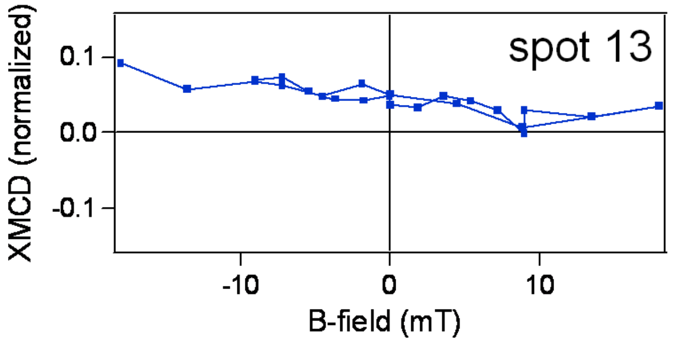

SEM overview

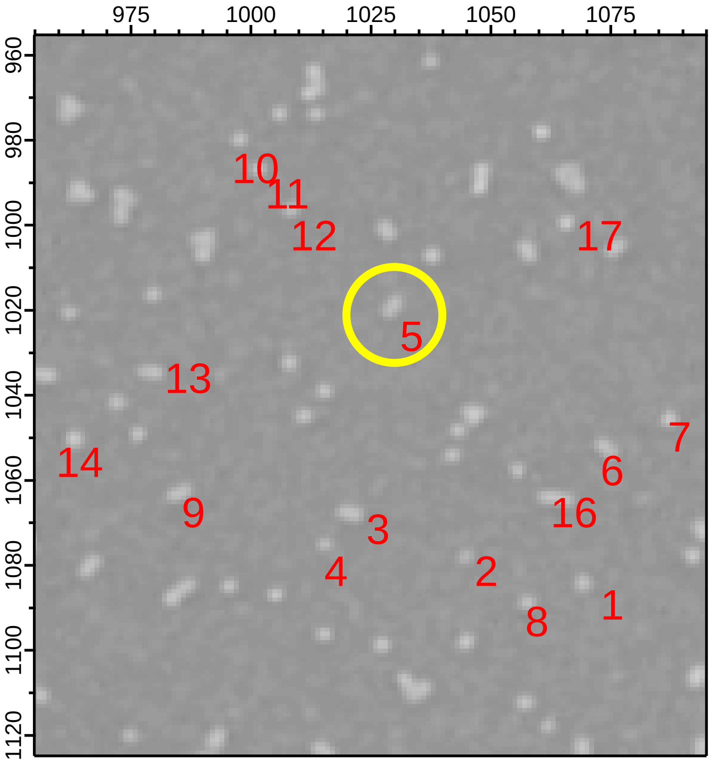

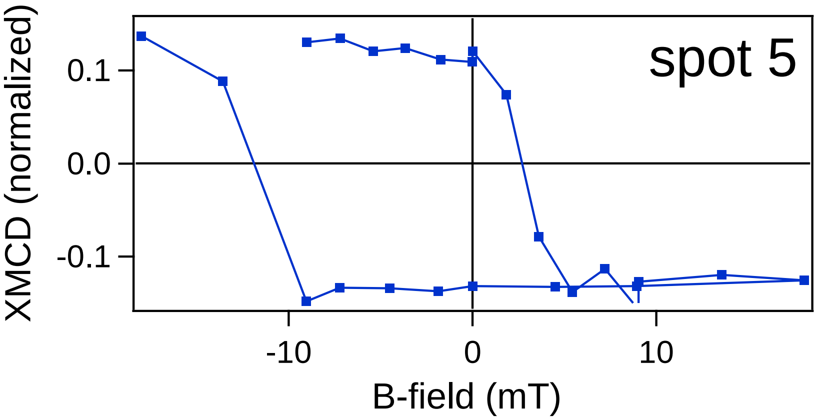

Micromagnetic simulations for selected configurations

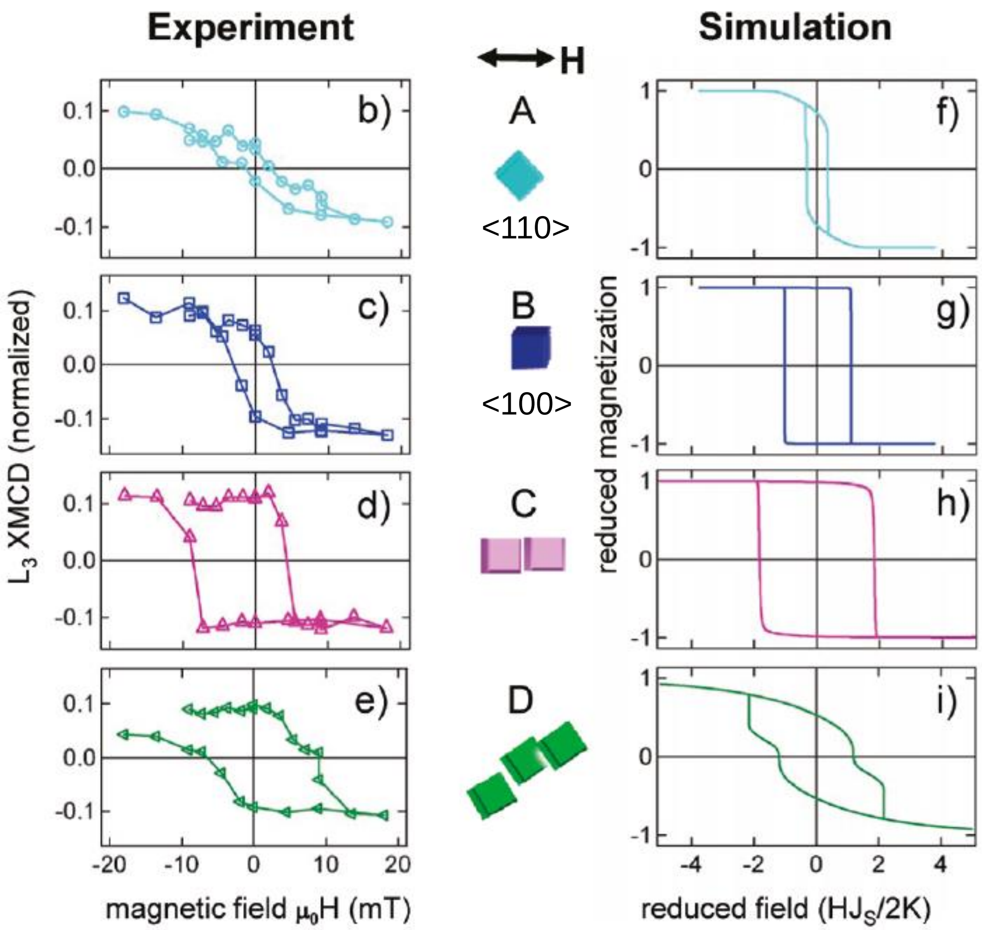

strongly reduced coercitive field close to the blocking temperature

evidence for magnetocrystalline anisotropy

dipolar coupling enhances shape anisotropy and increases blocking temperature

complex switching in non-collinear alignments

material parameters for (bcc) Fe :
A = 21 pJ/m (exchange constant)
$\mu_0 M_s$ = 2.15 T (M_s: saturation magnetization).

F.Kronast et al.,Nano Lett. 2011, 11, 1710–1715

3d imaging part I

Three-dimensional magnetization configurations in core-shell nanotubes

Imaging 3d nanomagnets

Field distortion and different emission angels cause imaging artifacts

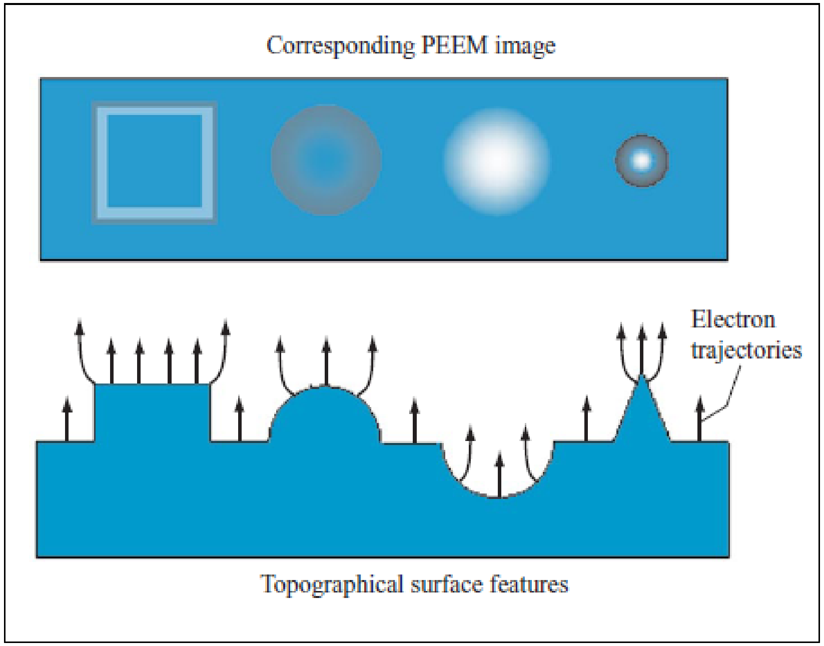

Sources of topographical contrast in PEEM

IBM J. RES. DEVELOP. VOL. 44 NO. 4 JULY 2000
J. STÖHR AND S. ANDERS

Transmitted x-rays probe bulk magnetization with enhanced spatial resolution (works for structure sizes 50nm ~ 400nm)

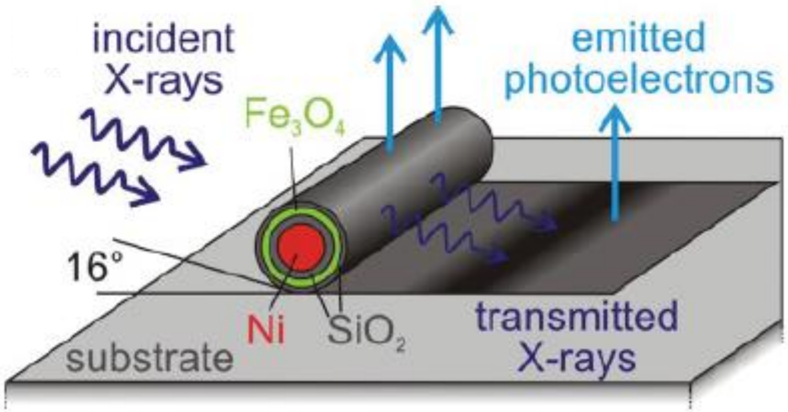

J. Kimling, F. Kronast, et al., PRB **84,** 174406 (2011)

Probing bulk and surface in coaxial nanomagnets

Iron oxide tube partially
filled with a nickel core (SEM)

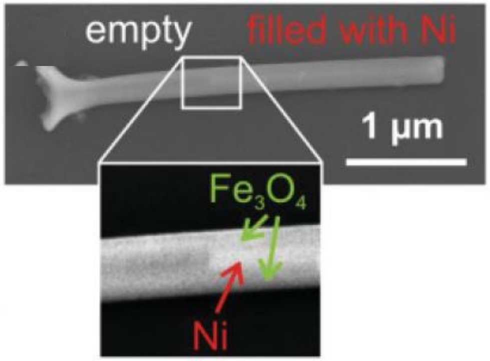

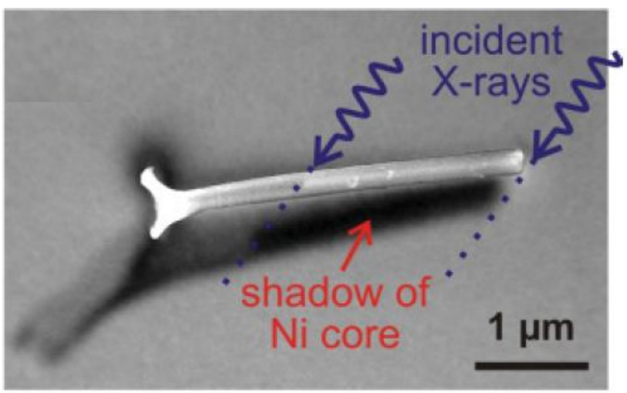

XAS spectra recorded on the wire (A),
In the shadow of the empty tube (B)
In the shado of the Ni core (C)

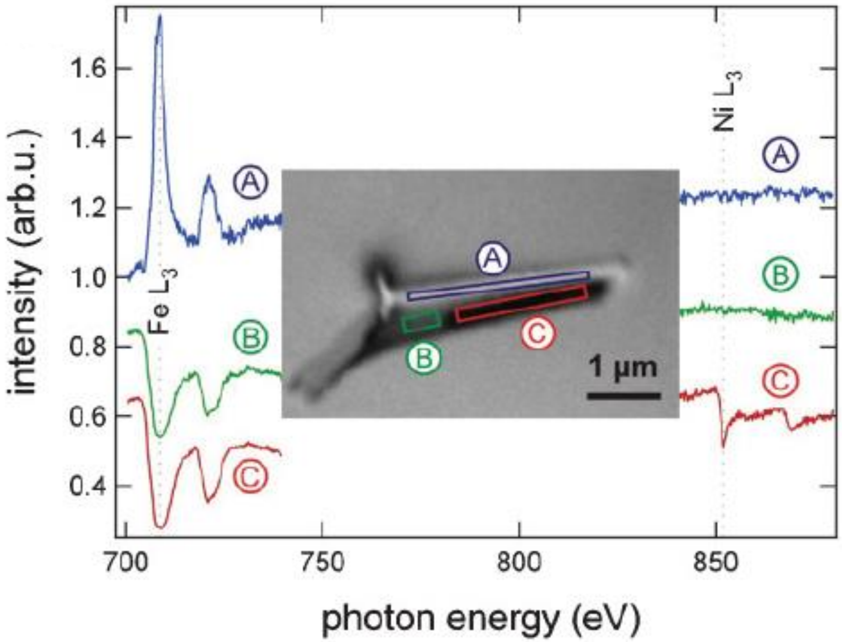

J. Kimling, F. Kronast, et al., PRB **84,** 174406 (2011)

Magnetization reversal in coaxial nanomagnets

PEEM image / Iron L_3 edge

magntic contrast

(measured in remanence after applying different field values)

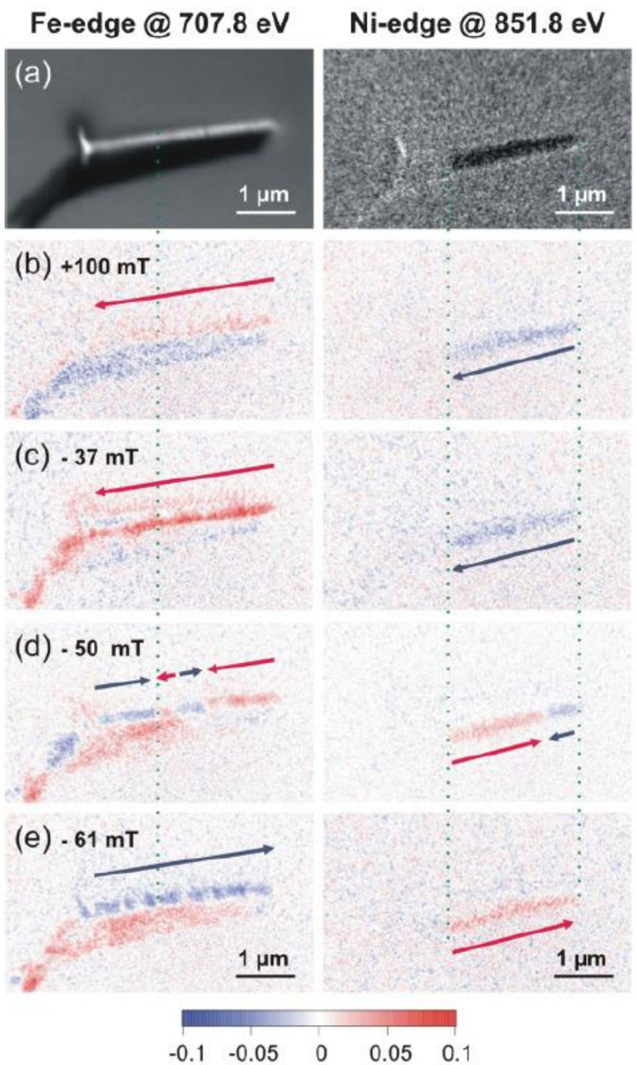

Ni L_3 edge

parallel state

Fe_3O_4 tube magnetization tilted

multi-domain state

parallel state

J. Kimling, F. Kronast, et al., PRB **84,** 174406 (2011)

Ni core: low magnetic anisotropy –
dominant shape anisotropy
magnetic moments align along the axis
magnetization reversal by domain wall motion

Fe_3O_4 tube: competition between
magentostatic energy, exchange energy,
and magnetocrystalline anisotropy

Magnetostatic energy pref
magnetization curling radially

Exchange energy prefers
magnetization parallel to the Ni core

Fe3O3 tube magnetization

virgin state saturated state

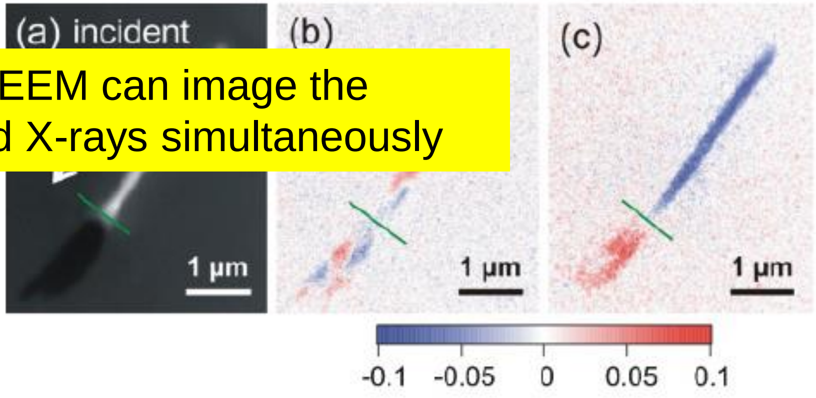

In 3d nanostructures PEEM can image the surface and transmitted X-rays simultaneously

J. Kimling, F. Kronast, et al., PRB **84,** 174406 (2011)

Magnetic patterns in ferromagnetic tubes

SEM

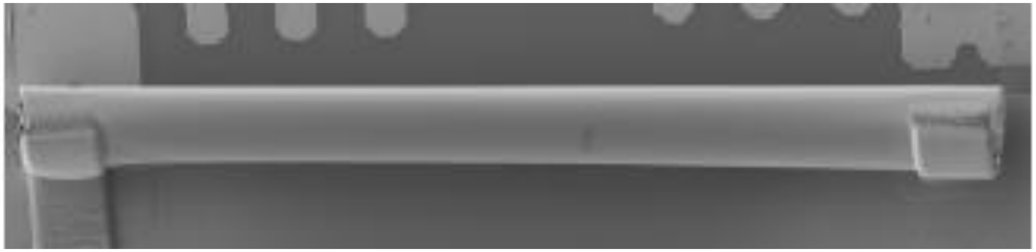

Strain engineering

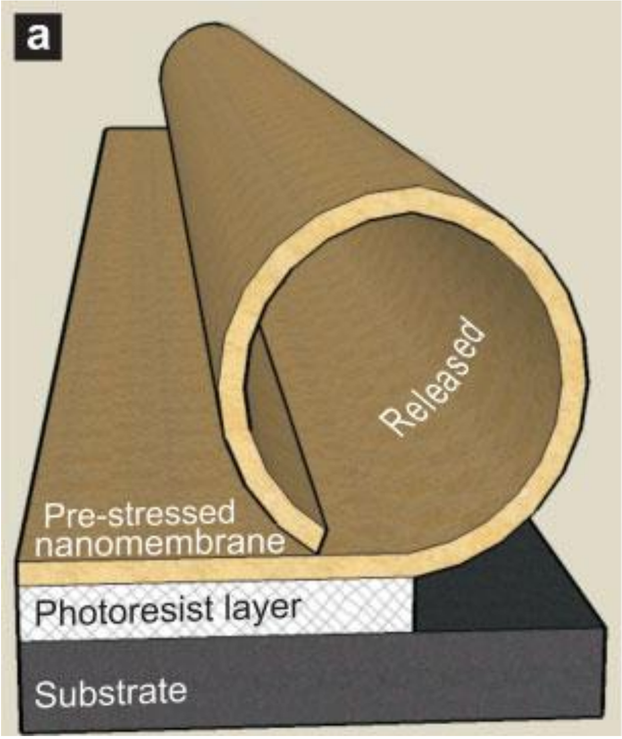

Mei et al., *Adv. Mater.* **20**, 4085 (2008)

Kerr effect microscopy

(d) Ni – length: 100 µm; ∅ = 12 µm

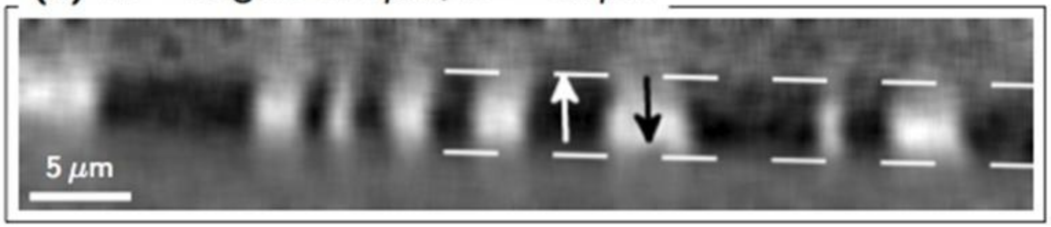

Azimuthal 180deg domains

Streubel, DM et al., *Adv. Mat.* **26**, 316 (2014)

Streubel, DM et al., *SPIN* **3**, 1340001 ('13) & *Adv. Mat.* **26**, 316 ('14) & *Nano Lett.* **14**, 3981 ('14)

IFW DRESDEN INSTITUTE FOR MAGNA INTEGRATIVE NANOSCIENCES

Magnetic patterns in ferromagnetic tubes

SEM

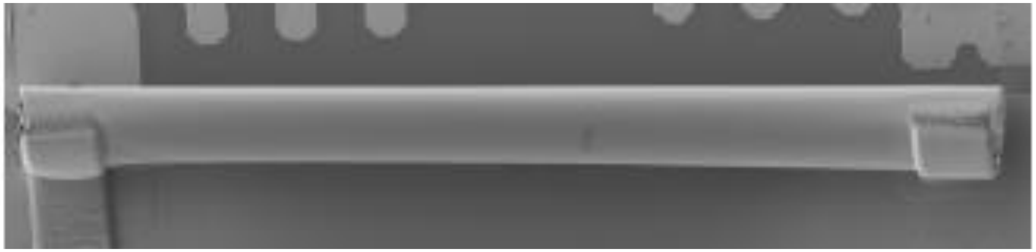

Compact sensorics for magneto-encephalography

Human – Machine interface

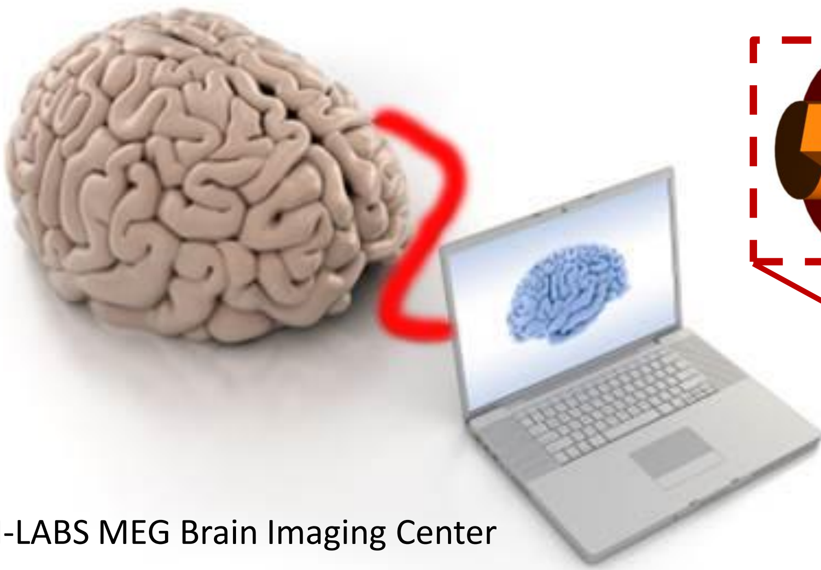

GMI⇔ SQUID

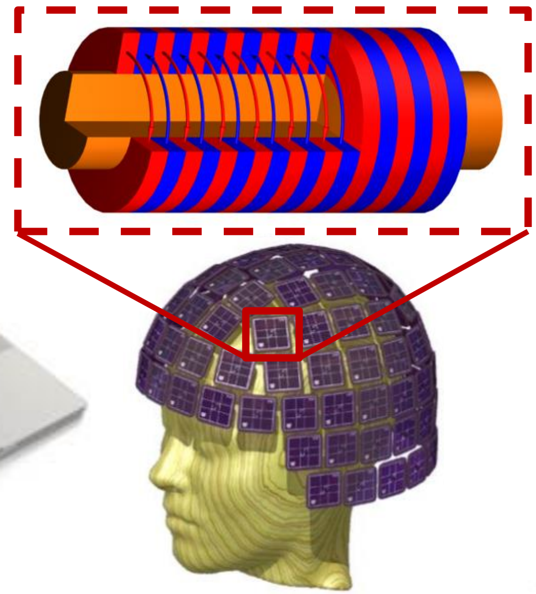

Kerr effect microscopy

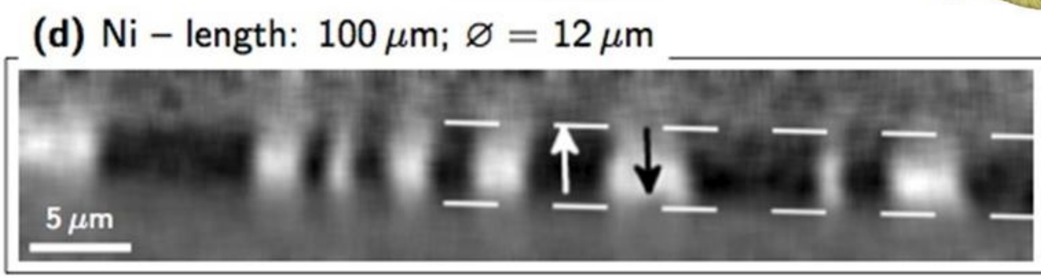

Azimuthal 180deg domains

Streubel, DM et al., *Adv. Mat.* **26**, 316 (2014)

IFW DRESDEN INSTITUTE FOR MAGNA INTEGRATIVE NANOSCIENCES

Collaboration: R. Schäfer (IFW-IMW); F. Kronast (BESSY II); P. Fischer (ALS Berkeley)

Magnetic patterns in ferromagnetic tubes

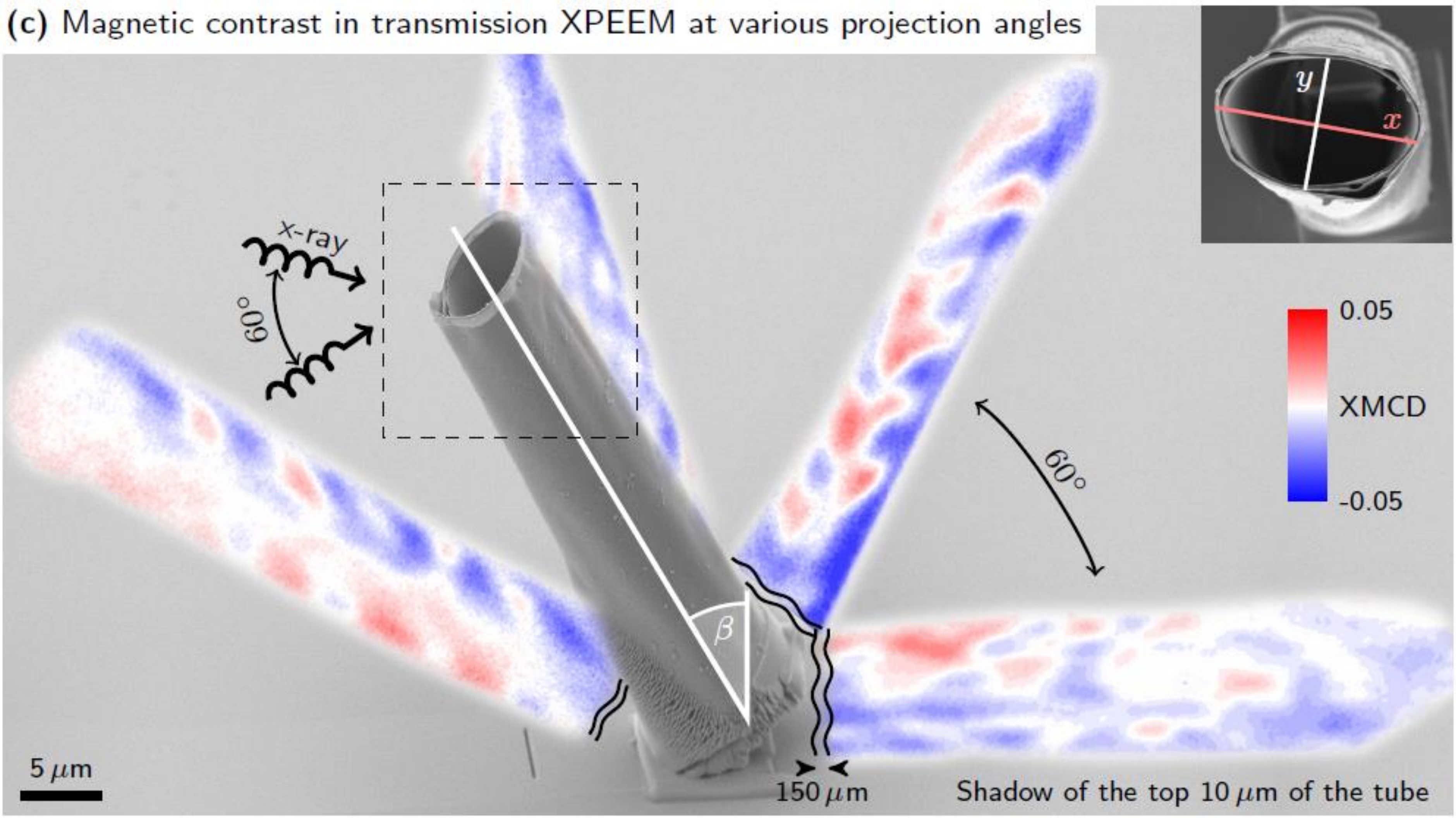

R. Streubel, F. Kronast, et al, Nat. Comm. accepted (2015)

Modeling the XPEEM shadow contrast

- ❑ Considering azimuthal and helical magnetization
- ❑ Precise spatial orientation of tube
- ❑ Angle series reveals distinguishable features

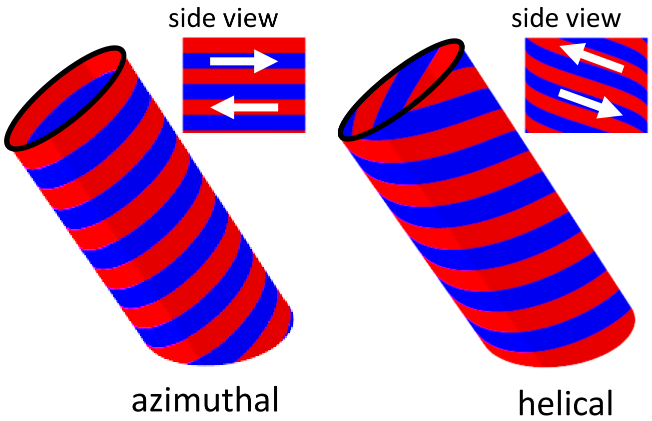

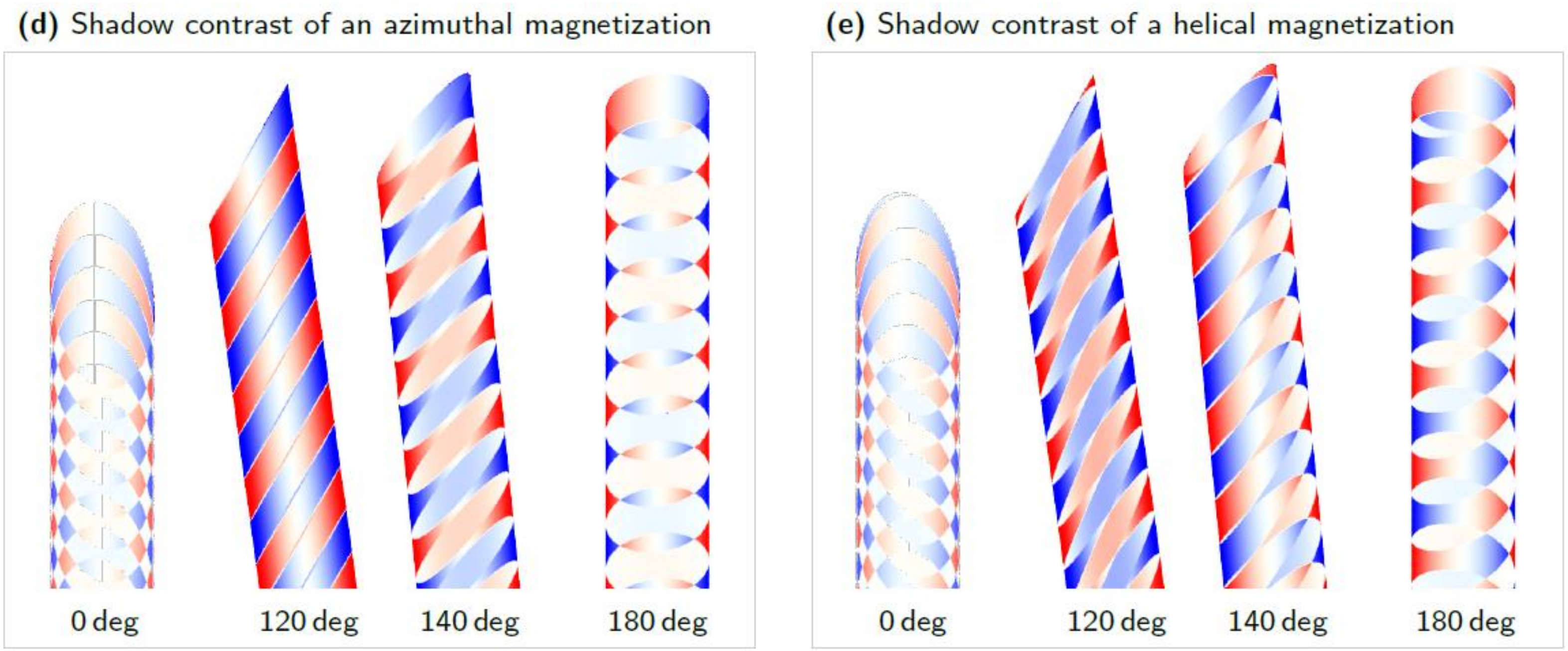

R. Streubel, F. Kronast, et al, Nat. Comm. accepted (2015)

IFW DRESDEN Institute for MAGNA Integrative Nanosciences

Modeling the XPEEM shadow contrast

- ❑ Considering azimuthal and helical magnetization
- ❑ Precise spatial orientation of tube
- ❑ Angle series reveals distinguishable features

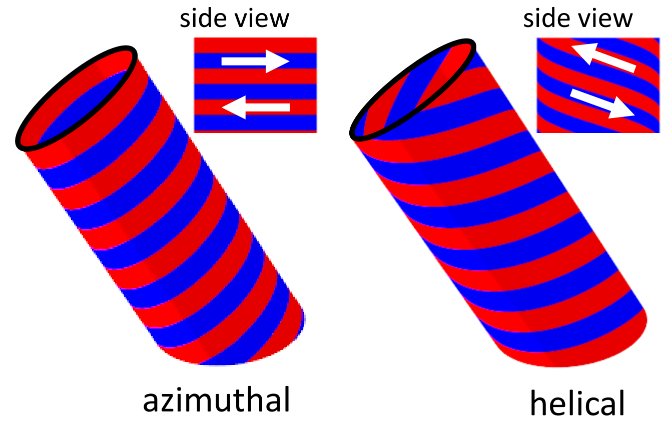

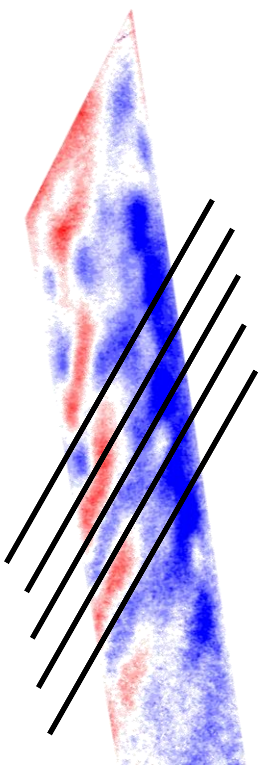

120 deg

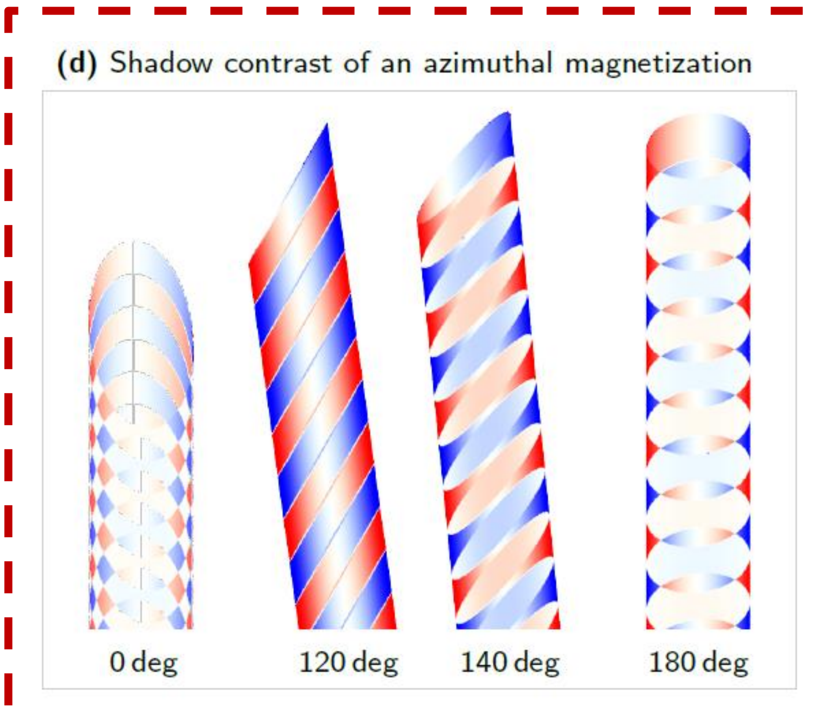

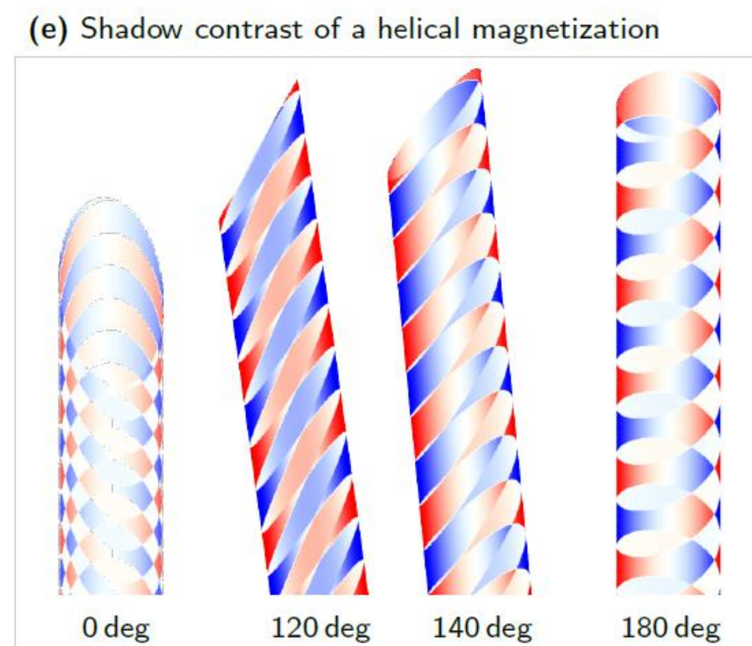

R. Streubel, F. Kronast, et al, accepted at Nat. Comm. (2015)

IFW DRESDEN INSTITUTE FOR MAGNA INTEGRATIVE NANOSCIENCES

Magnetic Soft X-ray Computed Tomography

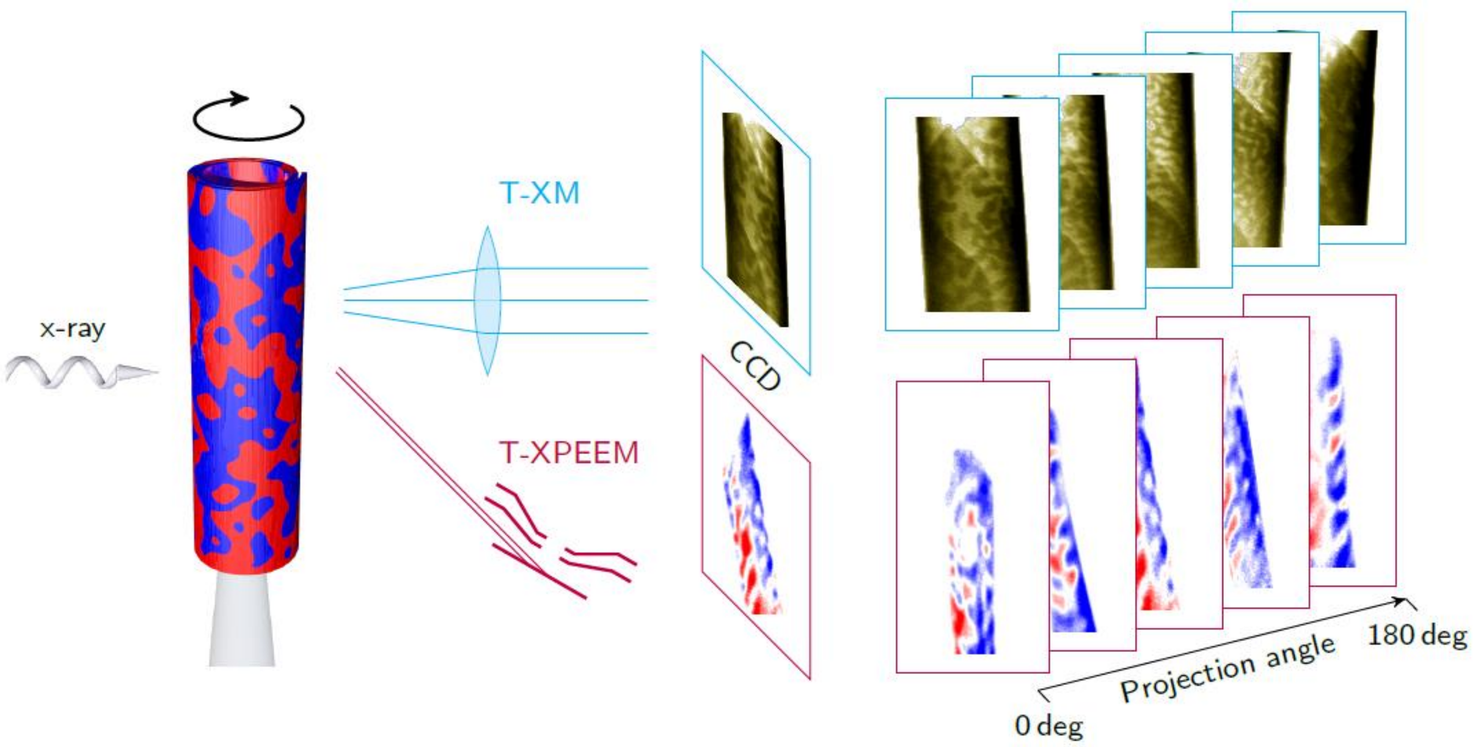

- ❑ Proper choice of sample for development of measurement technique
- ❑ Post-processing of acquired data (development of reconstruction algorithm)
  - ○ Accounting vector properties of magnetization

outline

Nanoparticles and 3d objects

-> Thin films and wedge profiles

- Exchange bias
- Phase transition

XPS PEEM & SW excitation

PEEM with laser excitation

Exchange Bias

Applications

- Permanent magnets
- Hard disk drives
- Magnetic random access memories
- …

Challenges

- Understand its microscopic origin
- Influence of finite size effect
- Training effects
- Access to the AFM-FM interface
- …

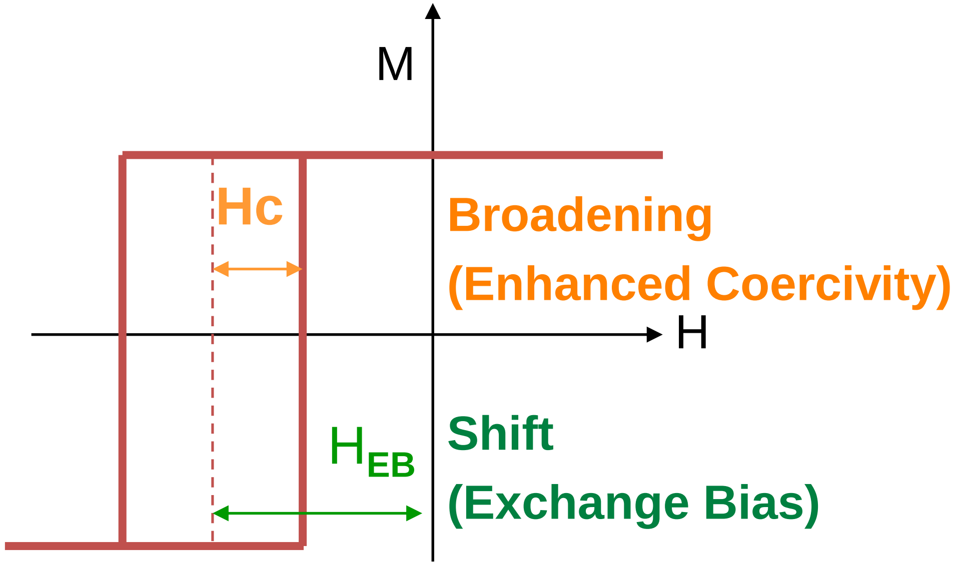

Magnetic interaction exerted by the antiferromagnet (AFM) onto the ferromagnet (FM)

⇓

Only **one** stable configuration for the direction of the FM magnetization

Magnetic switching of the Co layer

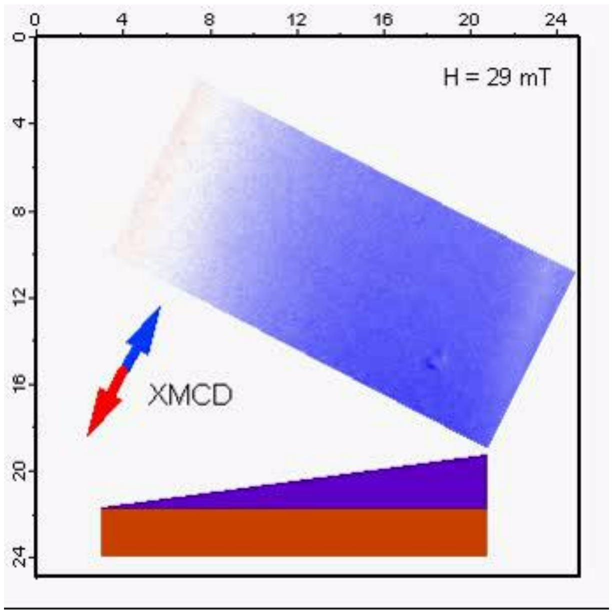

25 μm field of view

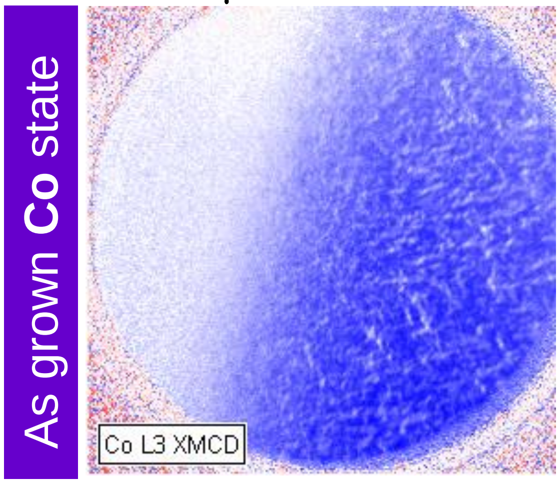

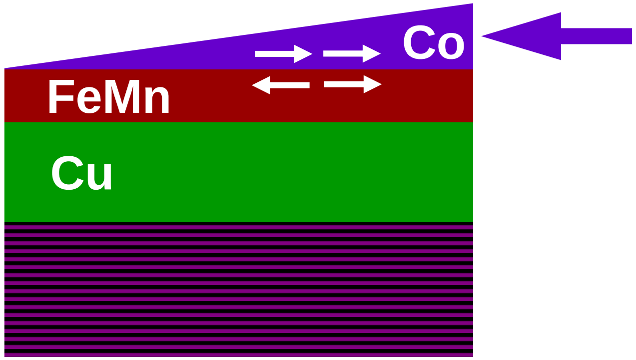

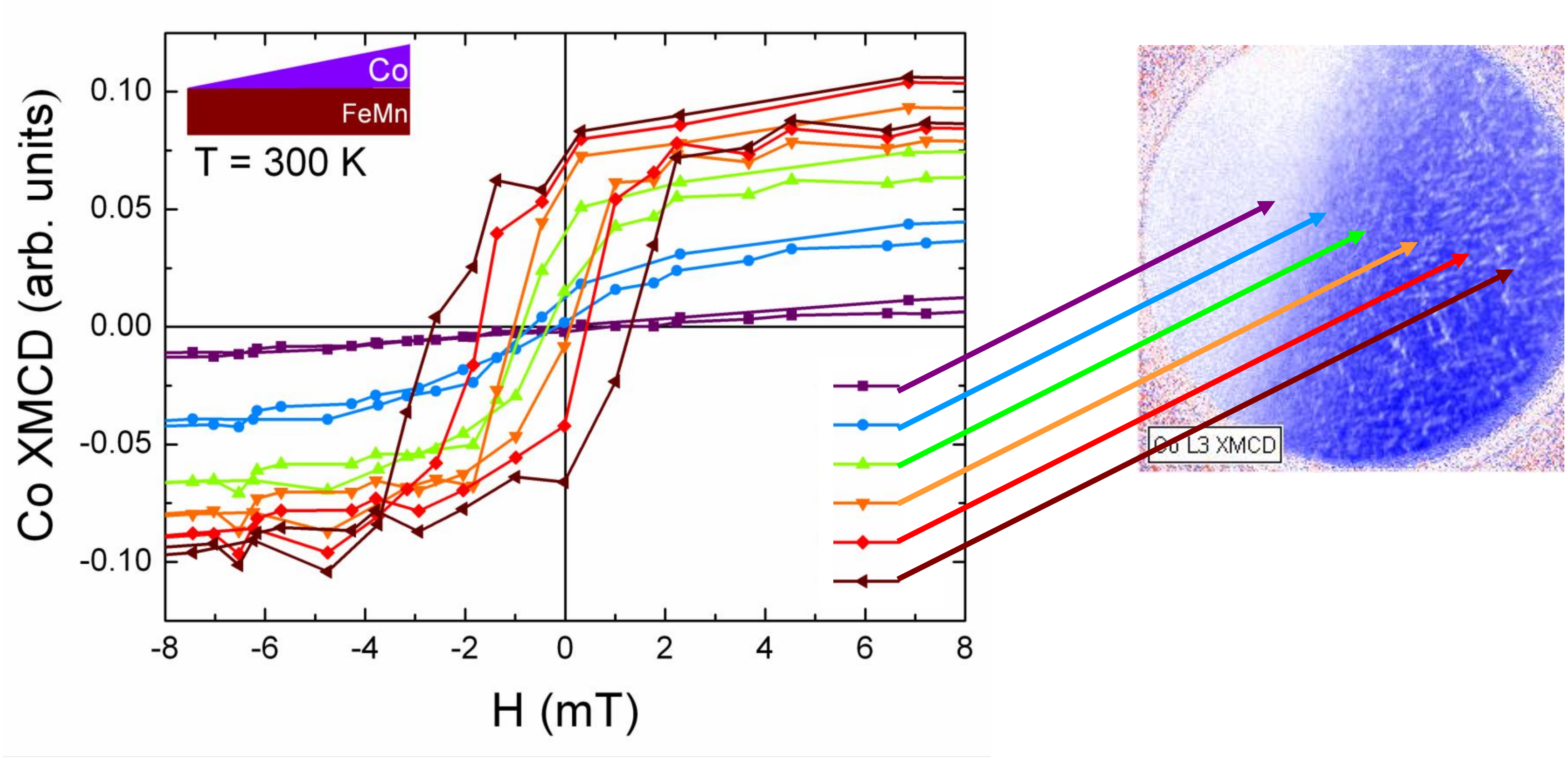

Hysteresis loops of individual pixels

…to calculate the lateral distribution of coercivity & exchange bias

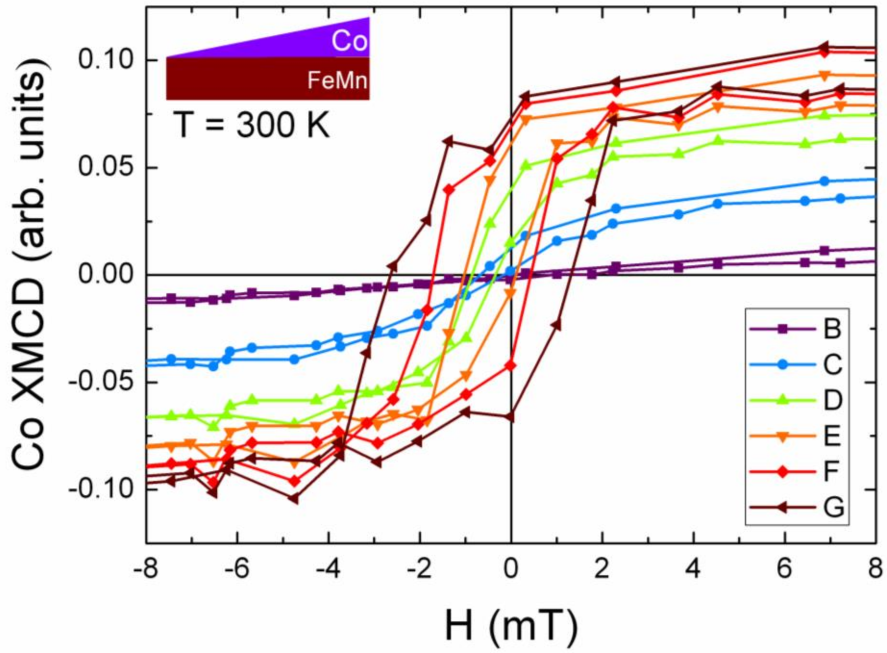

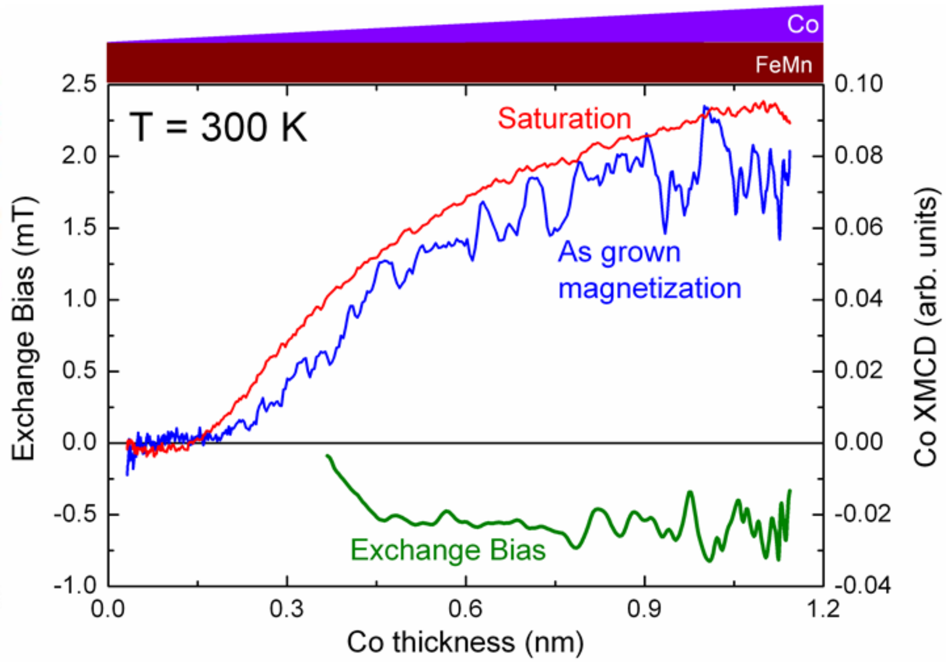

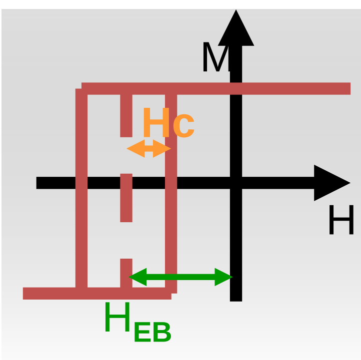

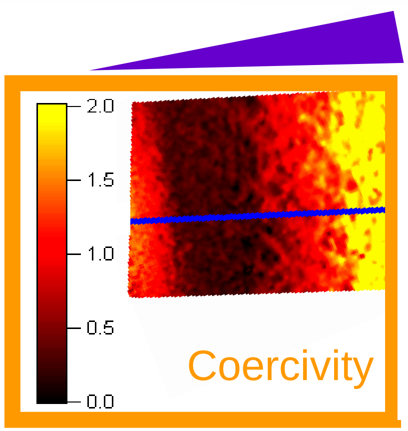

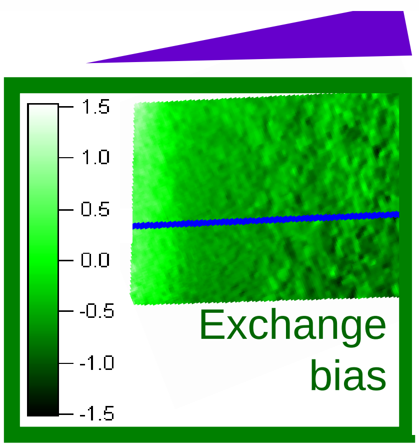

J. Herrero-Albillos, F. Kronast, L. Bismaths, C. Papp, and C. Fadley, unpublished

Imprinting of ferromagnetic domains

• Domain pattern in the Co layer

(as grown Co magnetization far from saturation)

⇒ Small Exchange Bias.

• Exchange bias mimics the as grown Co magnetization:

Imprinted FM domains on the AMF layer

Coercivity

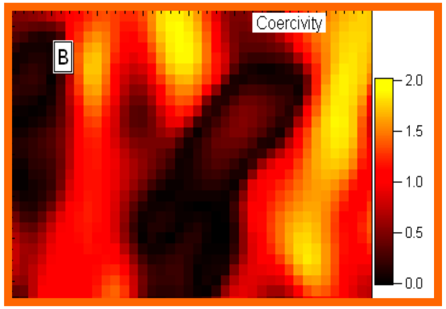

Magnetization

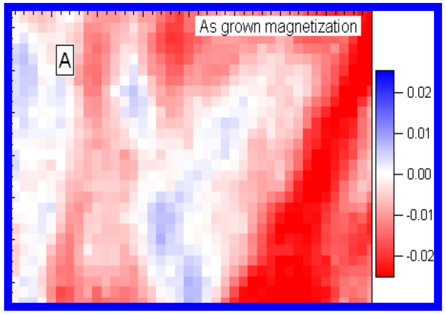

Exchange bias

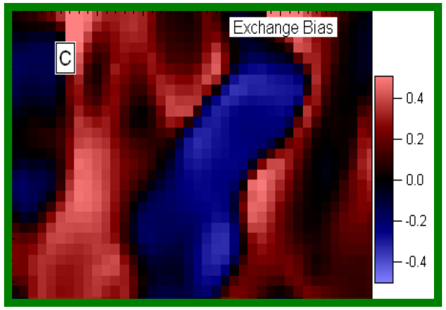

temperature-driven AF- FM phase transition in FeRh thin films

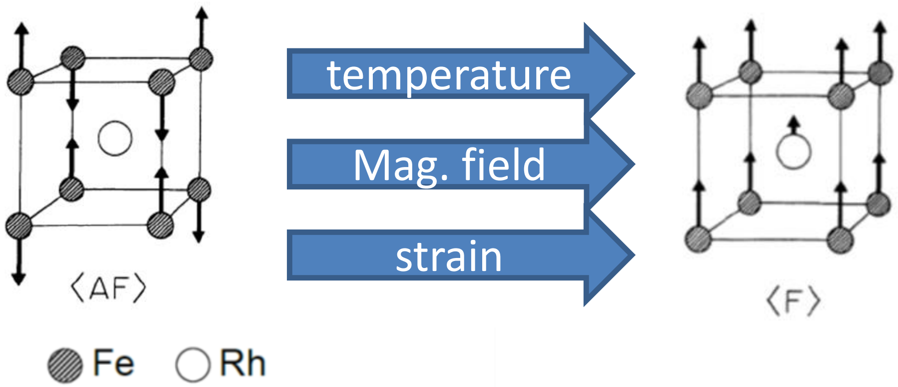

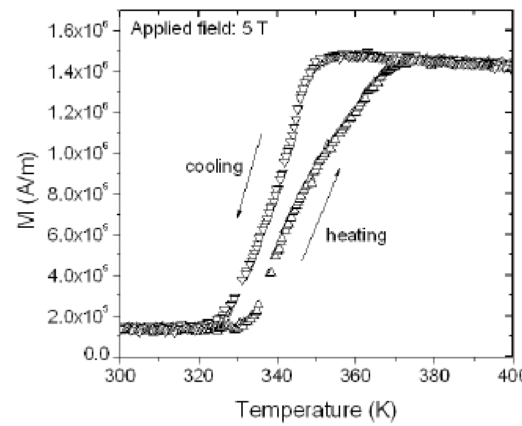

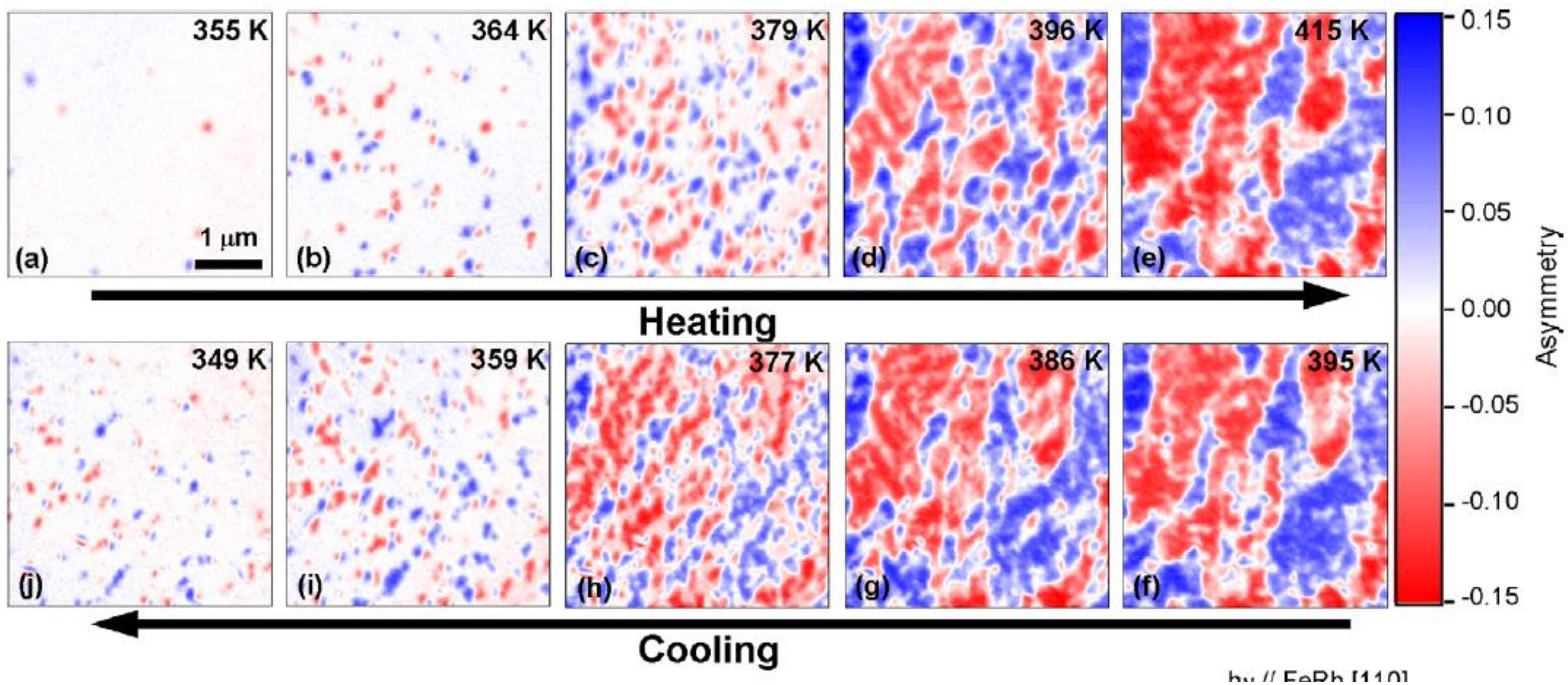

Baldasseroni et al. APL 100, 262401 (2012)

Using strain and charge from ferroelectric BaTiO3 to control the magnetic phase of FeRh

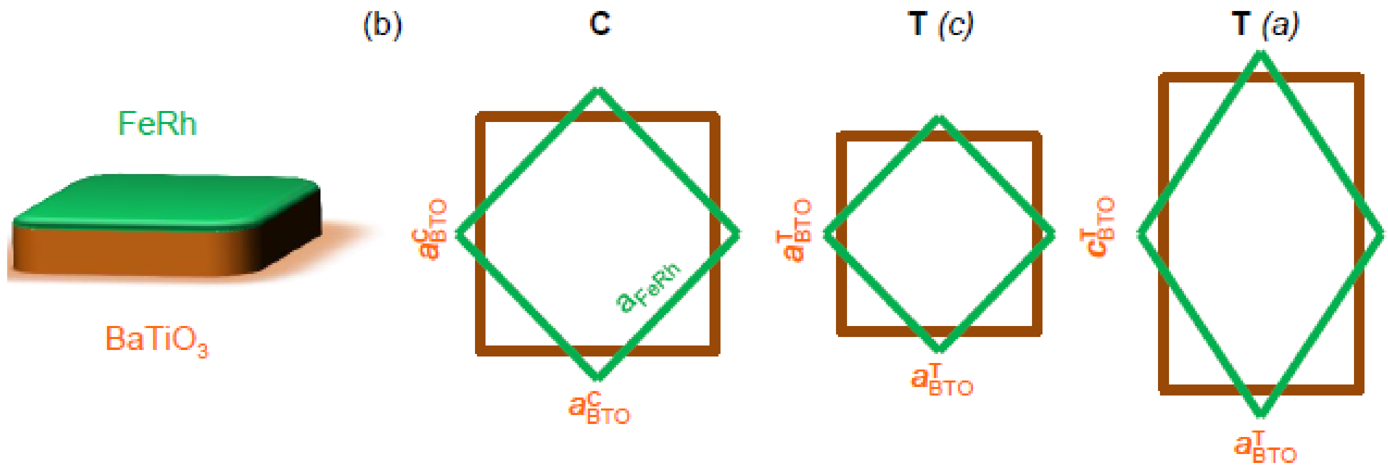

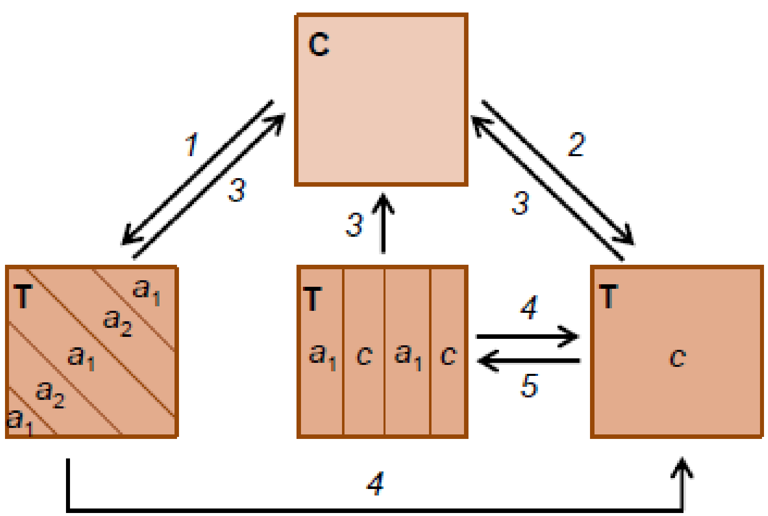

1 - cool through T_c without V

2 - cool through T_c in applied V

3 - heat through T_c

4 - apply V

5 - remove V

Electric field / strain controlled AF/FM phase transition on FeRh

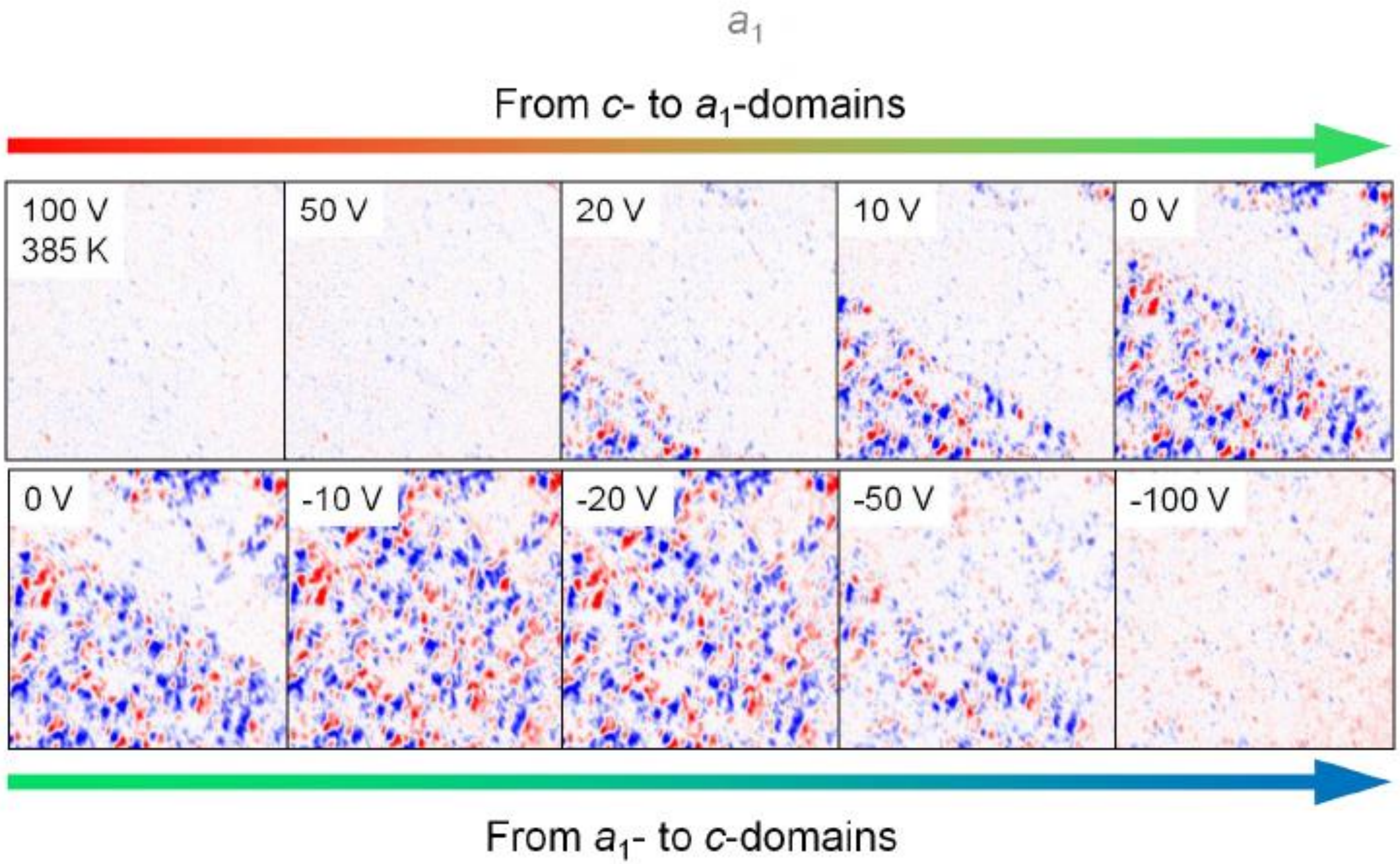

L.C.Phillips et al., Nature Scientific Reports, 5, 10026 (2015)

Electric field control of magnetic properties at room temperature

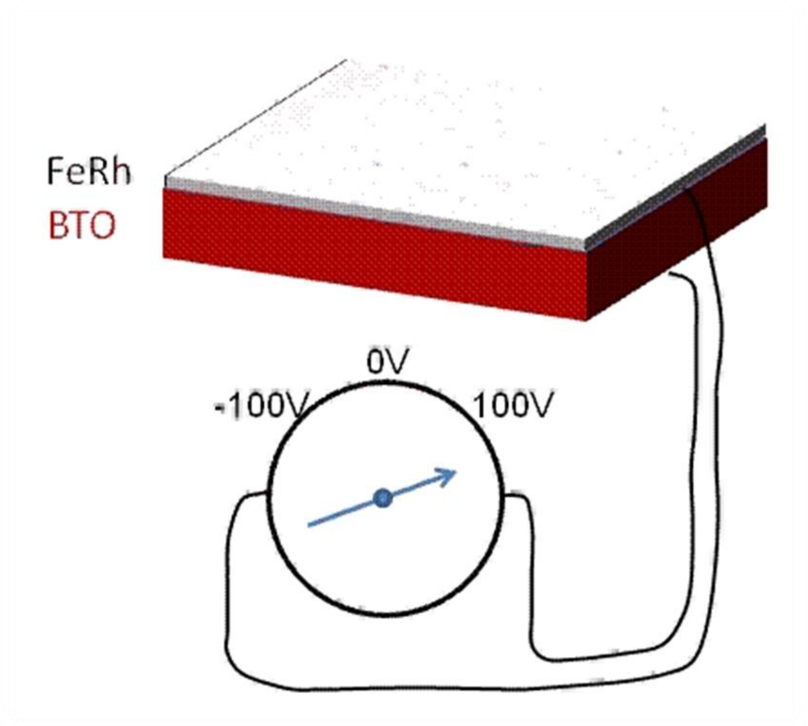

- **Electric-field controlled spintronics**
- **Multi-state data storage**
- **Low power dissipation**

R. O. Cherifi et al., Nature Materials, 13, 345-351 (2014)

Square lattice of $Pd_{0.87}Fe_{0.13}$ islands

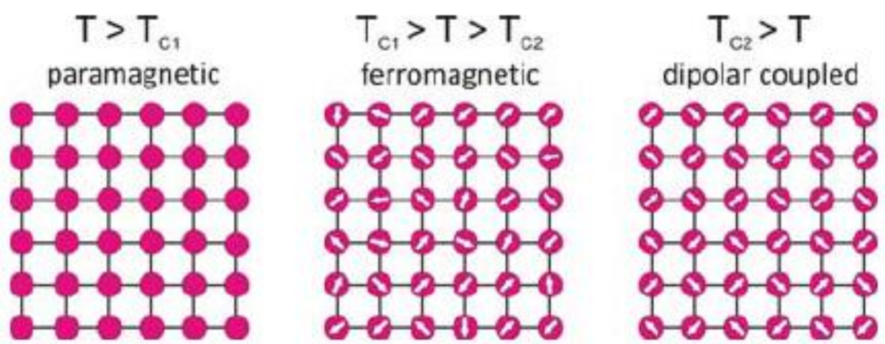

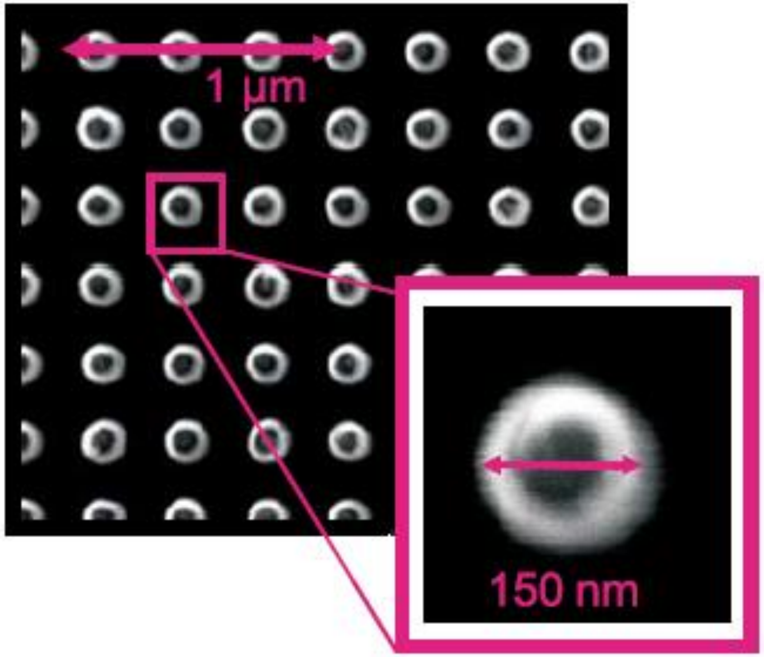

Ewerlin et al. PRL 110, 177209 (2013)

Two-step phase transition

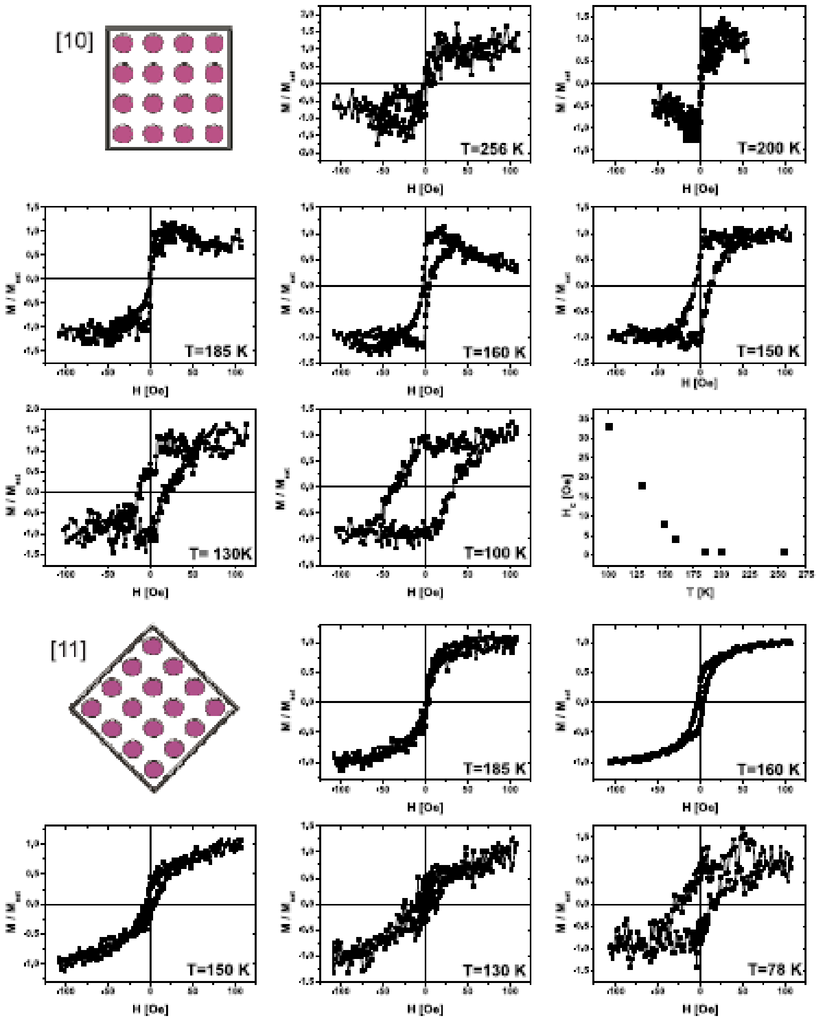

Tc = 260K
Pole interaction ~ 160K

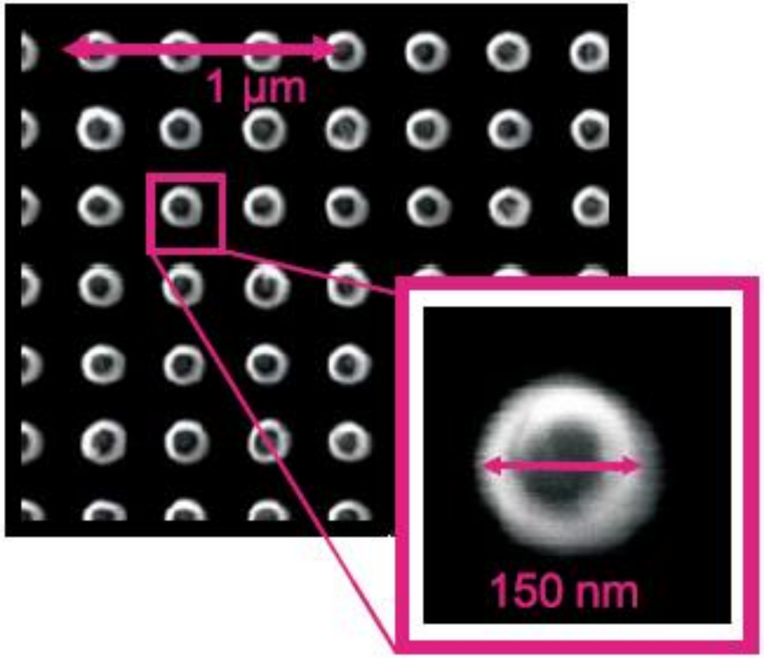

Ewerlin et al. PRL 110, 177209 (2013)

Higher pole interaction lead to the formation of Characteristic string patterns.

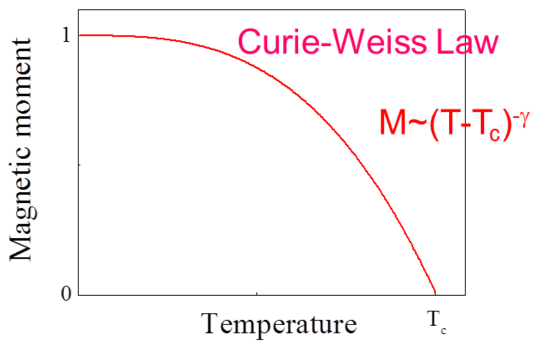

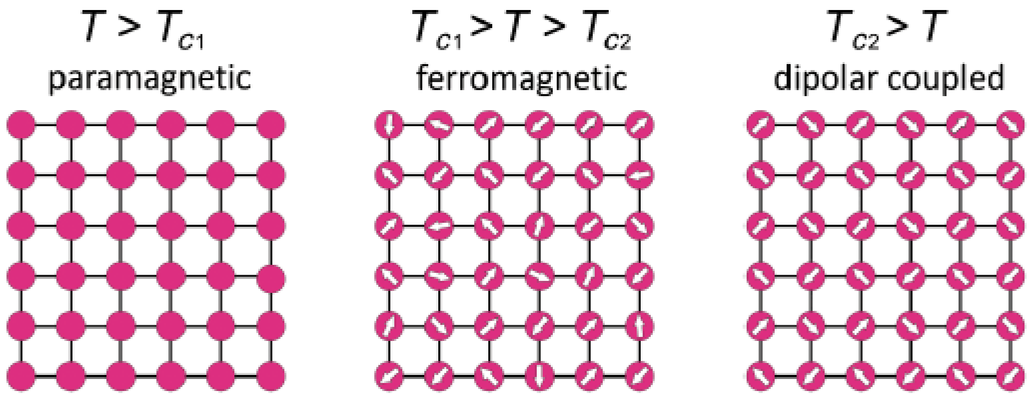

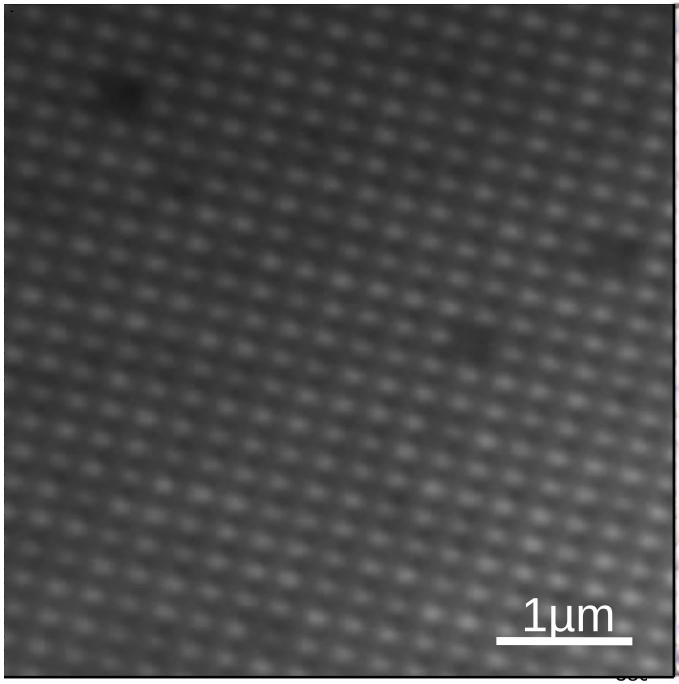

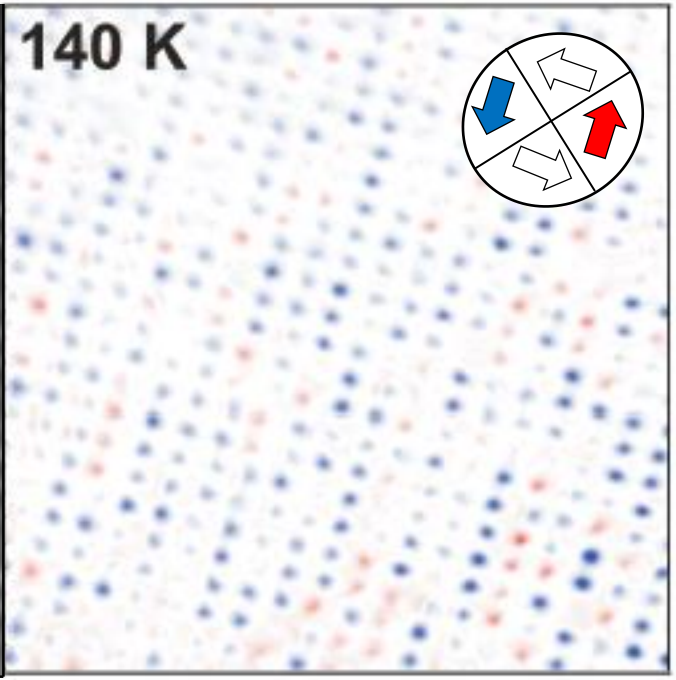

Ewerlin et al. PRL 110, 177209 (2013)

Spatially resolved measurements of AC-susceptibility

Synchronizing the camera with an alternating magnetic field

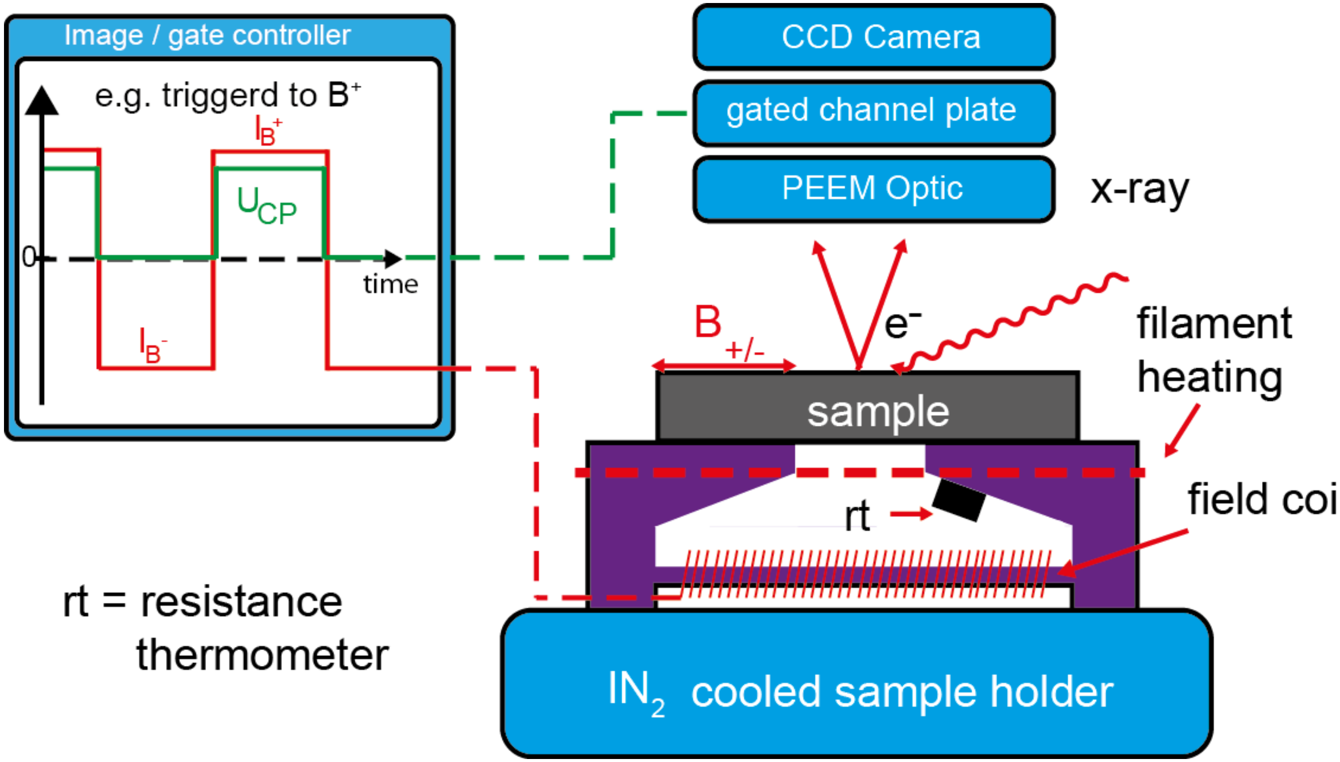

rt = resistance thermometer

F. M. Römer, F. Kronast, et al., *Appl. Phys. Lett. 96, 122501 (2010)*

Observing T_C in an epitaxial Fe wedge

Fe magnetic contrast

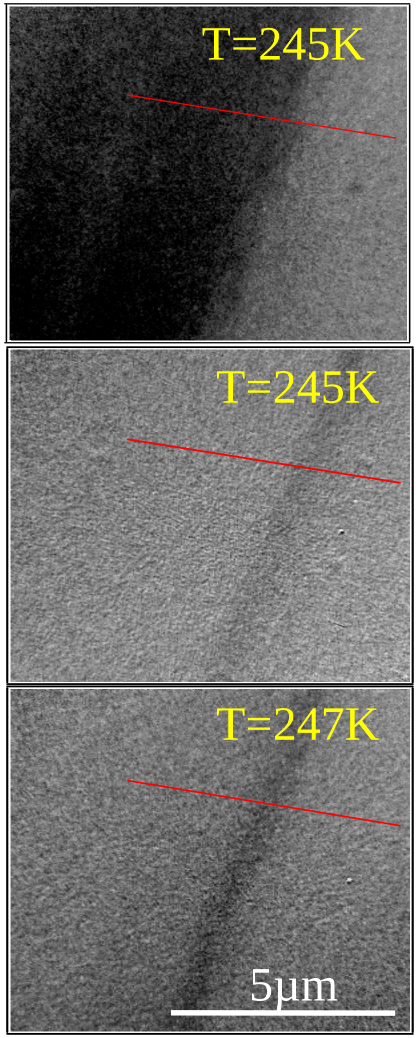

saturation magnetization

AC susceptibility

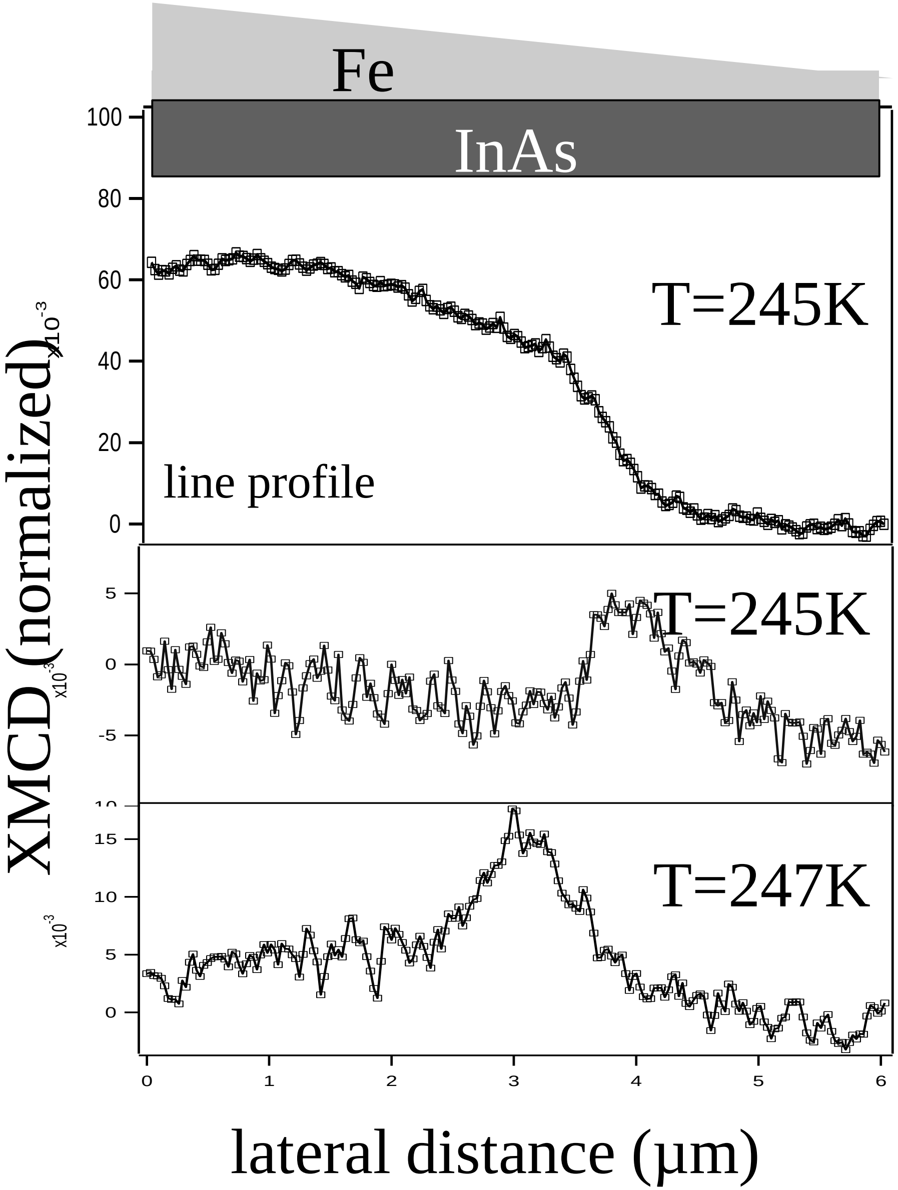

outline

Nanoparticles and 3d objects

Thin films and wedge profiles

-> PEEM with laser excitation

laser induced switching in TbFeCo, GdFeCo

XPS PEEM & SW excitation

SPEEM Laser system

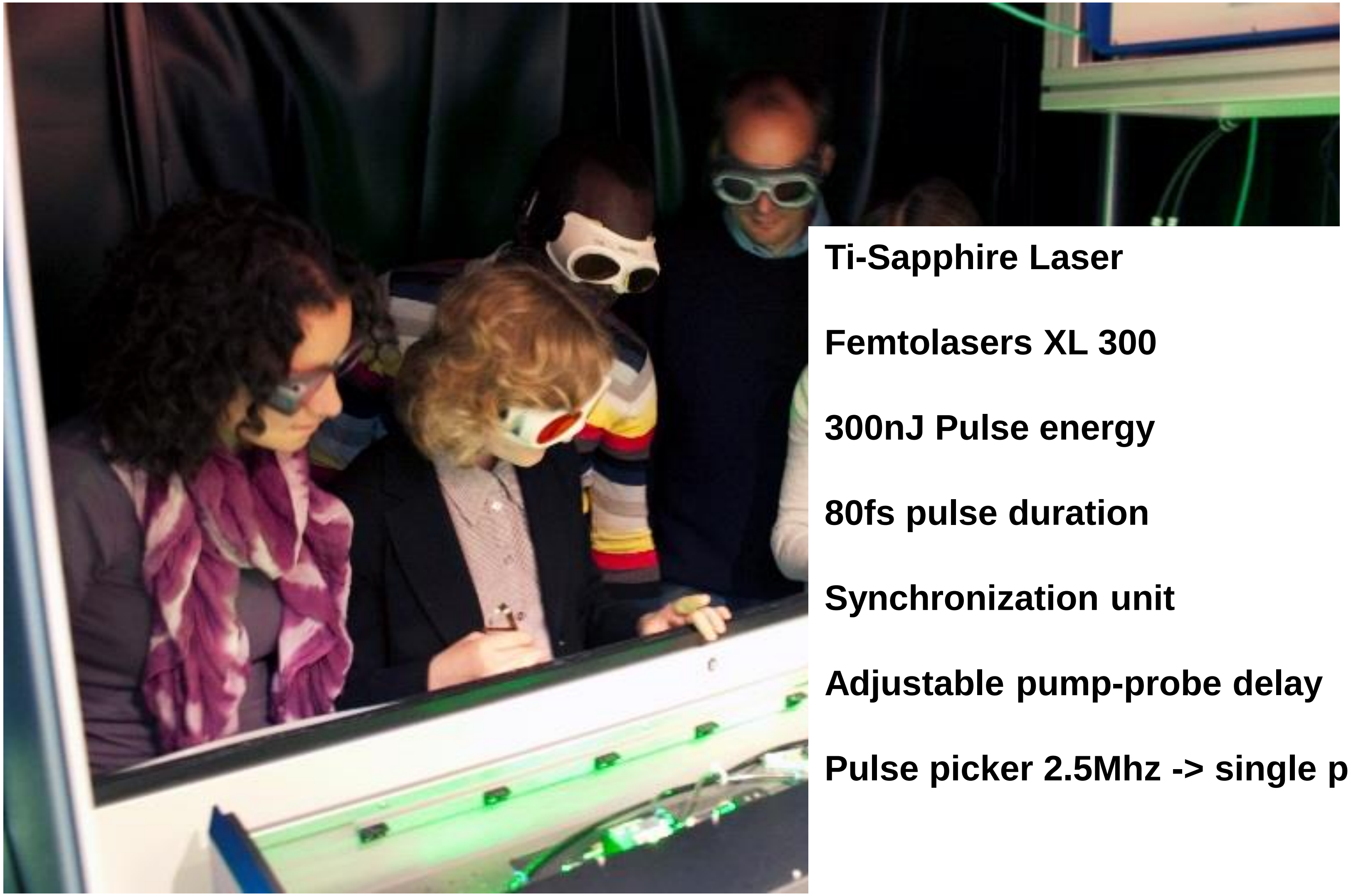

Ti-Sapphire Laser

Femtolasers XL 300

300nJ Pulse energy

80fs pulse duration

Synchronization unit

Adjustable pump-probe delay

Pulse picker 2.5Mhz -> single pulse

Experimental site at BESSY II

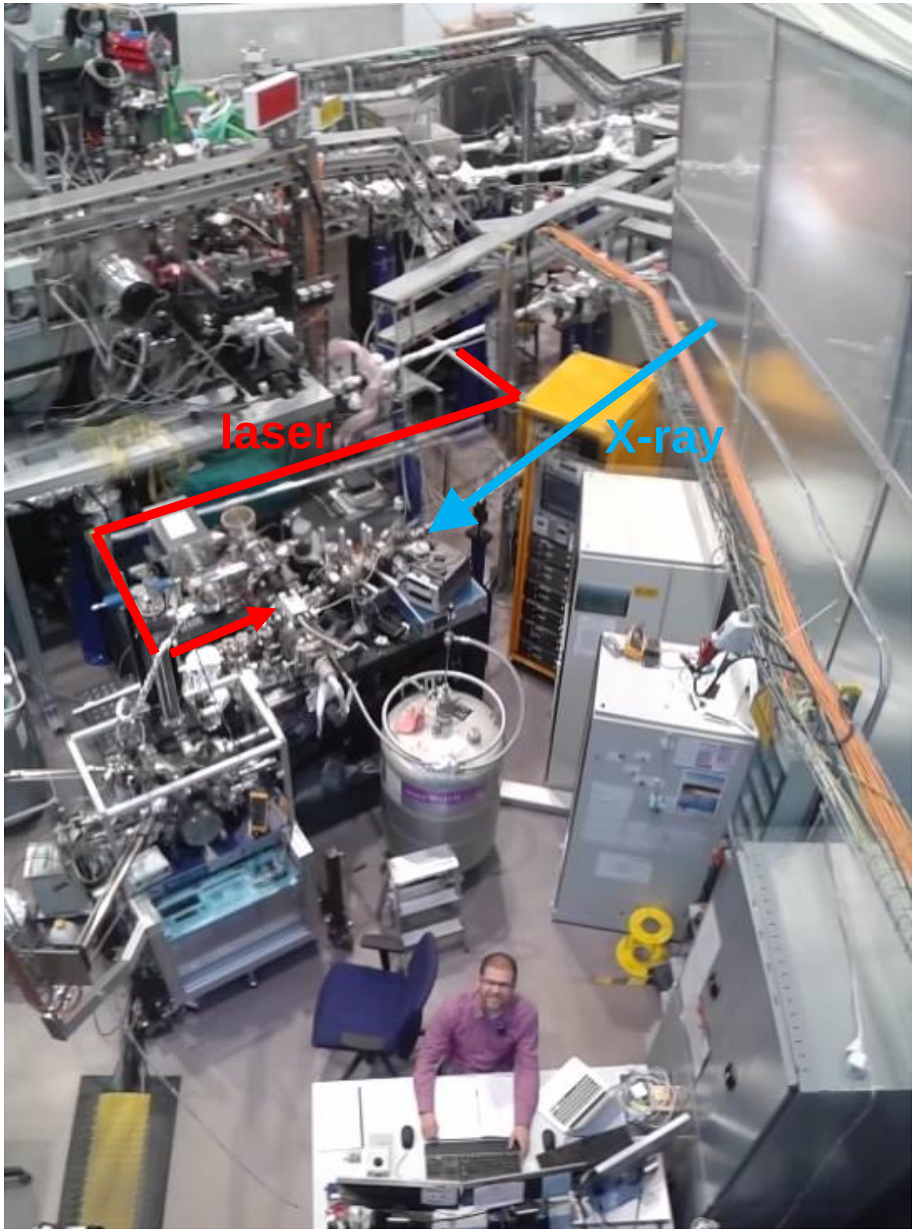

All optical switching in ferrimagnetic thin filmsTbFeCo / GdFeCo

Laser heating and the effect of circular polarization acting as effective magnetic field?

Or laser heating as a sufficient stimulus for magnetization reversal in a ferrimagnet?

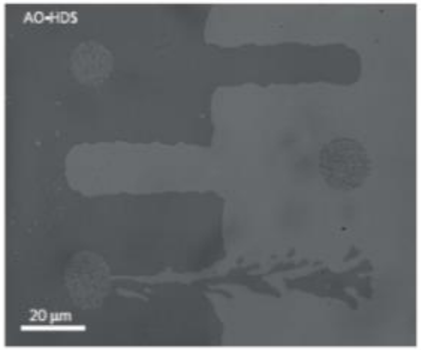

Mangin et al.,
Nature Materials DOI: 10.1038/NMAT3864 (2014)

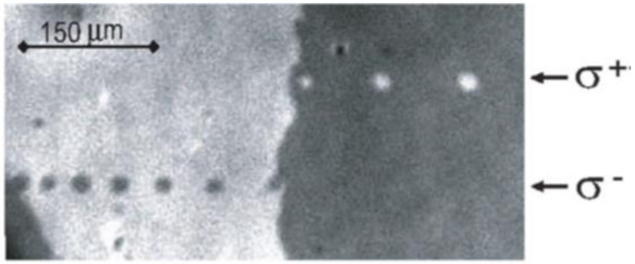

Stanciu et al.,
Physical Review Letters 99, 047601 (2007)

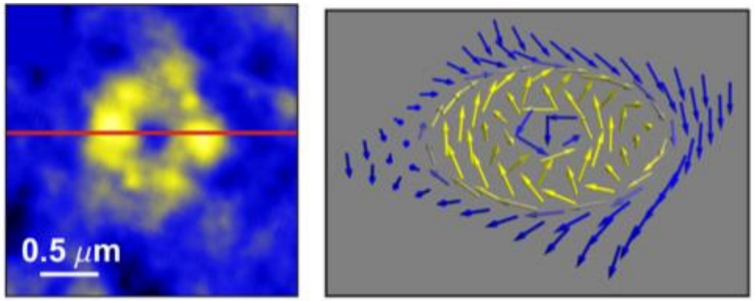

M. Finazzi et al,
Physical Review Letters 110, 177205 (2013)

Using a sample holder with integrated laser optics

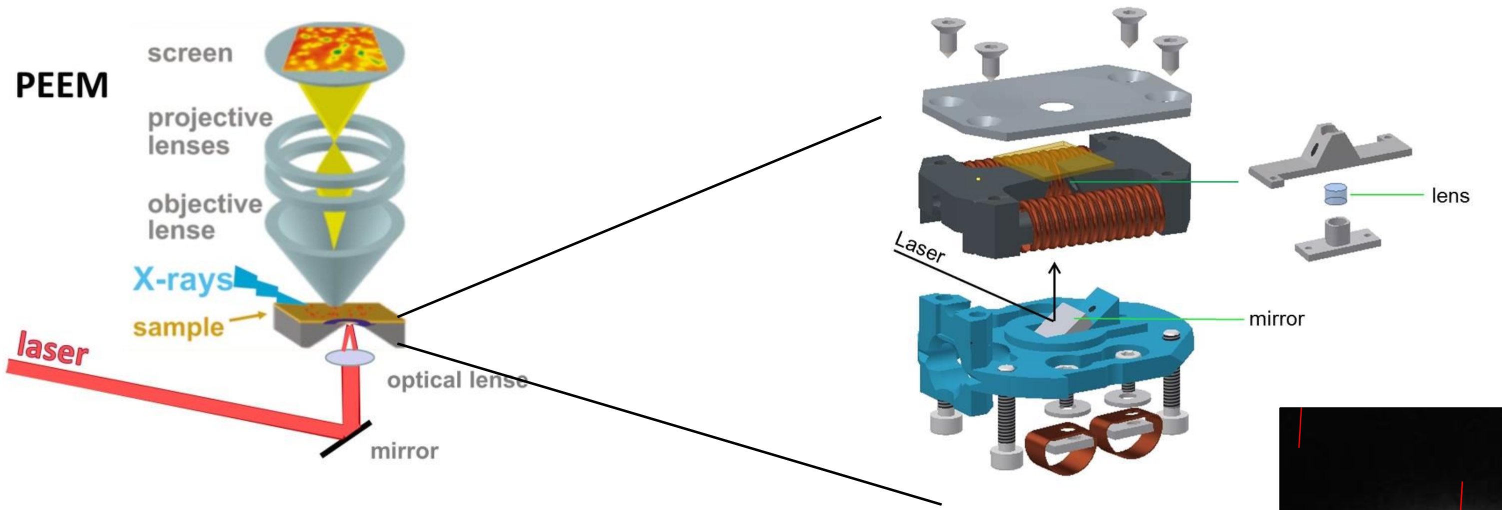

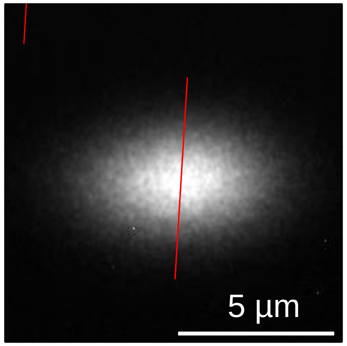

New possibilities for PEEM

Excitations of magnetic states on the micrometer-scale

Local heating -> thermomagnetic effects

Observation of plasmonic effects

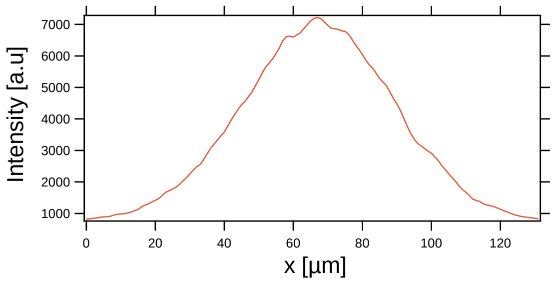

L. Gierster et al., Rev. Sci. Inst., 86, 023702 (2015)

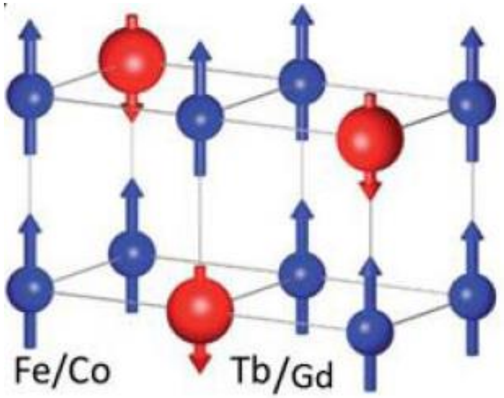
Fe/Co
Tb/Gd

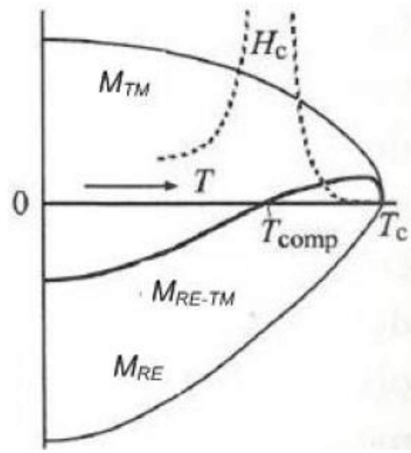
H_c
M_{TM}
T
0
T_{comp}
T_c
M_{RE-TM}
M_{RE}

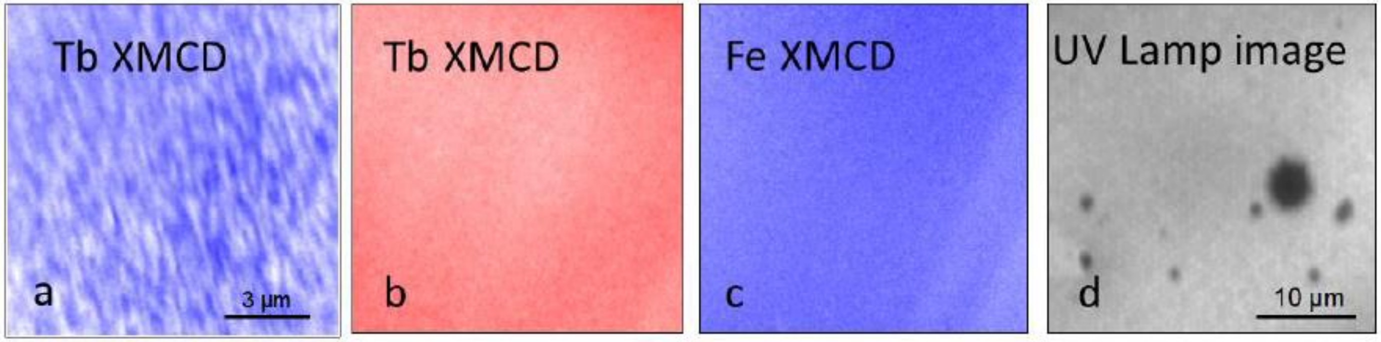
Tb XMCD
a
3 μm
Tb XMCD
b
Fe XMCD
c
UV Lamp image
d
10 μm

TbFeCo: laser induced switching with linear polarization

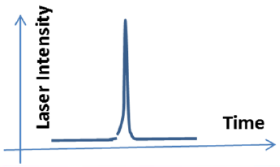

Single pulse switching / linear polarization

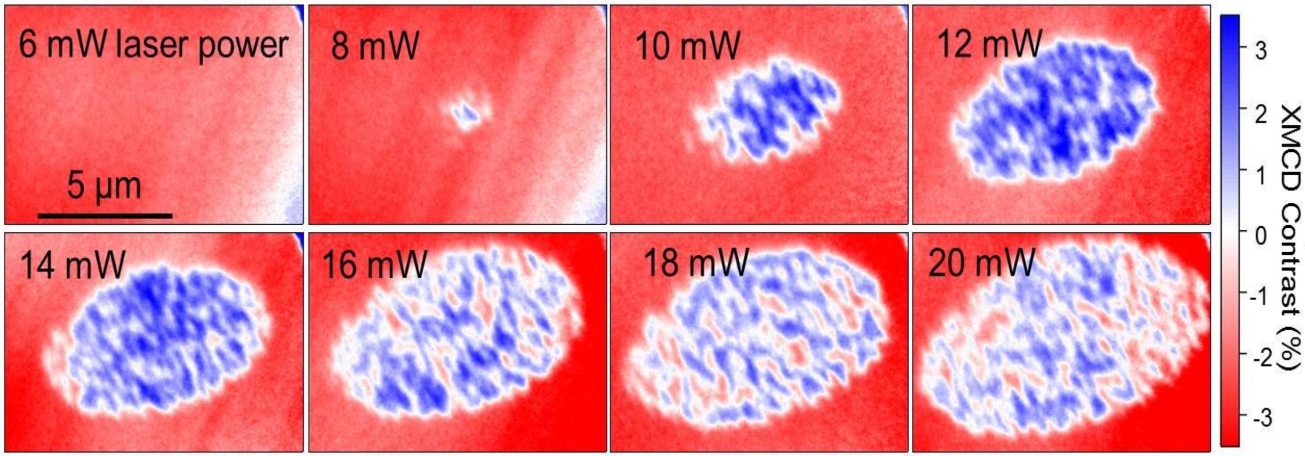

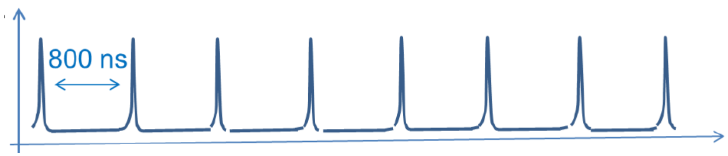

Pulse train switching / linear polarization

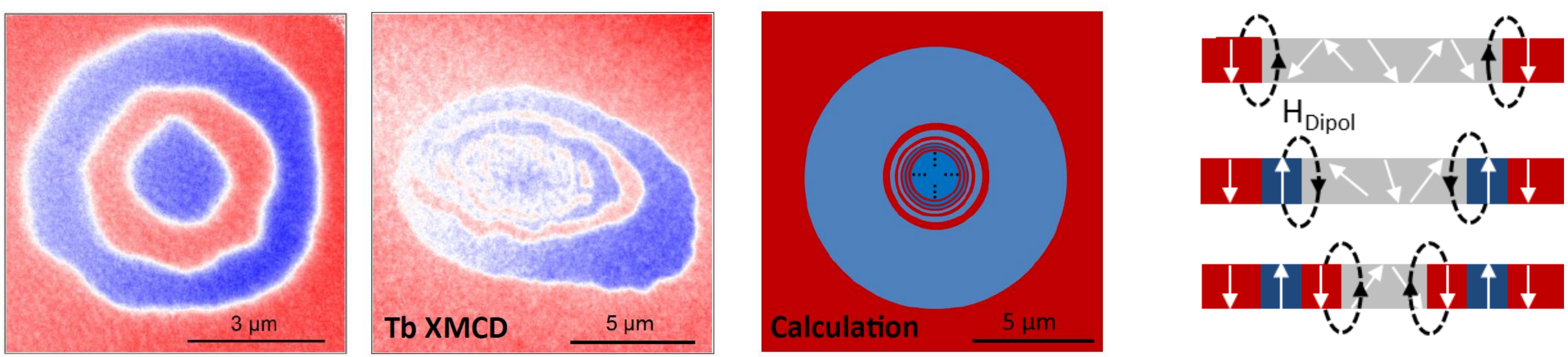

L. Gierster et al., Ultramicroscopy, (2015)

TbFeCo: laser induced switching with circular polarization

Measurement during excitation by circularly polarized laser pulses

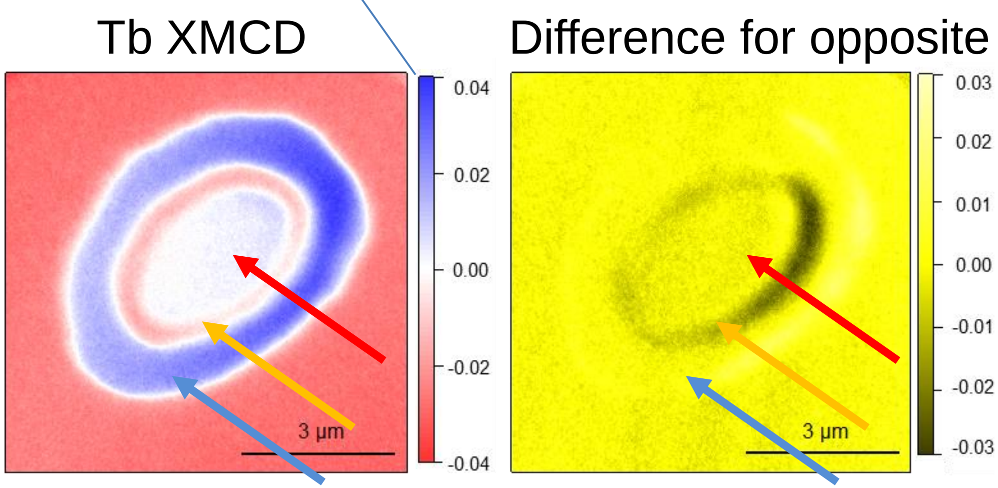

Three regions:

Inner area: thermally demagnetized

Outer circle: switched by dipolar fields

Ring-shaped region in between:
helicity dependent switching

L. Gierster et al., Ultramicroscopy, (2015)

Stroboscopic pump-probe setup for time-resolved x-ray microscopy

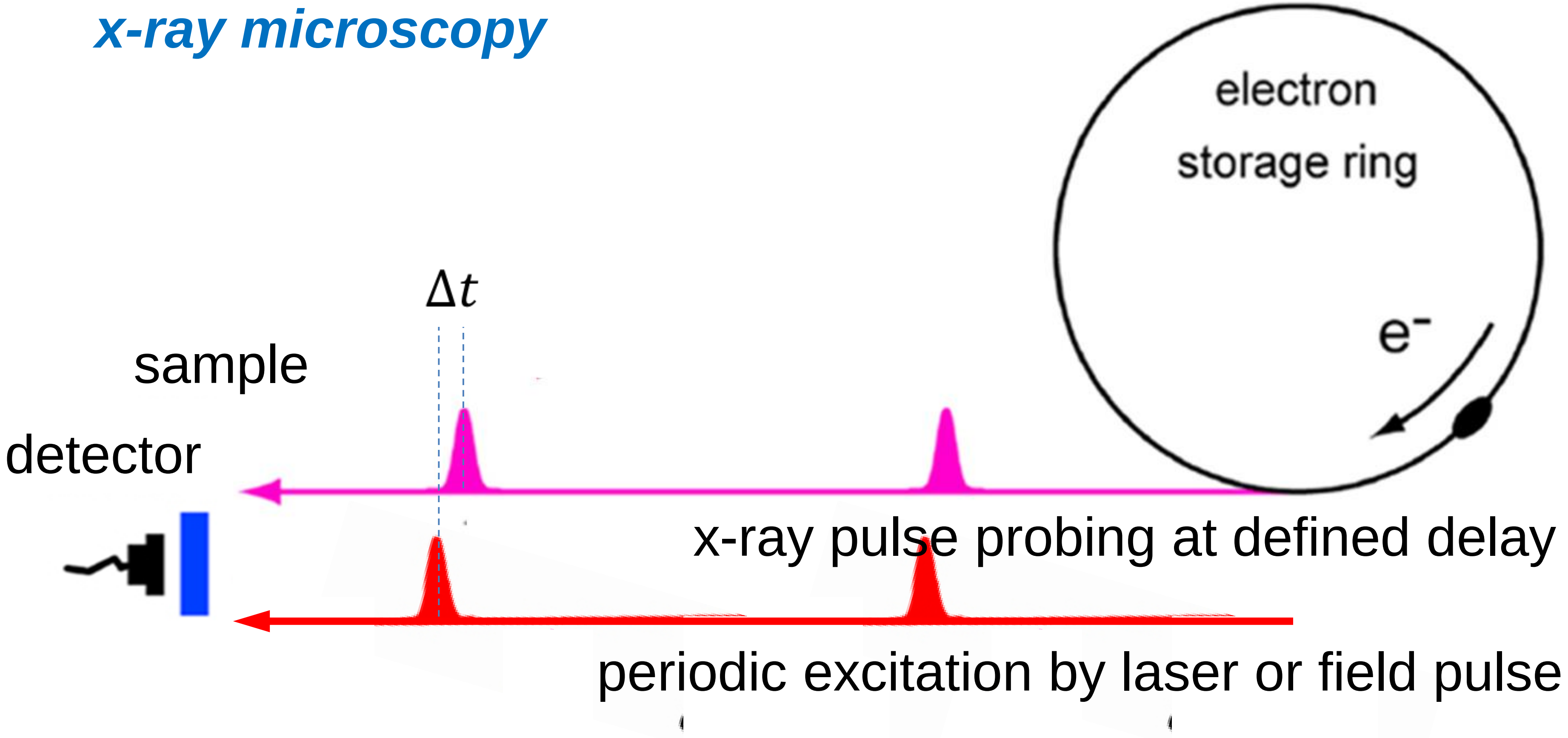

Stroboscopic pump-probe setup for time-resolved x-ray microscopy

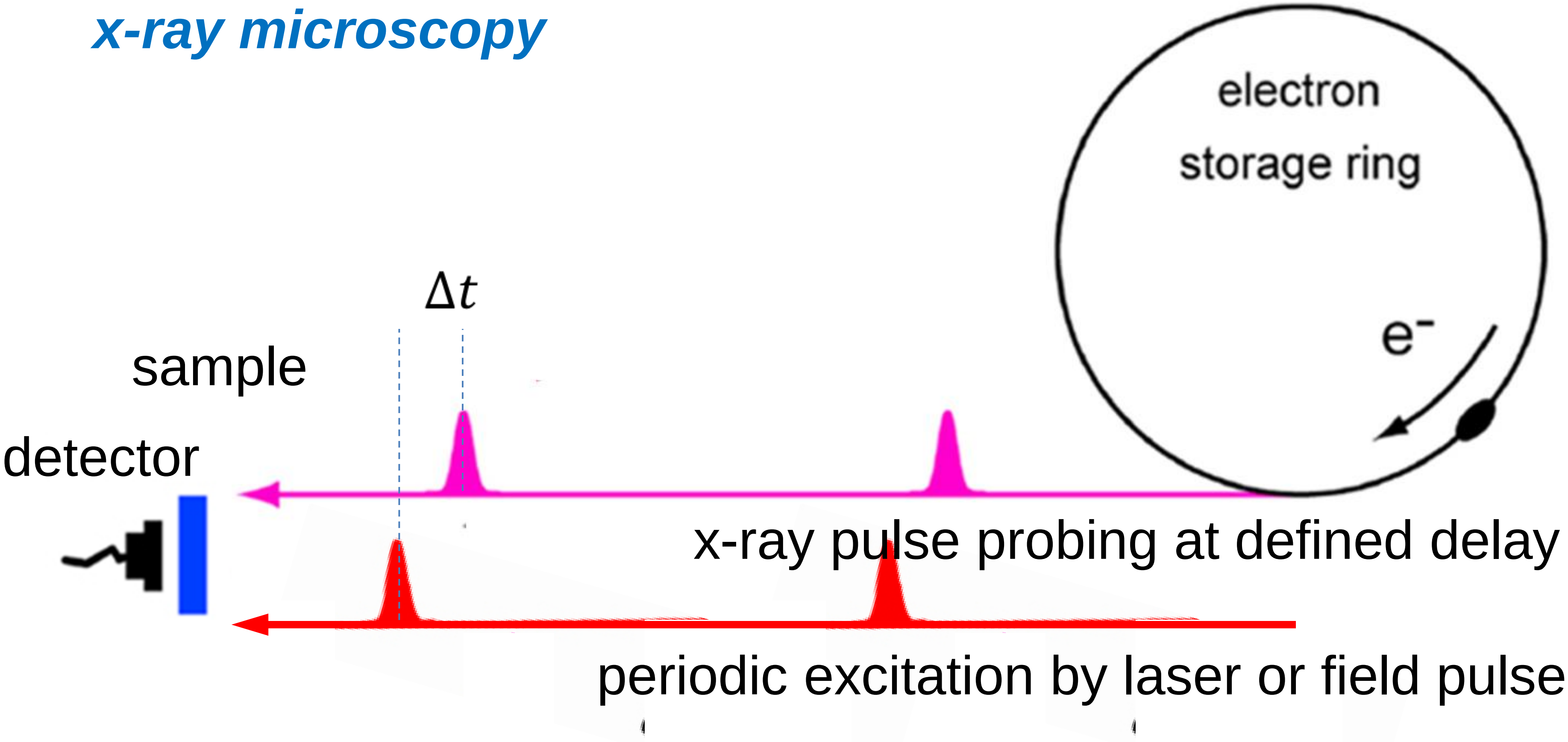

- Accumulation of large number of independent events necessary
- Only reversible processes can be imaged
- No acces to irreversible, stochastic processes e.g. fluctuations

Laser induced „bubble“ domains GdFeCo collapse

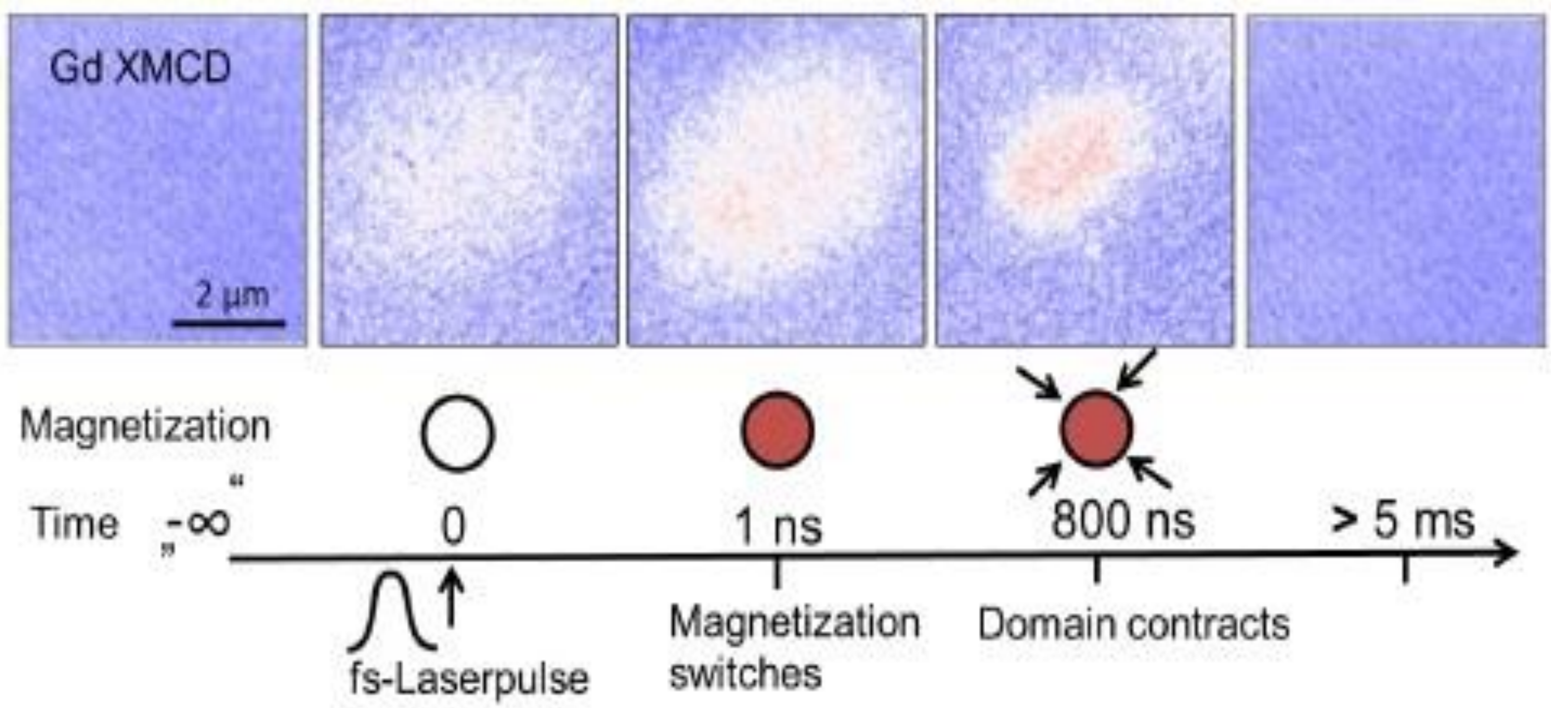

outline

Nanoparticles and 3d objects

Thin films and wedge profiles

PEEM with laser excitation

-> XPS PEEM & SW excitation

TMDs - for energy-efficient nano-optoelectronics

Transition-metal dichalcogenides (TMDs), such as:
Molybdenum disulfide (MoS2)
Molybdenum diselenide (MoSe2)
Tungsten disulfide (WS2)
Tungsten diselenide (WSe2).
The crystal structure consists of the metal atoms encapsulated between two layers of sulfur/selenium chalcogenide atoms. The bonding within a monolayer is strong while the bonding between monolayers is weak. Like with graphene/graphite, the monolayers of TMD can be exfoliated.

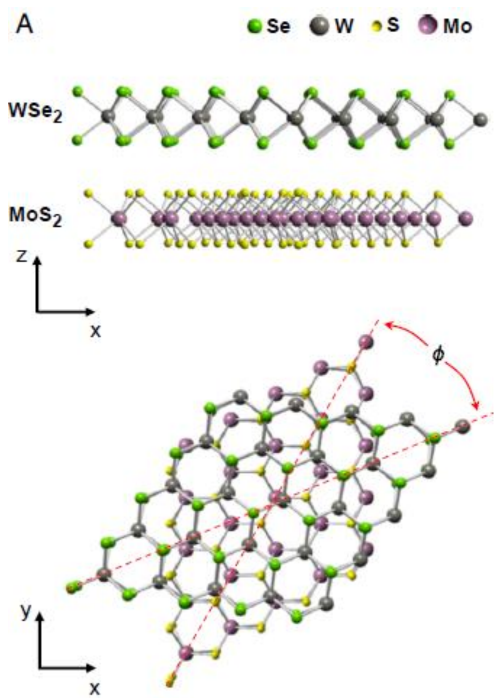

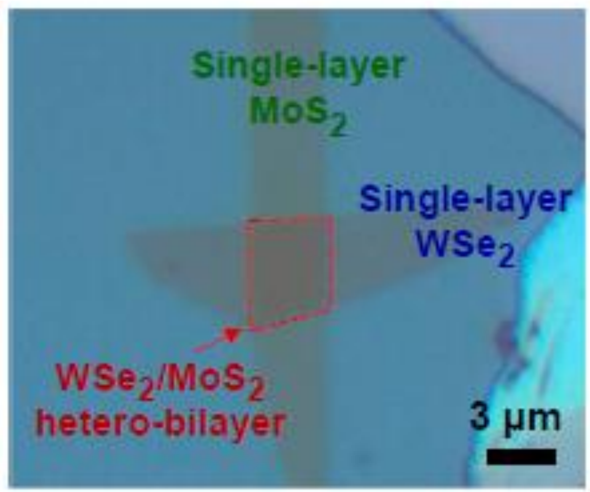

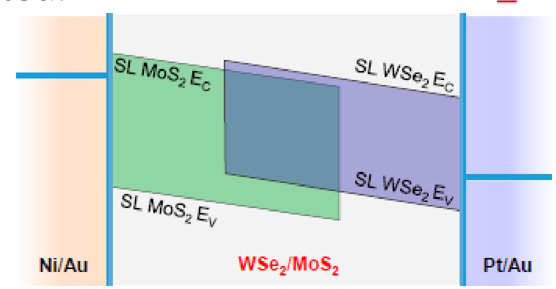

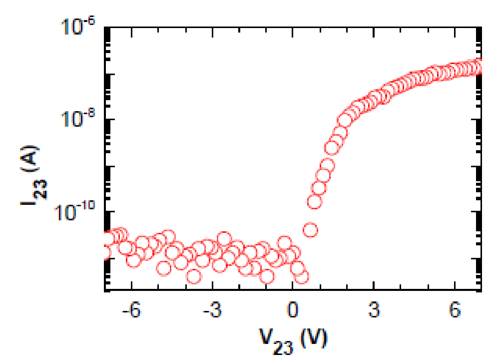

H. Fang et al., PNAS,111, 6198 (2014)

Electronic properties of TDM heterojunctions

local x-ray photoemission spectroscopy:

shows interlayer coupling and charge transfer in this new type of heterojunction

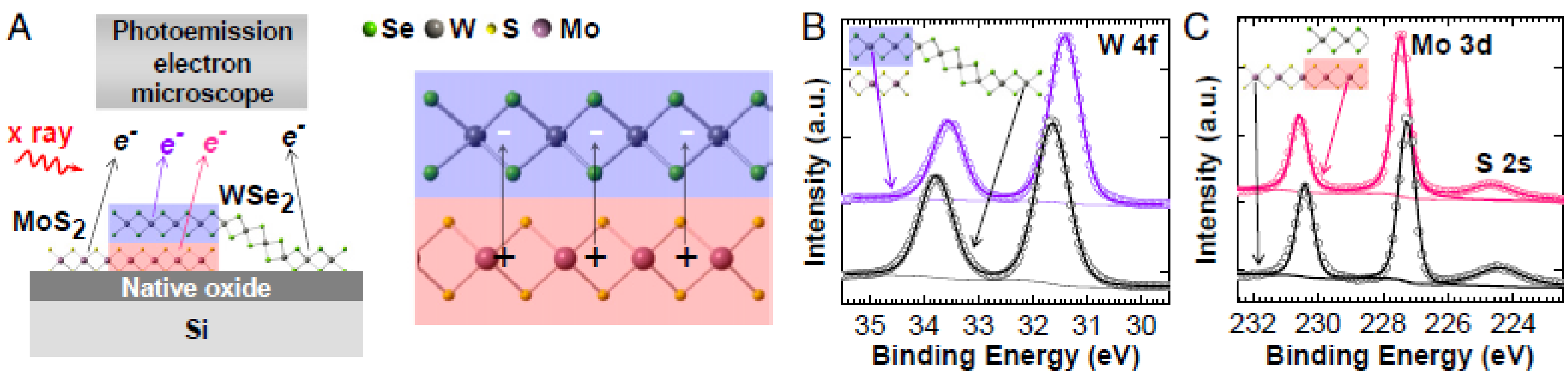

Fang et al., PNAS,111, 6198 (2014)

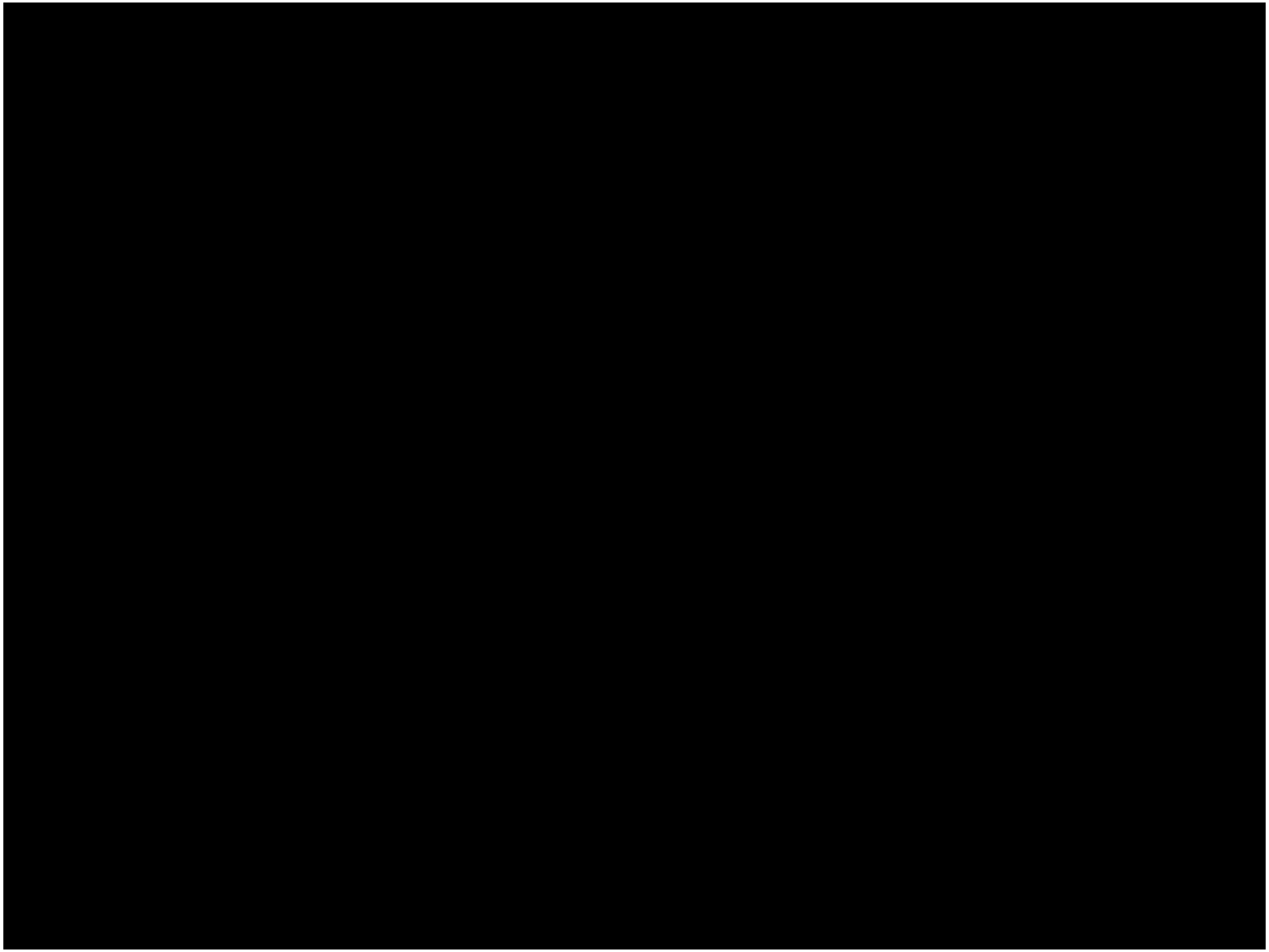

**PEEM / Nano-ARPES shows that Bulk TMDs show indirect-bandgap semiconductor behavior,
However, mono-layers of TMD have a wider direct bandgap!**

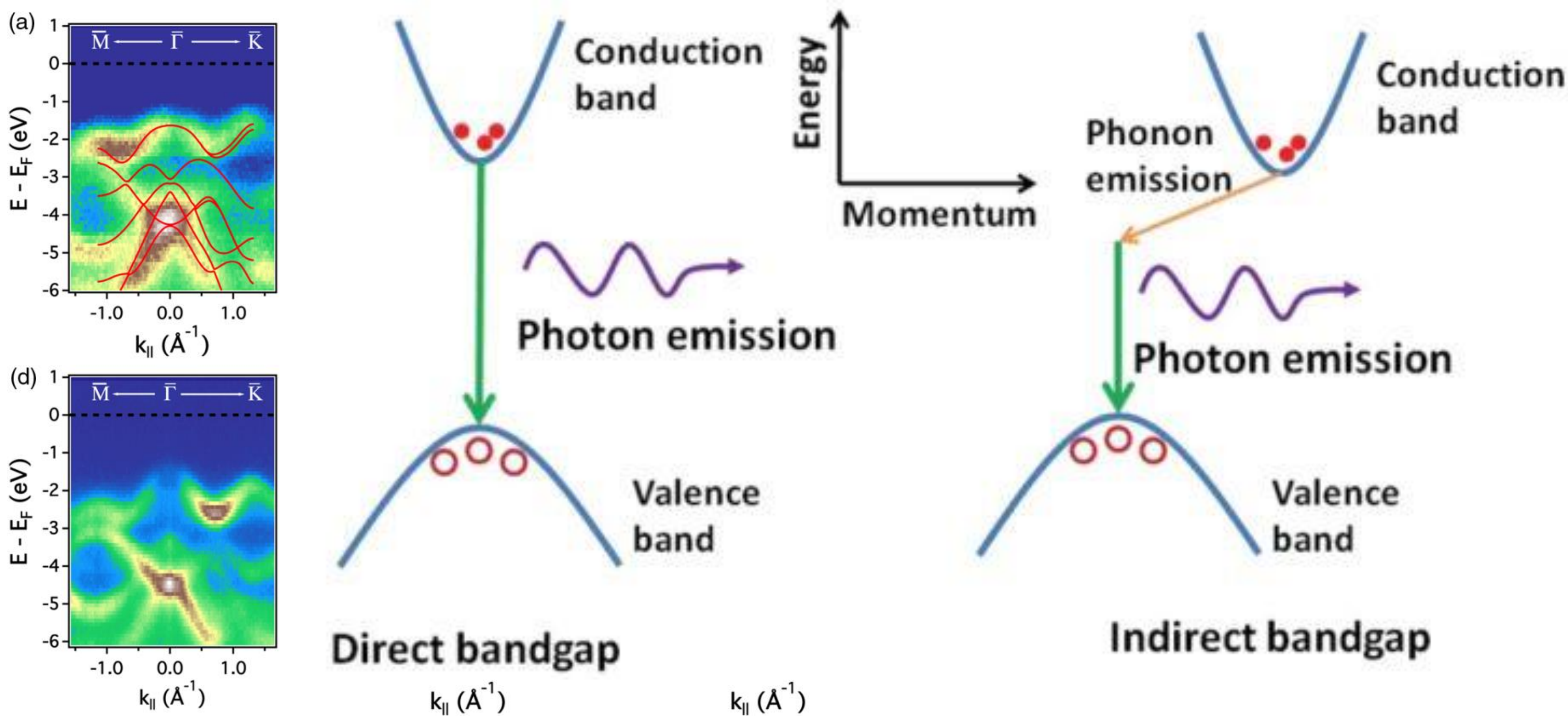

Jin et al., PRL 111, 106801 (2013)

TDMs - for energy-efficient nano-optoelectronics

-> Opportunities for creating optoelectronic devices such as solar cells and light-emitting diodes (LEDs). Monolayers have about 95% transparency, suggesting uses as transparent conductive electrodes. The transparency also points to stacking of devices for solar energy harvesting. Other possibilities include optical interconnect, logic and sensor applications.

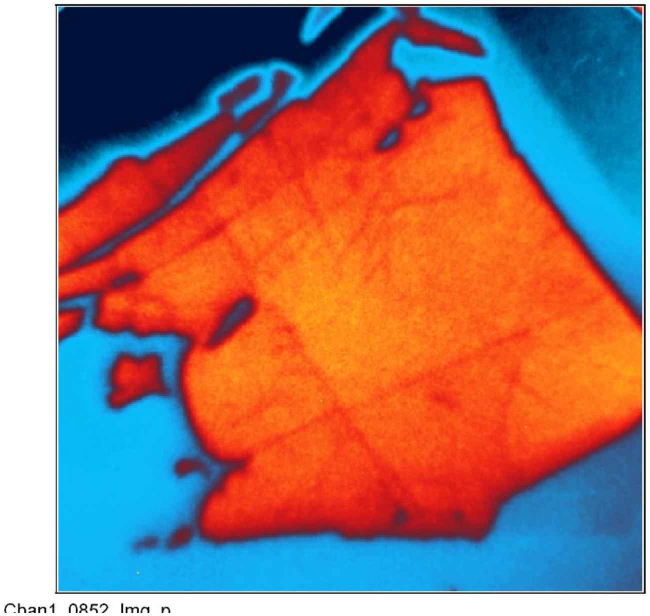

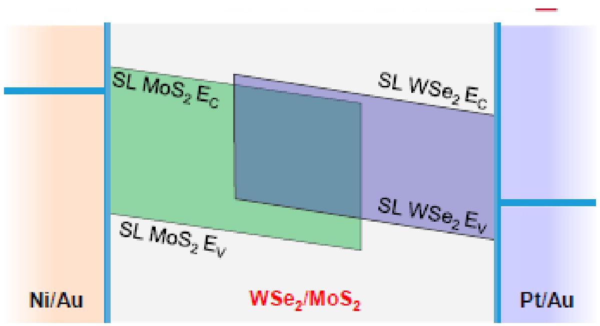

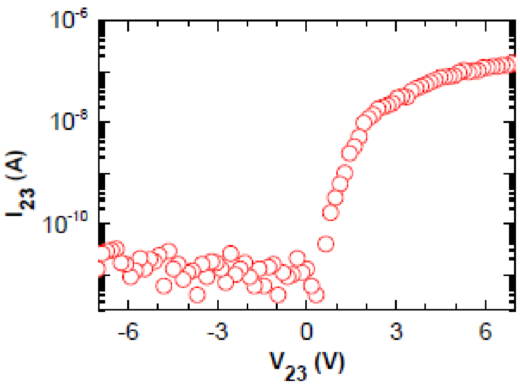

C 1*s* and Fe 3*p* images as function of photon energy

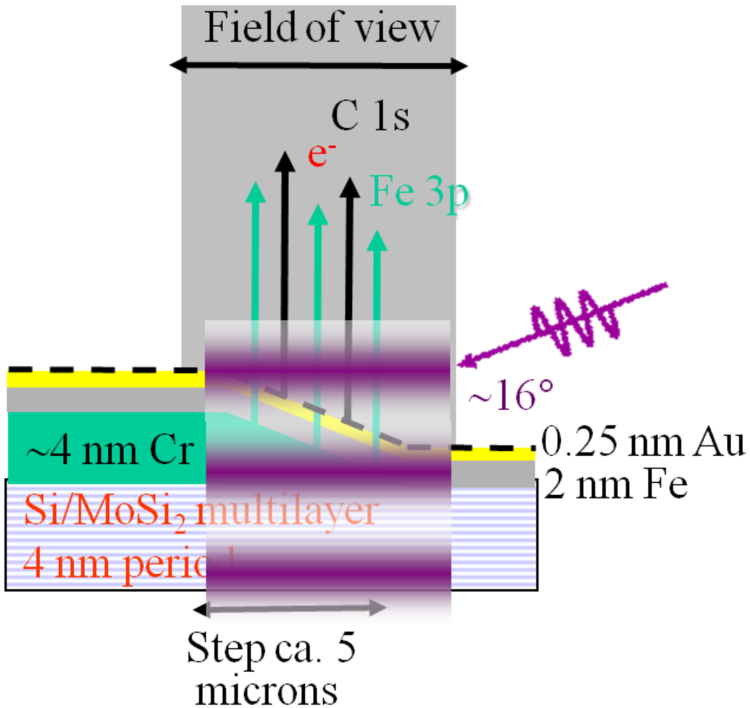

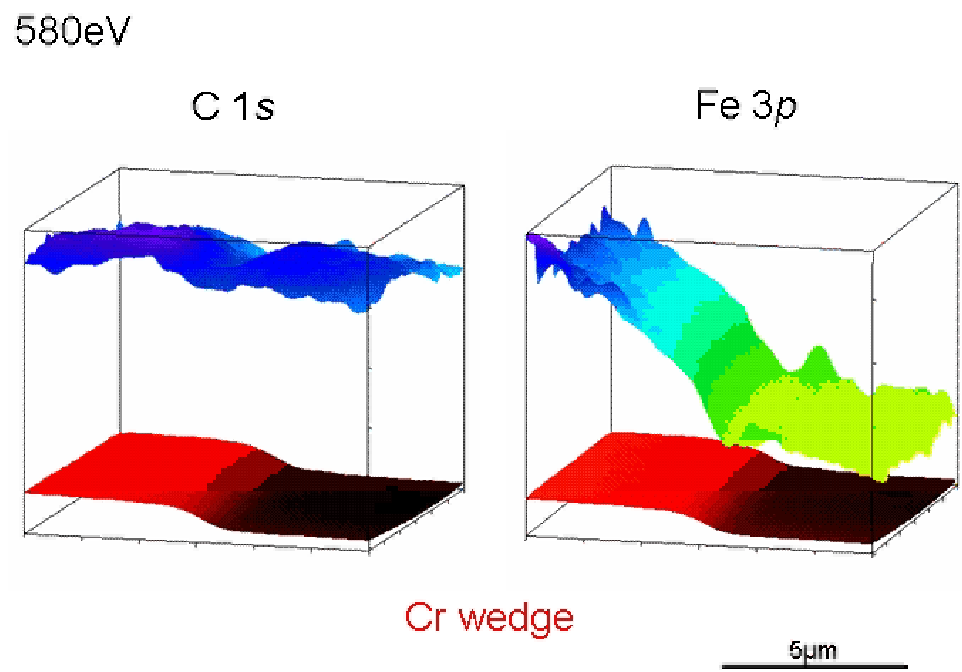

Sanding wave formation via Bragg reflection from a multilayer

Kronast et al., Appl. Phys. Lett. 93, 243116 (2008)

Depth profiling of Co Nanodot Magnetic Arrays

Co nanodots—4 nm thick, capping Al layer—2 nm thick
On Si/Mo multilayer, 4 nm period (2.4 nm Si, 1.6 nm Mo)

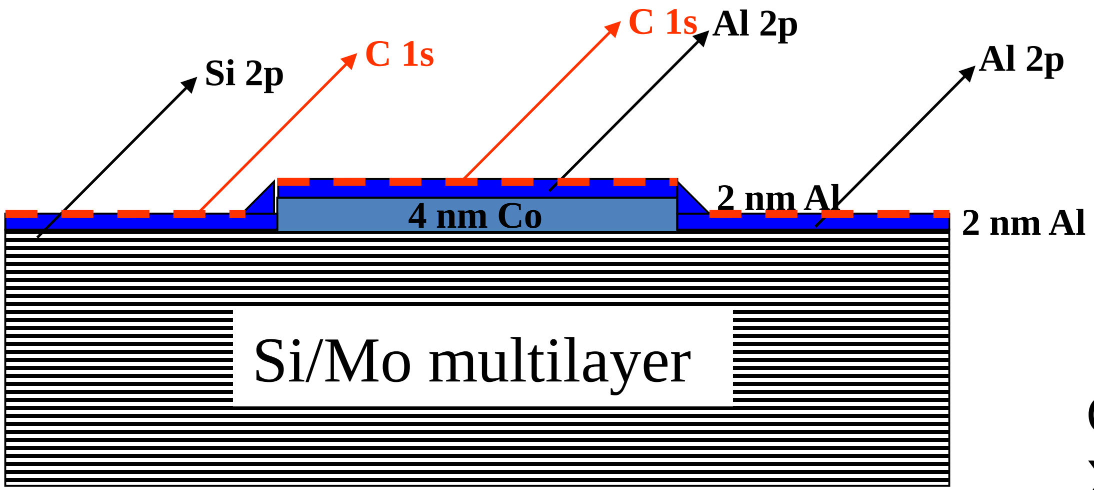

PEEM images

Co L_3

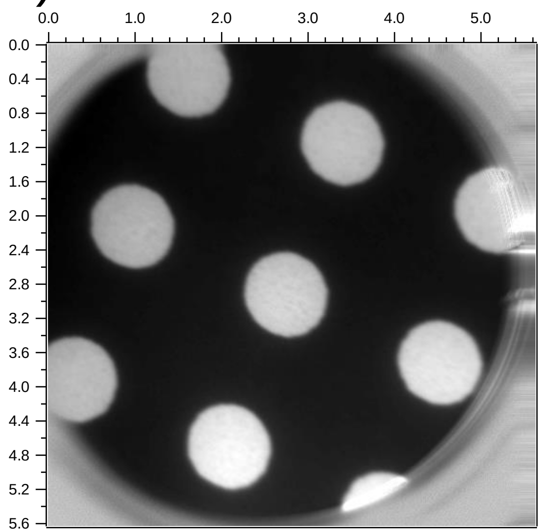

Co L_3 XMCD

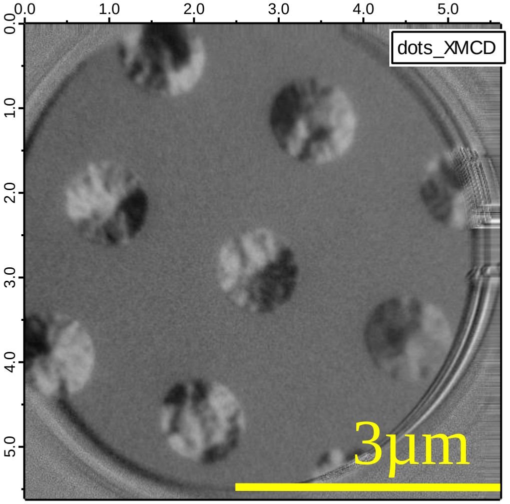

A. Gray, F. Kronast et al., *Appl. Phys. Lett.* **97**, 062503 (2010)

Separate animations of images via photoelectron peaks as photon energy is scanned through the Bragg condition

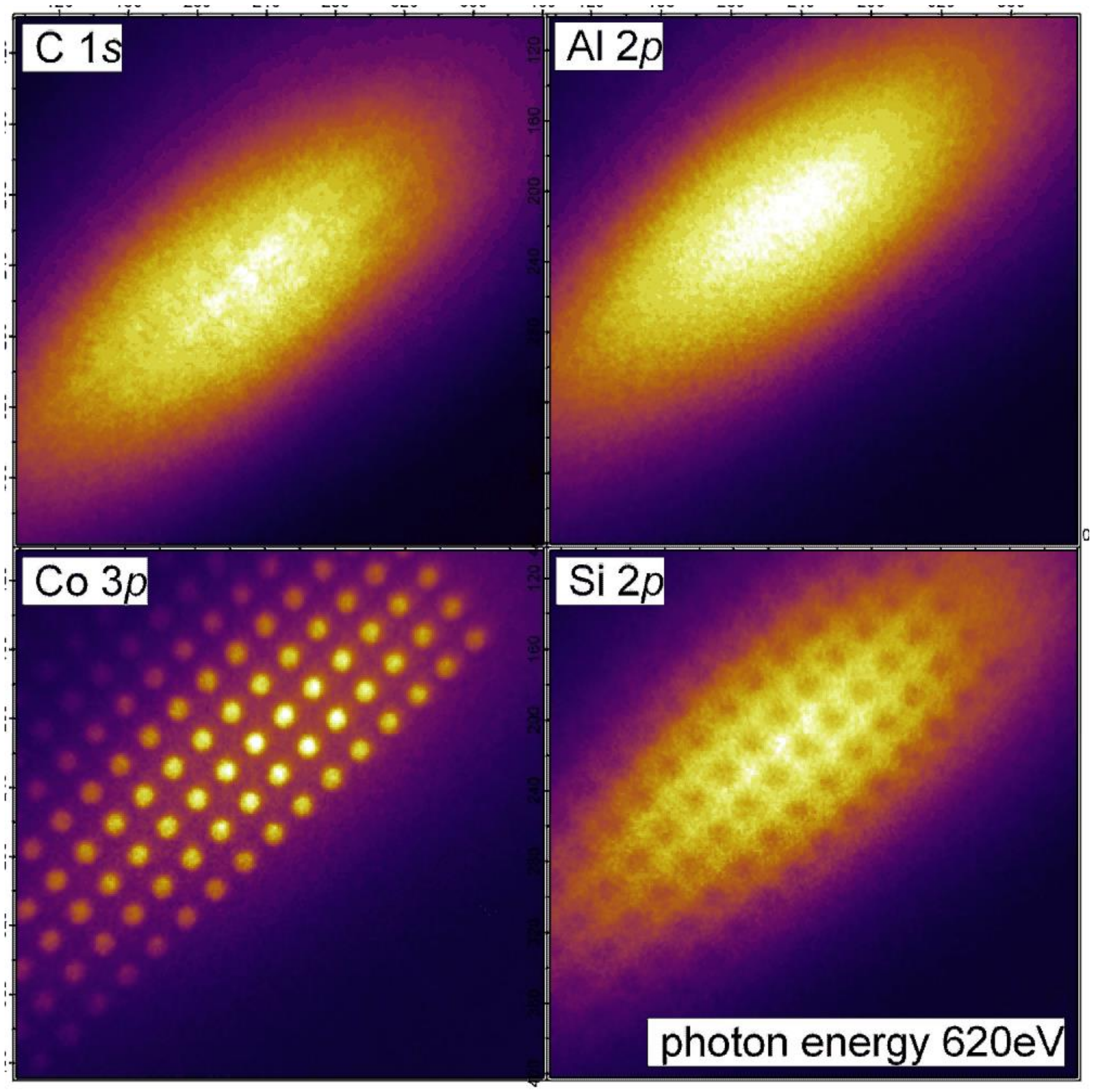

Modulation of the photoemission intensity by the standing wave on and off the dot

Photoelectron intensities

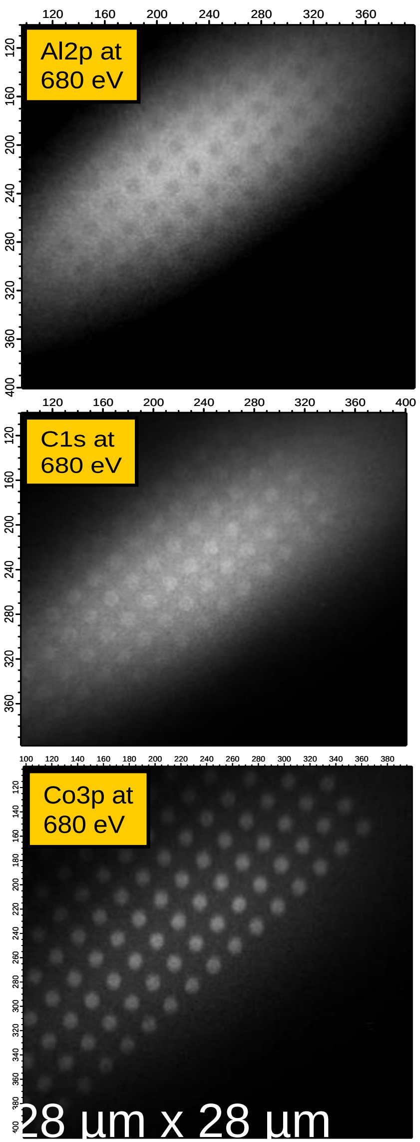

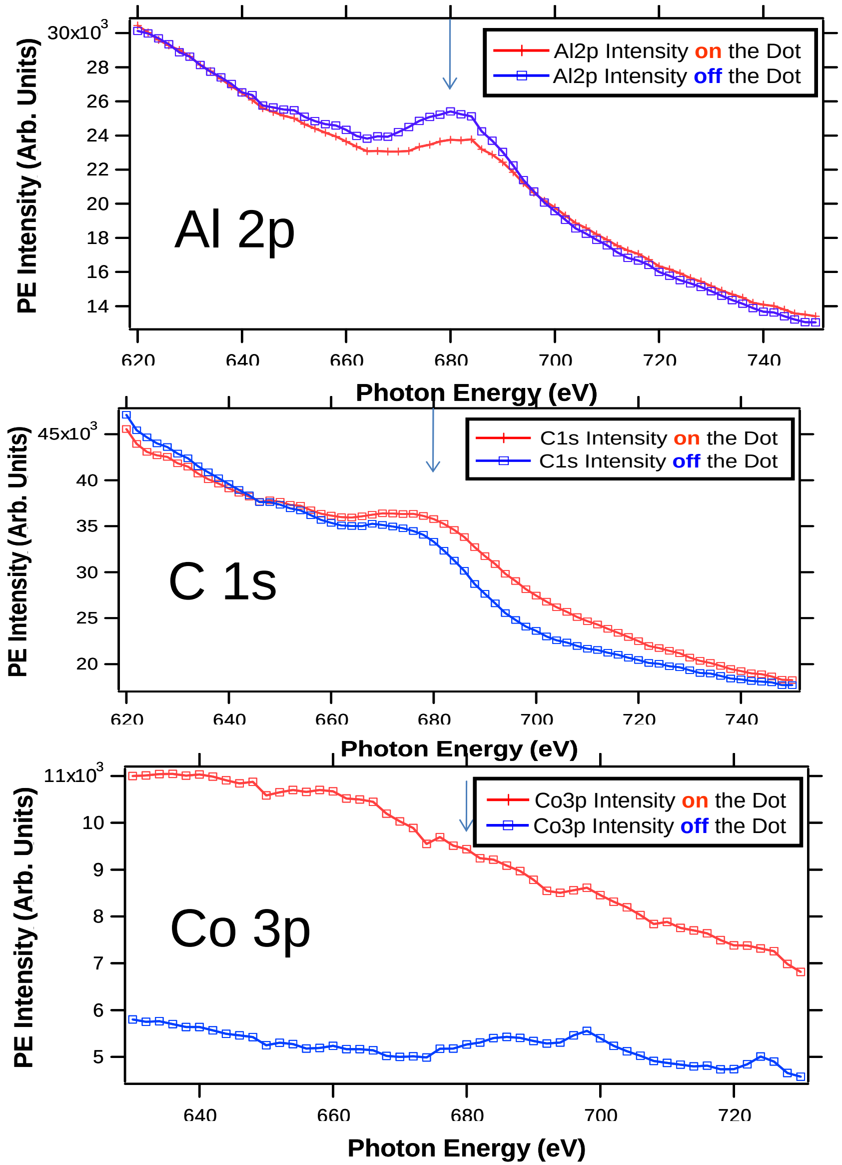

A. Gray, F. Kronast et al., *Appl. Phys. Lett.* **97**, 062503 (2010)

Self-consistent model of the film structure - result of simultaneous fitting of all the rocking curves

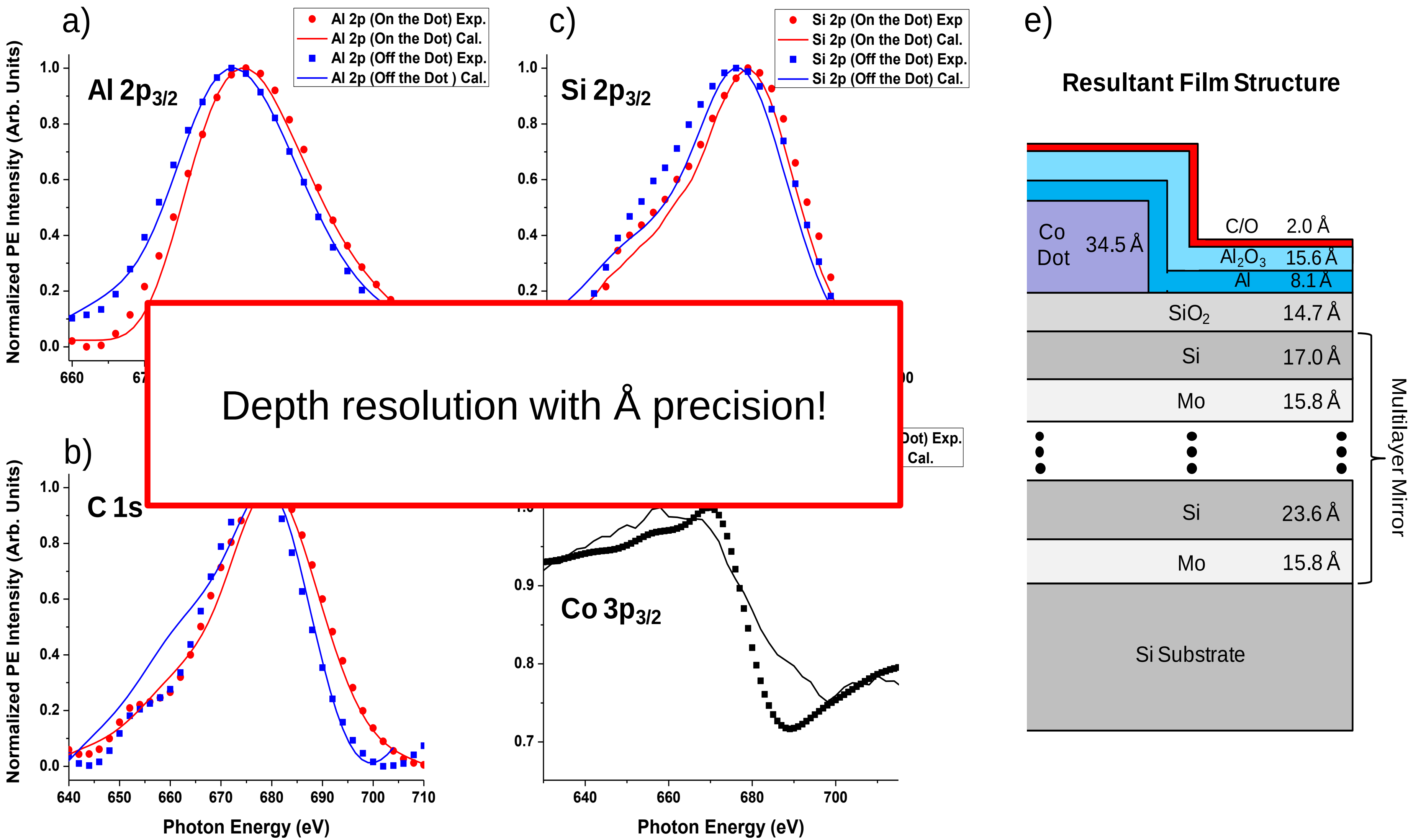

Depth resolution with Å precision!

A. Gray, F. Kronast et al., *Appl. Phys. Lett.* **97**, 062503 (2010)

- **Microspectroscopy**

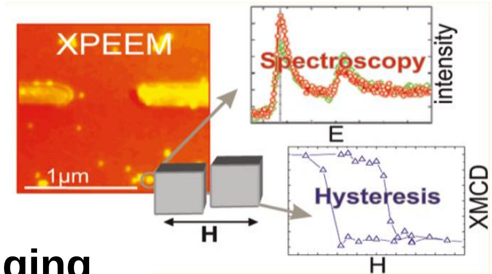

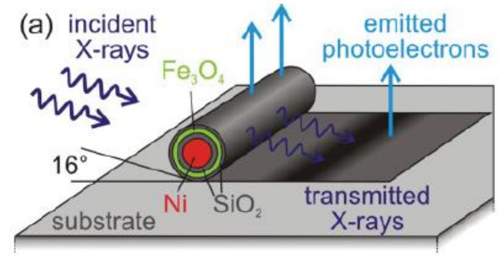

- **Element specifiy magnetic imaging**

- **XPS / ARPES spatially resolved / depth profiling**

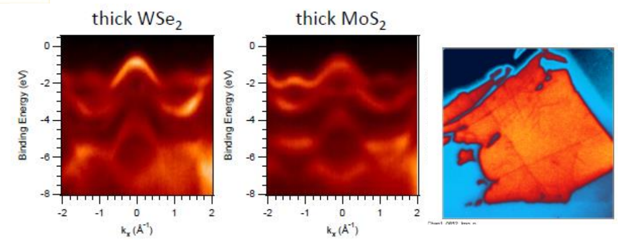

- **temperature dependent phase transitions**

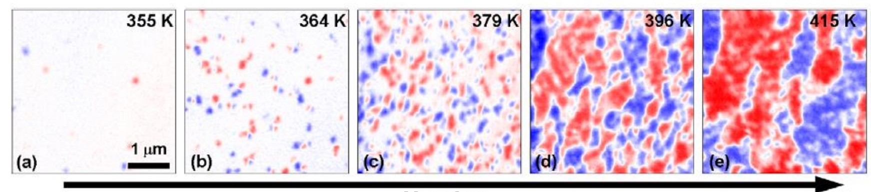

- **magnetic switching by magnetic or electric field**

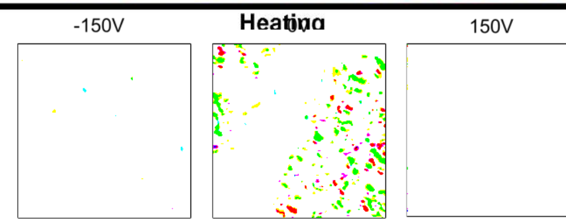

- **Laser excitation**

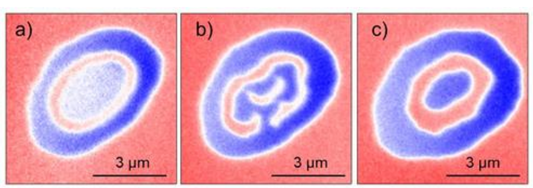

- **Dynamic pump-probe experiments**

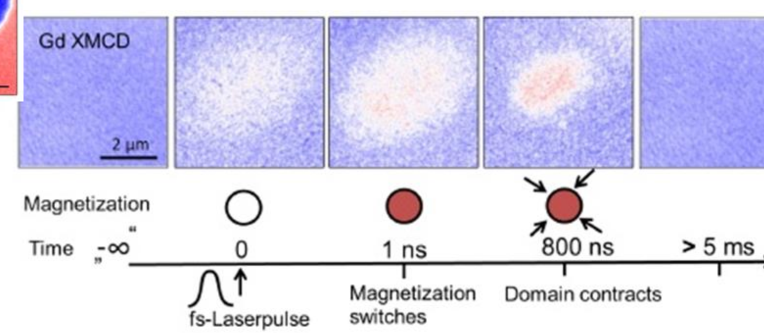

In collaboraion with

SW Project

Alexander Gray[1,2]
Christian Papp[2,4]
See-Hun Yang[5]
Stephan Cramm[6]
Ingo Krug[6]
Farhad Salmassi[7],
Dawn Hilken[7]
Eric Anderson[7]
Ruslan Ovsyannikov[3]
Alexander Kaiser[6]
Carsten Wiemann[6]
Roland Schreiber[6]
Daniel Bürgler[6]
Claus M. Schneider[6]
Hermann A. Dürr[3]
Charles S. Fadley[1,2]

Fe nanocubes

Nina Friedenberger[8]
Katharina Ollefs[8]
Hermann A. Dürr[3]
A. Shavel[9]
Michael Farle[8]

Coaxial nanomagnets

Judith Kimling[10]
Stephan Martens[10]
Tim Böhnert[10]
Michel Martens[10]
Julia Herrero-Albillos[3]
Logane Tati-Bismaths[3]
Ulrich Merkt[10]
Kornelius Nielsch[10]
Guido Meier[10]

SyntOrbMag MCRTN

SFB445

[1]Department of Physics, University of California, Davis, CA, USA
[2]Material Sciences Division, Lawrence Berkeley National Laboratory, CA, USA
[3]Helmholtz-Zentrum Berlin - BESSY II, Germany
[4]Physical Chemistry II, University of Erlangen, Germany
[5]IBM Almaden Research Center, San Jose, CA, USA
[6]Jűlich Research Center, Germany
[7]Center for X-Ray Optics, Lawrence Berkeley National Laboratory, CA, USA
[8]Department of Physics, Universität Duisburg-Essen, Germany
[9]Department of Physics, University of Vigo, Spain
[10]Institut f¨ur Angewandte Physik und Zentrum f¨ur Mikrostrukturforschung Hamburg , Universit¨at Hamburg

CeNIDE

In collaboraion with

Electric control of magnetism

A. Crassous
V. Garcia
L. Phillips
R.O. Cherifi
C. Deranlot
K. Bouzehouane
S. Fusil
F. Bruno
A. Barthélémy
M. Bibes

L. Bocher
A. Zobelli
A. Glotter

R. Abrudan

X. Moya
N. Mathur

Blanc programme

Magnetic tomography on tubes

R. Streubel
D. Makarov
O. Schmidt

Peter Fischer

Preparing samples for PEEM please consider...

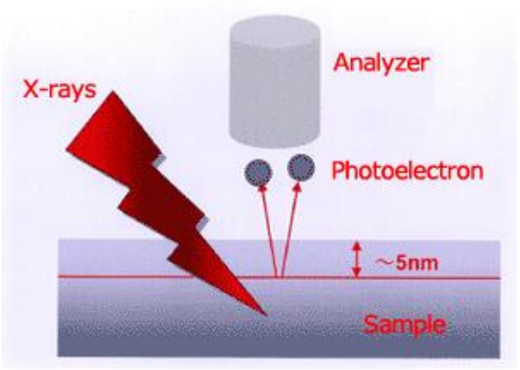

PEEM is surface / interface sensitive

(probing depth ~ 5nm in metallic samples)

If capping layer is required - consider using light elements such as Al or C

PEEM requires conducting samples

provides information on

- elemental composition
- chemistry
- structural parameters
- electronic structure
- magnetic properties
- topography

Native SiO_x layer usually works

Thicker SiO_2 layer might cause charging

Metallic structures on isolating substrates require connection to the potential of the sample holder